RESEARCH

UDOT Keeping Utah Moving

Utah Department of Transportation - Research Division
4501 South 2700 West - P.O. Box 148410 - SLC,UT 84114-8410

Report No. UT-21.19

EVALUATION OF COMMERCIALLY AVAILABLE CONCRETE BRIDGE DECK REPAIR MATERIALS

Prepared For:

Utah Department of Transportation
Research & Innovation Division

Final Report
July 2021

DISCLAIMER

The authors alone are responsible for the preparation and accuracy of the information, data, analysis, discussions, recommendations, and conclusions presented herein. The contents do not necessarily reflect the views, opinions, endorsements, or policies of the Utah Department of Transportation or the U.S. Department of Transportation. The Utah Department of Transportation makes no representation or warranty of any kind, and assumes no liability therefore.

ACKNOWLEDGMENTS

The authors acknowledge the Utah Department of Transportation (UDOT) for funding this research, and the following individuals from UDOT on the Technical Advisory Committee for helping to guide the research:

- Becky Nix
- Thad Pinkerton
- David Stevens
- James Corney
- Bryan Lee
- Scott Strader
- Jason Richins

TECHNICAL REPORT ABSTRACT

1. Report No.	2. Government Accession No.	3. Recipient's Catalog No.
UT-21.19	N/A	N/A

4. Title and Subtitle	5. Report Date
EVALUATION OF COMMERCIALLY AVAILABLE CONCRETE BRIDGE DECK REPAIR MATERIALS	July 2021
	6. Performing Organization Code: N/A

7. Author(s)	8. Performing Organization Report No.
Marc Maguire, Andrew D. Sorensen, Robert J. Thomas, Ali Banaei Pour, Md. Abdullah Al Sarfin	N/A

9. Performing Organization Name and Address	10. Work Unit No.
Utah State University Department of Civil and Environmental Engineering 4110 Old Main Hill Logan, UT 84322-4110	8RD2113H
	11. Contract or Grant No.: 18-8982

12. Sponsoring Agency Name and Address	13. Type of Report & Period Covered
Utah Department of Transportation 4501 South 2700 West P.O. Box 148410 Salt Lake City, UT 84114-8410	Final Report April 2018 to July 2021
	14. Sponsoring Agency Code: PIC No. UT17.105

15. Supplementary Notes

Prepared in cooperation with the Utah Department of Transportation and the U.S. Department of Transportation, Federal Highway Administration

16. Abstract

Extensive investigation on rapid repair materials for concrete bridge decks is of utmost importance to limit the impact on traveling vehicles as well as selecting suitable materials with acceptable mechanical properties and durability requirements. The objective of this research project is to evaluate eight commercial cementitious rapid repair materials for application to a concrete bridge deck in Utah. A robust laboratory study to quantify the mechanical performance and durability has been conducted and accompanied with evaluation of field performance. More than 450 specimens were prepared according to manufacturer recommendations and tested at ages of 4 hours, 24 hours, 7 days, and 28 days to measure their setting time, compressive and splitting tensile strength, elastic modulus, autogenous and drying shrinkage, restrained ring shrinkage, surface resistivity, and slant shear bond strength. Repair patches on the Layton, Utah, SR-193 bridge over US-89 (Structure Number 0F 575) have been inspected three times over an eight-month period by researchers, and crack development on these patches has been recorded. Based on this work, this report intends to assist the Utah Department of Transportation (UDOT) to identify the most influential factors in the success or failure of deck repair materials as well as which tests are most helpful in the process of evaluation and selection of deck repair materials.

17. Key Words	18. Distribution Statement	23. Registrant's Seal
rapid repair materials, partial-depth bridge deck repair, concrete bridge decks	Not restricted. Available through: UDOT Research & Innovation Div. 4501 South 2700 West P.O. Box 148410 Salt Lake City, UT 84114-8410 www.udot.utah.gov/go/research	N/A

19. Security Classification (of this report)	20. Security Classification (of this page)	21. No. of Pages	22. Price
Unclassified	Unclassified	116	N/A

TABLE OF CONTENTS

LIST OF TABLES

LIST OF FIGURES

UNIT CONVERSION FACTORS

Units used in this report and not conforming to the UDOT standard unit of measurement (U.S. Customary system) are given below with their U.S. Customary equivalents.

SI* (MODERN METRIC) CONVERSION FACTORS

APPROXIMATE CONVERSIONS TO SI UNITS

Symbol	When You Know	Multiply By	To Find	Symbol
		LENGTH		
in	inches	25.4	millimeters	mm
ft	feet	0.305	meters	m
yd	yards	0.914	meters	m
mi	miles	1.61	kilometers	km
		AREA		
in^2	square inches	645.2	square millimeters	mm^2
ft^2	square feet	0.093	square meters	m^2
yd^2	square yard	0.836	square meters	m^2
ac	acres	0.405	hectares	ha
mi^2	square miles	2.59	square kilometers	km^2
		VOLUME		
fl oz	fluid ounces	29.57	milliliters	mL
gal	gallons	3.785	liters	L
ft^3	cubic feet	0.028	cubic meters	m^3
yd^3	cubic yards	0.765	cubic meters	m^3
	NOTE: volumes greater than 1000 L shall be shown in m^3			
		MASS		
oz	ounces	28.35	grams	g
lb	pounds	0.454	kilograms	kg
T	short tons (2000 lb)	0.907	megagrams (or "metric ton")	Mg (or "t")
		TEMPERATURE (exact degrees)		
°F	Fahrenheit	5 (F-32)/9 or (F-32)/1.8	Celsius	°C
		ILLUMINATION		
fc	foot-candles	10.76	lux	lx
fl	foot-Lamberts	3.426	$candela/m^2$	cd/m^2
		FORCE and PRESSURE or STRESS		
lbf	poundforce	4.45	newtons	N
lbf/in^2	poundforce per square inch	6.89	kilopascals	kPa

APPROXIMATE CONVERSIONS FROM SI UNITS

Symbol	When You Know	Multiply By	To Find	Symbol
		LENGTH		
mm	millimeters	0.039	inches	in
m	meters	3.28	feet	ft
m	meters	1.09	yards	yd
km	kilometers	0.621	miles	mi
		AREA		
mm^2	square millimeters	0.0016	square inches	in^2
m^2	square meters	10.764	square feet	ft^2
m^2	square meters	1.195	square yards	yd^2
ha	hectares	2.47	acres	ac
km^2	square kilometers	0.386	square miles	mi^2
		VOLUME		
mL	milliliters	0.034	fluid ounces	fl oz
L	liters	0.264	gallons	gal
m^3	cubic meters	35.314	cubic feet	ft^3
m^3	cubic meters	1.307	cubic yards	yd^3
		MASS		
g	grams	0.035	ounces	oz
kg	kilograms	2.202	pounds	lb
Mg (or "t")	megagrams (or "metric ton")	1.103	short tons (2000 lb)	T
		TEMPERATURE (exact degrees)		
°C	Celsius	1.8C+32	Fahrenheit	°F
		ILLUMINATION		
lx	lux	0.0929	foot-candles	fc
cd/m^2	$candela/m^2$	0.2919	foot-Lamberts	fl
		FORCE and PRESSURE or STRESS		
N	newtons	0.225	poundforce	lbf
kPa	kilopascals	0.145	poundforce per square inch	lbf/in^2

*SI is the symbol for the International System of Units. (Adapted from FHWA report template, Revised March 2003)

LIST OF ACRONYMS

AASHTO	American Association of State Highway and Transportation Officials
ASTM	American Society for Testing and Materials
BRRFC	Black Rapid Repair Fiber Concrete
CAC	Calcium Aluminate Blended Cements
CSA	Calcium Sulfoaluminate
DOT	Department of Transportation
ECC	Engineered Cementitious Composites
FHWA	Federal Highway Administration
GGBS	Ground Granulated Blast Furnace Slag
HAC	High Alumina Cement
HES	High Early Strength
LMC	Latex Modified Concrete
MOE	Modulus of Elasticity
MSE	Mean Square Error
NCL	Normalized Crack Length
RCLMC	Latex-Modified Rapid-Set Concrete
RHA	Rice Husk Ash
RRM	Rapid Repair Material
SHRP	Strategic Highway Research Program
SRA	Shrinkage Reducing Agent
UDOT	Utah Department of Transportation
UFFA	Ultra Fine Fly Ash
VES	Very Early Strength
VHS	Very High Strength

EXECUTIVE SUMMARY

Eight commercially available cementitious repair media were investigated for rapid repair of concrete bridge decks in Utah. A robust laboratory study of mechanical performance and durability properties of the materials was conducted to measure their setting time, compressive and splitting tensile strength, elastic modulus, autogenous and drying shrinkage, restrained ring shrinkage, surface resistivity, and slant shear bond strength at ages of 4 hours to 28 days. Considerable variation was observed in the performance of the selected materials.

It was found that all repair materials evaluated in this study can be exposed to traffic after 4 hours and can meet the requirement of their compressive strength being equal to or greater than that of the substrate concrete. At the critical age of 4 hours, the materials had a compressive strength of 3,000-5,600 psi. At late ages (28 days), the compressive strength of the repair materials was 6,800-11,000 psi.

The time between the initial and final set for most materials was found to be between 5 and 15 minutes, and the materials commonly started to gain strength in less than 45 minutes. The elastic modulus of the repair materials at 4 hours and 28 days was 3,300-4,700 ksi and 4,500-7,500 ksi, respectively. Four materials demonstrated a splitting tensile strength of about 4,000 psi or higher at 4 hours, while all but one material had a tensile strength of higher than 4,000 psi at late ages. The chloride penetration potential of the materials at late ages was found to be very low.

Seven materials had a slant shear bond strength of over 1,600 psi at 4 hours, while all but one material showed a bond strength of over 3,000 psi at 28 days. Also, all possible failure modes were observed in the slant shear test: bond failure, substrate concrete failure, repair material failure, and a combination of the three failure modes. In four out of eight repair materials, the predominant failure mode was substrate and/or repair failures.

With regard to dimensional stability, all materials generally had a satisfactory performance but with different trends of autogenous (sealed) or drying shrinkage development. The highest observed autogenous shrinkage was 60 micro-strains (με). At 28 days, five materials had a free drying shrinkage of between 200 and 400 με, while for the other three materials it was

between 600 and 800 με, well below the ASTM C928 limit of 1,500 με. Only two of the materials developed cracks during the restrained ring shrinkage test. Four materials were found to register almost constant strain in ring specimens. It is recommended to use methods such as coarse aggregate extension or internal curing to reduce a high shrinkage cracking potential.

The field performance data, obtained from repair patches on the Layton SR-193 bridge over US-89 (Structure Number 0F 575), showed wide variation in crack formation and development in repair patches, which can be attributed to the different ambient conditions during pouring as well as patch size and shapes. Therefore, the laboratory experiments in a controlled environment have been found to be more suitable to compare the materials.

Overall, and based on the lab performance observations provided in this document, repair products P1 and P8 showed the best and the worst performance in terms of both mechanical and durability properties, respectively.

1.0 INTRODUCTION

1.1 Introduction to Rapid Concrete Repair

Concrete durability varies depending on exposure conditions; the presence and the localization of the reinforcement; and the placing, finishing, curing, and protection it receives. In service, concrete may be subjected to conditions of abrasion, moisture cycles, freeze-thaw cycles, temperature fluctuations, reinforcement corrosion, and chemical attacks, resulting in deterioration and possibly decreasing its service life [1]. Surface deterioration can develop in concrete transportation structures due to either mechanical loading or environmental exposure and can act to reduce the strength and stiffness of the concrete while permitting the accelerated ingress of water and other aggressive agents.

Studies have indicated that this type of deterioration can increase the permeability, increase the severity of reinforcing-steel corrosion, and lower the load-carrying capacity of concrete. As a result, surface deterioration should be repaired to reestablish the serviceability as well as the water-tightness of concrete transportation structures. Many of the bridges across the United States are deteriorated and need to be repaired. Concrete repair features several challenges and complexities. The steps involved in concrete repair include condition assessment of the existing structure, selection of appropriate repair materials as related to the exposure conditions, and implementation requiring a methodical approach. The repair system must eventually be a composite system and be durable enough to withstand different loading and environmental conditions during its service life [2].

A complete deck replacement is obviously not a feasible option because it is not cost-effective and requires closing the roads for long periods of time. Therefore, deck patching is often the most reasonable alternative [3]. Although conventional Portland cement-based concrete remains the most reliable repair material, the repair patch often requires time to cure before the structure can be reopened to traffic, which necessitates detours or lane closures. Also, repairs performed in high traffic areas and areas with severe environments require materials that have the ability to cure fast while having satisfactory strength and durability. Rapid repair of deteriorated bridge decks and pavements diminishes traffic interference, travel delays, and costs

[2]. As a result, in an attempt to reduce traffic disturbance, transportation authorities' often use rapid-hardening, prepackaged repair materials such as rapid-set, cement-based, and resin-based mortars or concretes. Therefore, these materials have been in great demand and are typically used so that the repaired pavement can be reopened to traffic about 4 hours after field placement [3].

Rapid-set cement-based materials are easier to mix and are more compatible with the substrate, but they are costly and can be more prone to dimensional instability. The primary categories of rapid-set cement are magnesium phosphate cement, calcium sulfoaluminate cement, calcium aluminate cement, and other blended cements.

One of the major concerns in rapid repair of concrete is the premature failure of the repair system, which is mainly caused by exposure to freeze-thaw cycles, aggressive chemical exposure, mechanical abrasion, loss of bond between the repair and the substrate, and dimensional stability of the repair material (elastic modulus, shrinkage, expansion, etc.). Most of the problems are related to durability and construction issues rather than structural failures [2]. Through follow-up inspection of repair patches, Ram et al. [2] reported that all but one patch in their study experienced premature failures, primarily cracking and edge de-bonding. For this reason, it is of utmost importance to properly select a repair material and then systematically evaluate its performance both in the lab and in the field.

In a previous research project funded by UDOT, an investigation to develop a full-depth durable concrete mixture, with minimum cracking potential, for pavement repair was carried out. The curing time and compressive strength of the mix were four hours and 4,000 psi, respectively. The researchers recommended a CSA mixture with internal curing [4].

1.2 Partial-Depth Repair

1.2.1 Introduction

Partial-depth repairs are referred to as the elimination and replacement of concrete pavement spalls. Spalling "describes the cracking, breaking, chipping, or fraying of concrete slab edges at joints and cracks" [5]. The spread of spalling distresses is slowed or eliminated by

performing a partial-depth repair. Deteriorated joints can also be repaired using this approach. As a result, partial-depth repairs reestablish the structural integrity and extend the service life of concrete pavements [5]. It should be noted that partial-depth repairs include shallow depth (0-2 in.) and moderate depth (2-5 in.) repairs.

1.2.2 Scope, Performance, and Failure Causes of Partial-Depth Repairs

A properly designed and placed partial-depth patch repair followed by adequate quality control can perform well, with a service life of 3-10 years or more. A poor performance is typically the result of poor design and construction, and improper quality control and condition assessment [5]. The most frequent causes of partial-depth patch failure are shown in Figure 1.1.

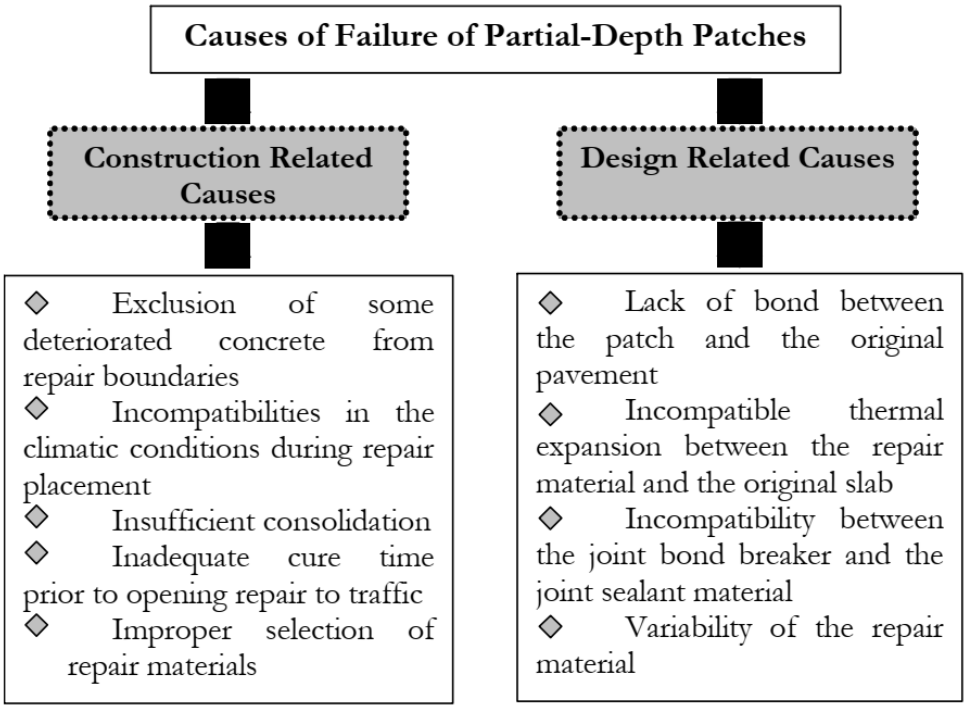

Figure 1.1 Causes of Failure of Partial-Depth Repairs [5]

1.3 Material Selection Process

1.3.1 General Steps in Material Selection

As discussed in the previous sections, the use of rapid-setting repair media has recently increased significantly. There are numerous commercially available rapid-setting repair materials

with a wide range of different mechanical and physical properties, shelf life, cost, performance, etc.; therefore, selecting a suitable material is difficult.

General steps to be followed in the material selection process are [2]:

- Condition assessment of the existing structure
- Identifying the deterioration cause(s)
- Establishing the nature and the severity of the environmental condition
- Determining the intended service life of the structure
- Evaluating alternative repair systems
- Appropriate repair system selection, design, and specifications
- Selecting repair materials to satisfy specifications
- Work execution in accordance with specifications

A flowchart showing general considerations for selecting a repair material is presented in Figure 1.2.

1.3.2 Different Types of Rapid-Setting Repair Materials

Rapid-setting repair materials generally fall into three main classes described below: cementitious materials, polymer-modified cementitious materials, and resinous materials.

Cementitious materials. These materials are easier to mix and more compatible with the substrate, but they are costly and can be more prone to dimensional instability. Examples include Portland cement (PC) based, gypsum-based, high alumina cement (HAC), magnesium phosphate cement, and calcium sulfoaluminate (CSA) cement.
Regular PC is the most common material used for spall repair but is not suitable if the road is to be opened to traffic quickly [5]. Gypsum-based (calcium sulfate) patching materials have a quick rate of strength gain, but their performance, when exposed to moisture or freezing weather, is not good [5]. Magnesium phosphate cement develops strength based on the hydration reaction

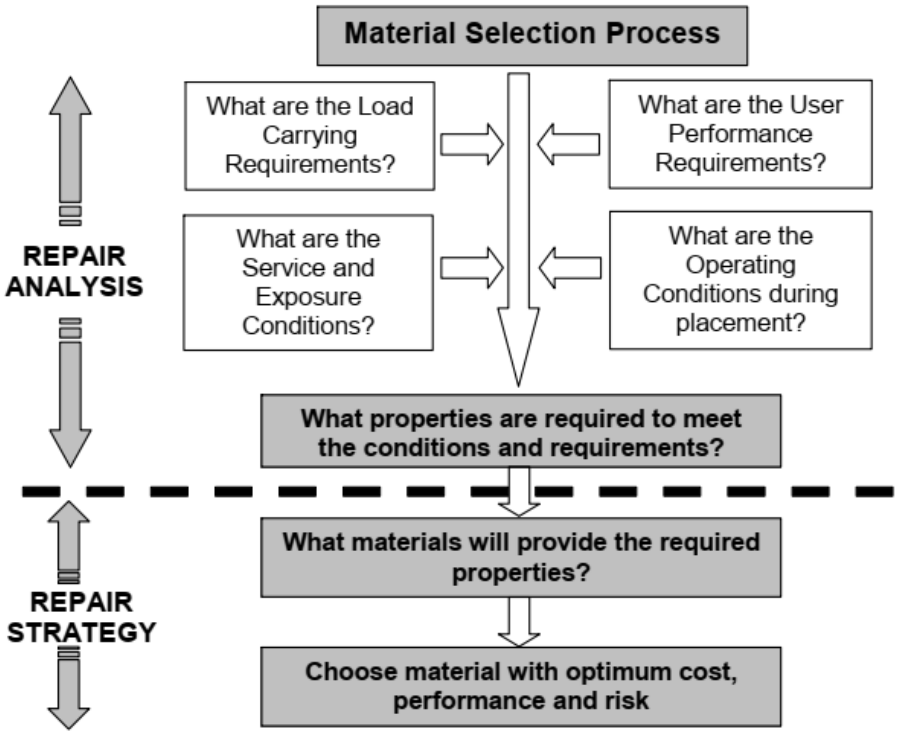

Figure 1.2 Material Selection Process [5]

between magnesium oxides and phosphates, leading to quick or flash setting, rapid strength development, and large amounts of heat generation. It has some limitations, such as those due to the large heat release, but on the other hand does not require moisture curing after placement due to the fact that the magnesium phosphate cement paste has negligible shrinkage upon drying [6]. CSA cement, despite having a relatively high cost, develops rapid early strength and high dimensional stability as a result of the fast hydration reaction of Ye'elimite (at an early age) and the formation of an expansive hydration product (ettringite) that compensates for shrinkage. Calcium aluminate cement (CAC) is also expensive but has the advantage of rapid setting and strength gain as well as enhanced resistance to high temperatures, abrasion, and chemical attacks [6].

Polymer-modified cementitious materials. "Polymer concretes are a combination of polymer resin, aggregate, and a set initiator. The aggregate makes the polymer concrete more economical, provides thermal compatibility with the pavement, and provides a wearing surface" [6]. Some types of polymer concretes include epoxy concrete, methyl methacrylate concrete, and polyurethane concrete.

Resinous materials. "Resin-based materials have extremely low permeability and low drying shrinkage as well as good adhesion with the substrate, but they are sensitive to moisture variations and are thermally incompatible with the substrate. These materials are preferred in thin applications, where low permeability and good adhesion are required [7]."

1.4 Characteristics and Properties of Repair Materials

A plethora of rapid-setting repair materials are available on the market, and there are considerable variations in their mechanical properties, durability, and the chemical composition. Important characteristics of a repair material should be identified with regard to the repair project at hand before selecting a specific repair material for the project [2].

1.4.1 General Requirements

Figure 1.3 outlines general performance criteria that are required for an ideal repair material. First, the repair system should be able to satisfy the structural requirements related to the load-carrying capacity of a given element. In addition, the repair material should be able to bond well with the existing concrete, which would enable the repair system to distribute the stresses throughout the structure. Also, the repair material has to be easy to mix and place. Another

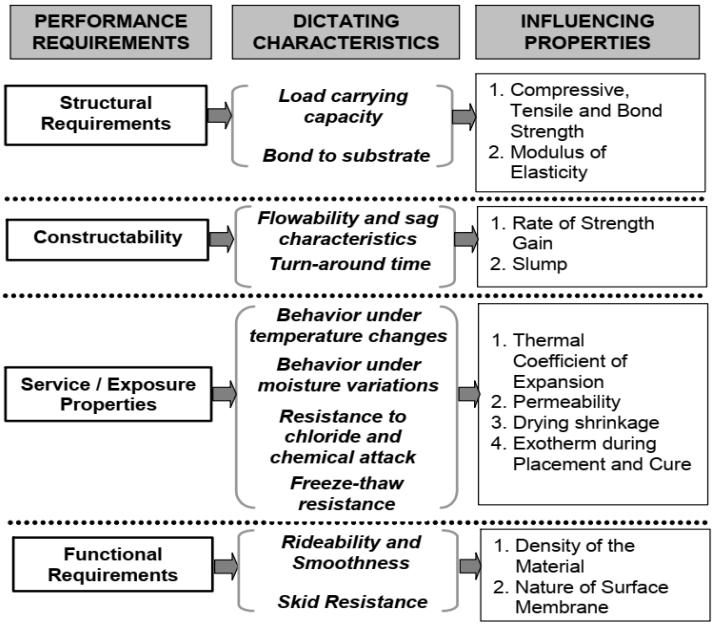

Figure 1.3 Required Performance Criteria for an Ideal Repair Material [5]

characteristic that is expected from a rapid-setting material is a fast rate of strength development to minimize the time of closure. Last, the adequate performance of the repair material when subjected to temperature and moisture changes, freeze-thaw cycles, and exposure to deicing salts is also required.

One of the greatest factors that govern the performance of a repair material is its compatibility with the existing structure. Table 1.1 presents the general requirements for structural compatibility of repair materials. The first requirement is that the strength in compression, flexure, and tension of the repair material should be greater than or equal to that of the substrate. Most repair materials meet this requirement. However, materials having a very high stiffness should be avoided because they can attract undesirable loads to the repair area [8].

Next, the repair material should have nearly the same Young's modulus and coefficient of thermal expansion as the substrate concrete to enable proper stress distribution within the structure. Many polymer concretes are problematic in terms of satisfying this requirement, whereas most Portland cement-based and polymer-modified repair materials meet this requirement [8].

Furthermore, the dimensional stability of the repair material relative to the substrate requires that the repair materials have low autogenous and free drying shrinkage as well as a coefficient of thermal expansion similar to the concrete substrate. Lastly, the repair material and the concrete substrate should be strongly bonded together [8].

Overall, the performance of repair materials is a function of various variables and depends on service/exposure conditions. Therefore, there is no ideal repair material, and the process of choosing the most suitable repair material for a specific application or project is a process of compromise and requires sound engineering judgment.

Table 1.1 General Requirements for Structural Compatibility of Repair Materials [8]

Property	Relationship of Repair (R) to Concrete Substrate (C)
Strength in Compression, Tension and Flexure	R>=C
Modulus in Compression, Tension and Flexure	R~C
Poisson Ratio	Dependent on modulus and type of repair
Coefficient of Thermal Expansion	R~C
Adhesion in Tension and Shear	R>=C
Curing and long-term shrinkage	R>=C
Strain Capacity	R>=C
Creep	Dependent on whether creep causes desirable or undesirable effects
Fatigue performance	R>=C

1.4.2 Critical Properties

A variety of options and considerations should be considered when choosing and evaluating a repair material, including key properties such as compressive strength, modulus of elasticity, thermal expansion, bonding strength, drying shrinkage, creep, and permeability.

A survey conducted by the departments of transportation of nine states identifies the important characteristics and mechanical properties of rapid-setting repair materials. The listed characteristics include setting time; durability (in general); working time; ease of mixing, placing, and finishing; cost; and similarity to the color of the existing concrete. The listed mechanical properties are bond strength to existing concrete, flexural strength, shrinkage, compressive strength, ductility, wear resistance, coefficient of thermal expansion, and modulus of elasticity. It is seen from the rankings that durability and bond strength ranked among the top characteristics [2].

1.4.3 Mechanical Properties

The most important mechanical properties to be considered and evaluated in a repair material are compressive strength, tensile strength, rate of strength gain, modulus of elasticity, setting time, workability, and bond strength.

1.4.3.1 Compressive and Tensile Strength

It is typically expected that the repair material will have a strength at least equal to the substrate. Currently, almost all rapid-setting repair materials satisfy this condition and reach high compressive and tensile strengths in a matter of hours. Yang et al. [7] evaluated the performance of 23 rapid-set prepackaged cementitious materials and reported that most materials showed fast setting, rapid strength development, high 28-day compressive strength, low permeability, and acceptable bond capacity, which are all essential properties for a successful repair. Hence, other aspects related to these high-early-strength materials should be considered as a part of repair material selection and evaluation.

A very crucial issue to be considered in this regard is that the mechanical properties alone, such as compressive and tensile strength, are not enough to determine the suitability of repair materials. For example, materials with high strength and rapid strength development typically exhibit high heat generation, high potential for shrinkage cracking, and high susceptibility to freeze-and-thaw deterioration [2]; thus, high-strength concretes guarantee good performance but also may cause long-term durability concerns.

Some of the interesting findings in recent literature related to compressive and tensile strength are presented as follows:

- Lee and Kim [10] reported that adding a Shrinkage Reducing Agent (SRA) to Latex Modified Concrete (LMC) can improve the compressive strength by 1.7-5.7%.

- Li and Li [11] reported that High-early-strength engineered cementitious composites (HES-ECC) can achieve a compressive strength of 3,422 ± 203 psi and 8062 ± 315 psi in 4 hours and in 28 days, respectively, which enables the repaired structure to return to service in 4 to 6 hours. Also, the tensile strain capacity is 2.5-5% (250-500 times that of normal concrete repair materials).

- Li et al. [12] reported that combining Emulsified Asphalt with Magnesium Phosphate Cement yields many advantages, such as enhancing bond strength, but also adversely affects compressive/flexural strength and abrasion resistance.

- Kastiukas et al. [13] reported that lactic acid at 2% wt. or below improves the strength of Portland/calcium aluminate blended cements (PC/CAC) at earlier ages, but citric acid reduces the strength of PC/CAC by blocking dissolution of cement grains.

- A mix proportion for High-strength, Roller-Compacted, Latex-Modified Rapid-Set Concrete (RCLMC) which achieved a compressive strength of 3,046 psi after 4 hours was proposed by Won et al [15]. The mix contains Type III cement, CSA admixture, and latex.

- Wang et al. [15] reported the development of a black rapid repair fiber concrete (BRRFC) for municipal pavement rehabilitation around manholes, which was found to be a super high-early-strength concrete, allowing the traffic to be reopened after 8 hours.

- A novel, low-cost, durable geopolymer-based rapid repair material (RRM) with a hydrophobic surface and high strength derived from fly ash, ground granulated blast furnace slag (GGBS), and rice husk ash (RHA) was developed by Song et al [16]. With the optimal content of RHA equal to 10%, the RRM yields high early compressive and bonding strength.

- A High-Performance Fiber Reinforced Concrete was developed by Roy et al. They reported that higher curing temperatures result in higher compressive and flexural strength [17].

- A new type of super-lightweight magnesium phosphate cement foamed concrete was developed by Yue and Bing. The authors reported that when all fine sand is replaced by fly ash, the 28-day compressive strength can be increased by 40% [18].

- Ghasemzadeh et al. [19] reported that a combination of pozzolanic materials, silica fume, and slag in the repair concrete improves its mechanical properties.

1.4.3.2 Rate of Strength Gain and Setting Time

As discussed previously, rapid-setting materials are used mainly to finish repair projects so that roads or pavement can be re-opened to traffic in about 4 hours. In order to achieve this goal, the repair material must have a quick set time and a rapid rate of strength gain. Setting time

also plays a vital role in quality control; therefore, the total time required to mix, place, and finish the repair material should be carefully considered. Otherwise, the material becomes hard too soon and a good bond will not be achieved [6].

Ambient temperature is a crucial factor governing the setting time and the rate of strength gain. For example, cold weather extends the setting time. Therefore, the repair materials, which are used on sites that are supposed to be opened to traffic in 4 hours, may not reach the laboratory-achieved 4-hour compressive strength, even after 4 hours. As a result, the low early-age-strength may lead to a premature failure of the repair. Hence, Ram et al. [2] suggested using warm water in cold weather conditions to accelerate hydration and using cold water in hot weather conditions to prevent flash-set of repair materials.

Some of the other important aspects related to the setting time and the rate of strength gain found in recent literature are as follows:

- Li et al. [12] reported that emulsified asphalt is more efficient at extending the setting time than traditional retarders (borax and fly ash)

- Laskar and Talukdar [20] reported the development of an ultrafine slag-based geopolymer repair mortar with an alkali activator composed of sodium hydroxide solution and which has higher setting time, better workability, and superior strength gain. Alkali concentration has a significant role in regulating these properties.

- Yue and Bing [18] reported that their super-lightweight magnesium phosphate cement foamed concrete exhibits high early strength, can be demolded after 3 hours, and develops more than 40% of its 28-day strength within one day.

1.4.3.3 Workability

Achieving the expected strength and durability requires the repair mixture to flow and to be placed with ease. In this regard, a key element of field placement is workability [2]. ASTM C 125 [21] defines workability as “the property determining the effort required to work with a freshly mixed concrete with minimum loss of homogeneity.” Consistency (ease of flow) and cohesiveness (tendency to bleed) are the two components of workability.

An important factor to be considered with respect to workability is the addition of extra water, beyond the manufacturer's specifications, to the repair mixture since many repair materials are very sensitive to excess water. Excess water can adversely affect setting time or cohesiveness, both of which play a significant role in workability. Therefore, this practice should be avoided [2].

Some of the recent findings with respect to workability include:

- Jeon et al. [22] reported that a rapid-setting concrete using ultra fine fly ash (UFFA) combined with calcium hydroxide advanced the workability better than normal fly ash. It also decreased the water/cement ratio of concrete.

- Yue and Bing [18] reported that their super-lightweight magnesium phosphate cement foamed concrete had appropriate workability at water/solid ratio of 0.30.

1.4.3.4 Surface Preparation and Bond Strength

Proper surface preparation of the substrate concrete is the first requirement of an effective repair. Lack of proper surface preparation makes failure of the repair system inevitable. According to Roy et al. [17], a bond surface roughened with only mechanical means results in a better performance. When preparing concrete substrates by means of mechanical removal such as chipping hammers and other impacting devices, and when preparation is not followed by sandblasting or high-pressure water blasting, "a bruised layer of micro-fractured aggregate and crushed mortar can be left at the exposed surface. This results in a plane of weakness just below the bond interface" [23, 24]. Techniques such as wire-brushing, grinding, and light-duty sandblasting may result in short-term bond strengths, but the durability can be compromised [25]. Increasing the surface roughness of the substrate can enhance mechanical interlocking, which is a basic adhesion mechanism. Nonetheless, some problems may arise from the effects of the treatment, especially due to the development of microcracks inside the substrate. Courard et al. [26] have proposed a bond strength estimation and a method for selecting a suitable surface treatment technique by studying the effect of concrete substrate surface preparation for patch repairs.

The performance of repair systems is greatly dependent on how well the repair material is bonded to the substrate concrete, and it is one of the basic performance requirements for repair systems. A good bond ensures composite action between the two layers; therefore, a highly penetrable repair material that can enter the open pores of a substrate is preferred [7]. Bond strength is strongly affected by "adhesion in interface, friction, aggregate interlock and time-dependent factors" [27]. "Adhesion to interface depends on bonding agent, material compaction, cleanness and moisture content of repair surface, specimen age and roughness of interface surface. Friction and aggregate interlock on interface depend on aggregate size, shape and surface preparation" [27]. Bond failure is a key cause of deterioration of pavement repairs, and the shear bond strength between the repair and the substrate is the most important bond performance criteria [2].

There are many different methods used to evaluate bond strength for concrete and repair materials, and the bond strength is significantly reliant on the test method used. Also, rough surface preparation results in a higher bond strength. The most common test methods include the pull-off test, slant shear test, splitting prism test, and the Iowa shear test. Momayez et al. [27] have proposed a new test called the direct shear or bi-surface shear test by comparing different test methods. A summary of each test method is presented next.

Splitting prism test. This test evaluates the bond strength when the repair-substrate interface is in a state of tension and can be a proper indicator of the tensile bond strength [2].

Pull-off test. Similar to the splitting prism test, there is a state of tension at the repair-substrate interface in the pull-off test [27]. The test is done following the ASTM C1583 specification [28], "Standard test method for tensile strength of concrete surfaces and the bond strength or tensile strength of concrete repair and overlay materials by direct tension."

Slant shear test. In this test, the interface between the repair material and the substrate concrete is in a state of combined compression and shear stress [26], and it is carried out based on the ASTM C882 specification [29], "Standard test method for bond strength of epoxy-resin systems used with concrete by slant shear." Slant shear and pull-off tests measure the shear strength from the tensile strength results.

Bi-surface shear test. A state of shear at the repair-substrate interface is the most common state of stress. In the bi-surface shear test, the loads are applied symmetrically, and a state of shear develops in the interface. The test also directly measures the shear strength [27]. Figure 1.4 displays the different setups of the discussed test methods.

The Iowa shear test. This test is typically used to assess the bond strength between asphalt overlays and the concrete substrate and features a state of pure shear at the interface between two layers.

Soliman and Shalaby [30] discussed how the failure mode of bond test specimens can be used to evaluate the bond quality at the repair-substrate interface. A clean failure at the repair/substrate joint signifies a poor-quality bond, whereas failure due to crushing of repair material, concrete, or a combination of the two modes shows a quality bond. They also report bond improvements in materials with wet-dry and freeze-thaw conditioning, which may be due to the ongoing hydration of the cementitious repair materials [30].

1.4.4 Dimensional Compatibility

Repair materials should be compatible; otherwise, they may not act together as expected, as the properties of one material can cancel those of the other. Compatibility is the "balance of

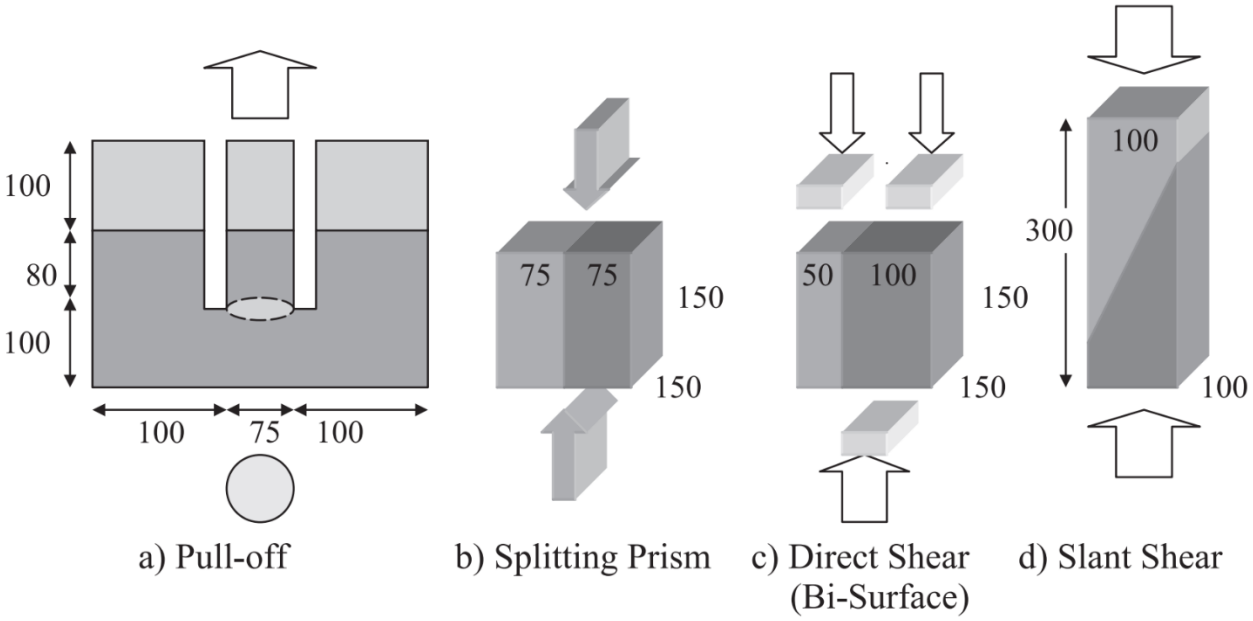

Figure 1.4 Different Setups of Shear Test Methods [27]

physical, chemical, and electrochemical properties and dimensions between a repair material and the existing substrate that will ensure the repair can withstand all the stresses induced by volume changes and chemical and electrochemical effects without distress and deterioration over a designated period of time" [23].

Dimensional compatibility is one of the most important deciding factors in a repair material's performance and is defined as "the ability of the repaired area to withstand volume changes without loss of bond and delamination, and the ability of the repaired area to carry its share of the applied load without distress" [23, 31]. Dimensional compatibility is a common issue in the repair industry. A lot of parameters influence dimensional compatibility, including shrinkage, thermal expansion or contraction, creep properties, modulus of elasticity and Poisson's ratio, geometry of sections, the amount of reinforcing and anchorage, and strain capacity. Any difference in the parameters between the repair material and the substrate concrete can result in dimensional incompatibilities, which can cause premature cracking in the repair material or debonding at the interface since the stresses are not distributed uniformly [2].

Shrinkage, or volume change, of the repair material relative to the substrate is a very crucial property to be considered. Cracking or bond failure can occur if there is a significant difference between the two layers in terms of volume change. The repair materials start to shrink as they lose moisture, but the concrete substrate has a relatively low shrinkage as it is typically aged. As a result, the drying shrinkage of the repair material is restrained by the aged concrete substrate, which could result in tensile stress development and premature failure. In addition to free shrinkage measurements, which are useful for comparing different mixtures, the cracking tendency of the repair material should also be evaluated [2]. The length changes of a hardened cementitious repair mortar or concrete due to drying shrinkage can be measured based on ASTM C157 [32]. The cracking tendency of a repair material under restrained shrinkage conditions can be evaluated using ASTM C1581 [33]. Another shrinkage type to be measured in the cementitious repair materials is called autogenous shrinkage, and it occurs when the cement mortar or paste is cured in a sealed condition and volume change is allowed. Autogenous shrinkage is caused by the reduction of the cement paste due to the hydration process and can result in microcracking, which reduces a material's penetration resistance [34]. It can be measured following the specifications of ASTM C1698 [35].

An important consideration in measuring the drying shrinkage of rapid-setting repair materials is that if the length change measurements started 24 hours after water touched the cement, as ASTM C157 specifies, a substantial amount of shrinkage that has already been developed in the specimen would be missed [36]. Thus, ASTM C928 [37] specifies that for packaged, dry, rapid-hardening cementitious repair materials, the first measurement be taken at 3 to 3.5 hours after water addition. This modification is very important in terms of evaluating materials for rapid repair of concrete, as the repair is expected to be re-opened to traffic after about 4 hours. Ram et al. [7] also suggest that the first shrinkage measurement be taken within 2 hours of water addition since in the rapid-setting repair materials the majority of the hydration process is completed in the first few hours.

Some of the recent findings on shrinkage of repair materials are presented next:

- Yang et al. [36] reported that half of the 23 rapid-set prepackaged cementitious materials investigated for drying and restrained shrinkage had rapid drying shrinkage development within the first week. Also, they observed almost no drying shrinkage for the magnesium phosphate cement–based materials. Sixty percent of the investigated materials had a low 28-day drying shrinkage (less than 0.05%), but 65% of the materials cracked during the restrained shrinkage ring test, indicating that a low shrinkage material does not guarantee proper shrinkage performance. The observed restrained shrinkage cracking mainly depended on the drying shrinkage rate, modulus of elasticity, and creep relaxation of the materials tested. Lower creep coefficient and/or higher modulus of elasticity raised the probability of restrained cracking development. Finally, extending the materials with coarse aggregate reduced both the drying shrinkage and restrained shrinkage cracking of materials.

- According to Hwang and Khayat [38], adding more synthetic fibers to the self-consolidating concrete (SCC) used in repair can reduce its restrained shrinkage cracking potential. Also, a considerable reduction in drying shrinkage occurs due to using a shrinkage-reducing admixture (SRA). Finally, a lower elastic modulus can decrease the cracking potential of SCC at a given level of drying shrinkage.

- Myintlay [39] reported the development of a new approach using digital image analysis to monitor the very early age shrinkage of fresh cementitious materials 30 minutes after adding water to the mixture, and identified the three most significant affecting factors as moisture loss, time of hardening, and W/C ratio. Decreasing the W/C ratio increased the very early age shrinkage. A very substantial reduction occurred in the very early age shrinkage when covering the specimens with aluminum tape. SRA addition also decreased the early age total shrinkage. Also, adding silica fume to the mixture resulted in a higher shrinkage rate. Finally, decreasing the substrate moisture content increased the shrinkage rate.

- Based on early age restrained shrinkage cracking, Richards and Xi [9] found that a higher and quicker temperature profile in repair materials can lead to incompatibility between the repair and concrete substrate. They also suggested testing fracture properties of the repair materials as a compatibility measurement, since higher fracture energy means higher crack propagation resistance.

- Cervo and Schokker [3] reported the coefficient of thermal expansion of bridge deck materials by evaluating shrinkage of bridge deck materials based on ASTM C418 [40].

- Yang et al. [7] reported that when their tested prepackaged repair materials were exposed to harsh environments, the high shrinkage cracking potential could cause premature failure.

- Lee and Kim [10] demonstrated that the suitable amount of Shrinkage Reducing Agent (SRA) was 3% by weight of the binding material. No cracking was observed in their field testing; however, SRA in amounts of over 5% resulted in excessive air content and slump loss.

- Li and Li [11] demonstrated that high-early-strength engineered cementitious composites (HES-ECC) have relatively low Young's modulus and significant resistance to shrinkage-induced microcracking. Microcracks have a self-controlled width below 0.002 inches under restrained shrinkage conditions. Also, the shrinkage strain is below 0.3%, and the

ductility of the material can cause shrinkage deformation by means of developing several microcracks during the strain-hardening stage.

- The shrinkage of nano-modified fly ash concrete to be used as a repair material was investigated by Ghazy and Bassuoni [41]. The material was a mixture of general-use cement, fly ash (class F), commercial Nanosilica sol, and a non-chloride accelerator. Nanosilica increased the autogenous, free, and restrained shrinkage, but adequate curing plus adding 30% fly ash controlled that adverse effect. Also, the moisture loss was reduced by using a curing compound. Overall, most nanomodified fly ash concrete mixtures showed low total shrinkage with adequate curing, despite having higher autogenous shrinkage.

- The effect of latex-solid content on early-age and autogenous shrinkage of very-early strength latex-modified concrete (VES-LMC) was analyzed by Choi and Yun [42]. Cement paste volume governed the autogenous shrinkage of VES-LMC. An increase of latex-solid content increased the total and autogenous shrinkage. Also, total shrinkage occurred very quickly, so that 80% of the maximum shrinkage took place during the first six hours. To minimize early age shrinkage cracking, a minimum of six hours of wet curing was needed.

- Wang et al. [15] observed good drying shrinkage performance and wear resistance in black rapid repair fiber concrete (BRRFC).

- A low-shrinkage, high-early-strength, fiber-reinforced, rapid-set material (HES-FR-RSM) was developed and evaluated by Mansi et al., and it achieved a free shrinkage of less than 300 microstrains [43].

1.4.5 Durability

One of the most challenging aspects of rapid concrete repair is the long-term durability of cementitious materials. Multiple factors affect the durability of repair materials, including chemical compatibility, electrochemical compatibility, permeability compatibility, and dimensional compatibility between the substrate and the repair overlay. In Utah, which has a

relatively harsh climate and cold winters, evaluating the resistance of repair materials to freeze-thaw cycles and deicing salts should be considered. ASTM C666 [44] can be used to evaluate the resistance of repair materials to adverse freeze-thaw effects. Other durability considerations include surface scaling, corrosion, and chloride penetration. Some of the recent findings on the durability of repair materials are presented as follows:

- The abrasion resistance of the repair material by running the test based on ASTM C418 [44] at 3-hours strength (when the bridge is reopened to traffic) was evaluated by Cervo and Schokker [3]. A corrosion test to determine the ability of the repair patch to protect the substrate reinforcement from corrosion was also performed.

- Ram et al. [7] demonstrated that several materials are very sensitive to excessive water addition to the mixture, which can cause a reduction in their freeze-thaw resistance.

- Lee and Kim [10] reported that adding a Shrinkage Reducing Agent (SRA) can ensure the durability of latex modified concrete (LMC). Also, LMC/SRA had high resistance to chloride ion penetration.

- The durability of rapid-strength concrete produced with ettringite-based binders was investigated by Moffat and Thomas [46]. They reported that the chloride permeability of calcium sulfoaluminate belite was the lowest among the evaluated non-proprietary repair materials.

- Song et al. [16] reported that a complete surface hydrophobic modification resulted in higher chloride permeability, freeze-thaw resistance, and surface abrasion resistance.

- Jeon et al. [22] reported that ultra-fine fly ash can significantly increase the chloride ion penetration resistance of concrete.

- Moffatt and Thomas [47] observed an increased resistance to chloride ion penetration in Portland cement combined with CSA cement.

- Ghasemzadeh et al. [19] reported that silica fume was more effective than slag in terms of durability.

- Maler et al. [48] reported that CSA cement had a weak frost resistance.

One of the interesting emerging methods for repairing spall damage to concrete roads is utilizing the 3D printing technology, as studied by Yeon et al. [49]. The repair time is 2 hours, and the associated indirect losses can be reduced from $140,000 to $1,700. Also, currently available adhesives can handle 91% of the shear stress on this type of concrete patch, but further evaluation is needed. The repair steps are as follows:

1. Photographing the spall damage,
2. Turning that information into a 3D model using photogrammetry,
3. Printing the result as a plastic formwork using a 3D printer,
4. Fabricating a concrete patch using this formwork, and
5. Gluing that patch to the surface of the spall damage [49].

1.4.6 Performance Evaluation and Field Testing

Although numerous rapid-set repair materials are on the market, the lack of reliable information on how these materials behave in the field makes it difficult for repair professionals to decide which material is more suitable. Conventionally, the selection is made based on the material's data sheet provided by the manufacturer; however, these data sheets are often insufficient and sometimes misleading. For example, some materials are called "high-performance," but after undergoing severe exposure, they display premature deterioration. As a result, research is needed to systematically assess the performance-related properties of rapid-set prepackaged materials with the goal of thoroughly understanding their compatibility with field concrete.

It has been shown that satisfying performance and quality requirements in controlled laboratory conditions does not necessarily guarantee a decent field performance, as in most cases the properties of materials mixed on site are not consistent [2]. Richards and Xi [9] observed that the major issues in repairs are quality control and workmanship, both dictating the field performance of the repair, along with construction-related issues (consolidation and finishing).

Also, laboratory samples are made in several small batches since these materials set so quickly that making a single large batch would not be feasible. Hence, the water content and other mixing and pouring conditions could diverge, and even small differences in water content may cause a substantial impact on the material properties. This can be the reason why the mechanical properties obtained in the lab are sometimes lower than those provided by the manufacturers. These differences can be more significant in the field, increasing the difference between material performance in the laboratory and in the field [2].

The difference between controlled laboratory conditions and on-site conditions was also studied by Ram et al. [2]. While the mixes produced in the laboratory consistently showed acceptable performance, mixes produced on site were more variable. The reasons were "changes in the amount of aggregate extension used, moisture content of the aggregates, amount of water added and ambient temperature conditions." The researchers also found the uncertainties associated with the mixtures developed on site to be due to the amount of aggregate extension and amount of mix water added, deviations from recommended mix proportions (often to address the material's poor workability), rate of strength gain, and freeze-thaw resistance. To improve the uniformity of the field installations, they suggested "accounting for moisture content of the aggregate during the batching process and using calibrated buckets to control the amount of water and aggregates added into each mix" [2].

1.5 Objective

The objective of this research project is to evaluate eight commercial cementitious rapid repair materials for application to concrete bridge decks in Utah.

1.6 Scope

The scope of this research project is to identify and evaluate commercially available cementitious repair media for concrete bridge decks in Utah. Extensive laboratory studies to quantify the mechanical performance and durability properties of the repair materials have been performed. These laboratory tests include setting time, compressive strength, static modulus of elasticity, splitting tensile strength, surface electrical resistivity, slant shear bond strength,

autogenous shrinkage, drying shrinkage, and restrained ring shrinkage. Field performance of the materials has also been investigated.

1.7 Outline

This document is organized in five sections. A brief description of these sections is as follows:

Introduction: This section presents the background and significance of this research. A compilation of the existing literature discusses the past development and current significant research work undertaken by various researchers, the material selection process, and performance criteria. Finally, the section states the objective and scope of this work.

Experimental Procedure: This section presents a compilation of all the experimental methods, standards, and specifications pertaining to the project. A comprehensive description of the test methods, testing equipment, description, and required modification of standard testing and specimen preparation are discussed in detail.

Laboratory Results: The third section covers the laboratory results for mechanical and durability performances for the selected repair material.

Field Performance of Selected Repair Materials: The field performance of the repair materials is presented in the fourth section.

Conclusions: A summary of test results, a conclusion based on the experimental and fieldwork, and final recommendations are described in the fifth and final section of the report.

In addition to the abovementioned sections, a list of all the references cited in this document and an appendix with some test data, field pictures and repair information, and product information are included at the end of this document.

2.0 EXPERIMENTAL PROCEDURE

2.1 Introduction

In this section, the properties of the selected rapid repair materials as well as their mixing procedures are presented first. Then, the mechanical and durability testing methods, including casting of specimens and procedures for running the tests and taking measurements, are explained in detail.

2.2 Material Properties

After consulting UDOT-authorized product lists along with reviewing DOT and FHWA documents and related literature, eight proprietary rapid-setting repair materials from five different manufacturers were selected for evaluation. Four materials were pre-packaged mortars, while the rest were already extended with coarse aggregates. Among the mortars, material P4 was extended 100% by weight with locally available pea gravel. The maximum and nominal maximum sizes of the pea gravel used for extension were 0.5 inch (12.7 mm) and 3/8 inch (9.53 mm), respectively, with a specific gravity of 2.68 and absorption of 1.02%. The gradation curve of the pea gravel used is shown in Figure 2.1. All materials were cement-based and one-component. None of the materials contained Magnesium Phosphate, which is specifically excluded by UDOT. The reported properties and characteristics of the selected materials are presented in Table 2.1. Additional product information is given in Appendix C.

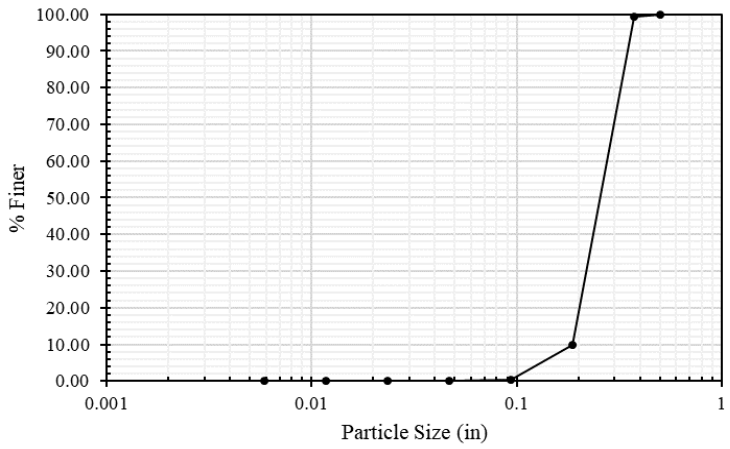

Figure 2.1 Gradation Curve of the Pea Gravel Used for Aggregate Extension of Material P4

Table 2.1 Summary of Properties and Characteristics of Selected Repair Materials Reported by Manufacturers

Property	Product							
	P1	**P2**	**P3**	**P4**	**P5**	**P6**	**P7**	**P8**
Base	Cement	Cement	Cement	Cement	Cement	Cement	Cement	Cement
One Component	Yes	Yes	Yes	Yes	Yes	Yes	Yes	Yes
Contain Fiber?	Yes	No	No	No	Yes	No	No	Yes
Weight of Bag, lbs.	53.5	65	65	55	60	50	50	50
Approximate Cost/Bag	$39	-	$15	$25-30	-	$22-25	-	$20
Primer Required?	No	-	No	No	-	No	-	No
Pre-Extended?	Yes	Yes	Yes	No	Yes	No	No	No
Yield/Bag, ft^3	0.40	0.5	0.5	0.5	0.42	0.43	0.43	0.42
Yield/Bag – Extended, ft^3	-	-	-	0.7 (60%) 0.9 (100%)	-	0.57 (50%) 0.77 (100%)	0.57 (50%) 0.77 (100%)	0.6 (60%)
Required Water/Bag, L	1.89	2.4	2.6+0.24	2.8-4.3	2.8-3.3	2.6	2.6	3.07
Ambient Temp. for Mixture, °F	40-120	> 45	> 40	45-90	45-90	> 40	> 50	> 40
Mixing Duration, min	7	3	3 (max)	1-3	3 (max)	3-5	3-5	2-3
Working Time, min	Varies	-	-	10-25	15-20	8	25	-
Setting Time								
Initial, min	20-25	40-50	-	-	-	16	50	15-20
Final, min	30-40	50-60	-	-	-	28	80	25-30
Compressive Strength (ASTM C39), psi				**(C109)**			**(C109)**	**(C109)**
1 Hour	-	-	-	3300	-	-	-	2000
2 Hours	> 2500	2500	3000	-	3000	-	-	-
3 Hours	-	3000	-	5000	-	-	3000	3500
24 Hours	> 5000	5000	4500	7000	4500	-	4000	5200
7 Days	> 7000	6000	6000	7500	6000	-	-	6500
28 Days	> 9000	7500	6500	9500	6500	7400	8000	7500
Modulus of Elasticity (ASTM C469), 10^6 psi								
7 Days	-	-	-	4.4	-	-	-	-
28 Days	5.41	-	-	5.1	3.6	4.4	4.6	-
Splitting Tensile Strength (ASTM C496), psi								
24 Hours	-	400	-	-	-	400	400	-
7 Days	-	600	-	700	-	-	-	-
28 Days	> 500	-	650	900	300	450	450	-
Length Change (ASTM C157), %								
7 Days	-	-	-	-	0.015	-	-	-
28 Days	< 0.035	< 0.06	0.016	0.08	0.035	0.05	0.05	0.11
Slant Shear Bond Strength (ASTM C882), psi								
24 Hours	> 1500	2500	1700	1500	1700	2300	2300	2000
7 Days	> 2000	3000	2300	2000	2300	-	-	2750
28 Days	-	-	3000	-	3000	2600	2600	-

2.3 Mixing and Casting Procedures

The proportionating of materials was done based on each material's product data sheet provided by the manufacturer. A rotating drum mixer with a capacity of 3 $ft.^3$ was used to mix the materials in the laboratory.

Manufacturers' instructions were strictly followed for mixing and casting of each product in the laboratory. Typical steps were as follows:

1. Precondition the materials to 70 °F; This is achieved through storing the product bags at the lab with a controlled temperature of 70 °F.
2. Rinse the mixer with water followed by removing any excess (puddled) water from the mixer.
3. Place water into the mixer (some or all of the required amount of water, depending on the manufacturer's recommendation).
4. (For material P4 only) Add the pea gravel.
5. Start the mixer.
6. Slowly add the cementitious repair material.
7. Mix for a time specified by manufacturer.
8. Add the remaining water (if any).
9. Mix for a time specified by manufacturer.
10. Pour the contents into container and start casting the specimens.
11. Clean mixer or repeat process for next batch.

Using a stopwatch, the time at which water touched cement was recorded to keep track of the age of specimens. Careful attention was made to not add extra water to the mixture more than the amount required by the manufacturer. Mixtures were visually inspected during and after

mixing to ensure a uniform consistency was achieved. Safety measures were taken during the process, including using eye protection, a mask, and gloves.

Specimens were cast in accordance with the specifications of ASTM C192 and the corresponding ASTM specifications for each test. The 4×8 in cylinders for compression, splitting tension, and elastic modulus tests were prepared by pouring the fresh mixture in two lifts with 25 times rodding per layer and 10-15 times tapping. However, this was not feasible with materials of very low working time (very quick setting time), since 36 cylindrical specimens were to be prepared per material. Therefore, in such cases, external vibrating for 10-15 seconds using a vibration table was performed to consolidate the specimens.

Once cast, cylindrical specimens were labeled, tightly capped to limit moisture loss, and immediately transferred to a moist curing environment meeting the specifications of ASTM C192.

Specimens prepared for the drying shrinkage test were covered with layers of plastic to avoid moisture loss and immediately moved to a temperature-controlled room (23±2 ˚C) with RH of 50±5% to be air-cured.

2.4 Testing Procedure

The mechanical and durability properties of the selected repair media were investigated through a robust laboratory study. The testing program along with the procedure for collecting data is explained in the following sections.

2.4.1 Testing Program

The following tests, tabulated in Table 2.2, were performed on each repair medium at early ages (~4 hours) through 28 days.

Table 2.2 Testing Program and the Specimen Type for Each Test

Test	Code	Specimen Type	Number of Specimens	Specimen Age				
				Final Set	4 h	24 h	7 d	28 d
Compressive Strength	ASTM C 39	4×8 in Cylinder	12		✓	✓	✓	✓
Splitting Tensile Strength	ASTM C 496	4×8 in Cylinder	12		✓	✓	✓	✓
Static Modulus of Elasticity	ASTM C 469	4×8 in Cylinder	12		*	*	*	*
Surface Resistivity	AASHTO TP 95	4×8 in Cylinder	This test is done on every cylinder before performing other tests at each age.					
Setting Time	ASTM C 403	6× 6 in Cylinder	2	✓				
Autogenous Shrinkage	ASTM C 1698	185 mL Tube	3	✓				
Drying Shrinkage	ASTM C 157	3×3×16 in Prism	6		✓	✓		
Restrained Ring Shrinkage	AASHTO T 334	6×6 in Ring	2		✓	✓		
Bond Strength (Slant Shear)	ASTM C 882	4×8 in Cylinder	9		✓	✓		✓

2.4.2 Compressive Strength Test

All the compression test procedures are performed according to ASTM C39 [50]. Three samples at each specimen age (i.e., 4 hours, 24 hours, 7 days, and 28 days) were tested at the

Figure 2.2 Compressive Strength Test Setup

recommended loading rate of 352-528 lb./s. Cylinders were capped with neoprene caps in accordance with the specifications of ASTM C39 prior to testing. The average strength of the three samples was reported as the compressive strength of that particular material at that age. Figure 2.2 shows the compression test setup. The testing machine is FX-600F/LA-270 from FORNEY.

2.4.3 Splitting Tensile Strength Test

Splitting tensile strength was evaluated in accordance with the specifications of ASTM C496 [51]. Three samples at each specimen age (i.e., 4 hours, 24 hours, 7 days, and 28 days) were tested. The test setup is shown in Figure 2.3. The test was conducted using the Instron universal testing machine. This machine was controlled by a computer software, so various testing procedures could be inputted into the system and the tests could be done automatically. It should be noted that splitting tensile strength is known to underestimate the tensile strength of concrete compared to direct tension or flexural testing [52].

2.4.4 Static Modulus of Elasticity Test

The static modulus of elasticity was evaluated in accordance with the specifications of ASTM C469 [53]. Three cylindrical specimens were tested for each product at each age using

Figure 2.3 Splitting Tensile Strength Test Setup

Figure 2.4 Static Modulus of Elasticity Test Setup

the same loading machine as the compressive strength test. Each cylinder was fitted with an axial compressometer in order to record their axial deformation corresponding to the desired compressive loads. Then, the specimens were loaded in uniaxial compression to a stress of approximately 40% of the compressive capacity. The compressive capacity was defined as the average of three compressive strength values obtained from the compressive test. In other words, at each age, the compressive strength test was performed first, and the average compressive capacity was obtained. Then, the static modulus of elasticity test was performed. The modulus of elasticity was calculated as the chord modulus according to ASTM C469 Eq. 3. The static modulus of elasticity test setup is shown in Figure 2.4.

2.4.5 Surface Electrical Resistivity Test

The surface electrical resistivity test uses the Wenner method to measure surface electrical resistivity of concrete. This test was performed according to Standard Method of Test for Surface Resistivity Indication of Concrete's Ability to Resist Chloride Ion Penetration [54]. A

low frequency alternating current (AC) goes through the two outer probes and the drop in voltage is measured by the two inner probes.

The testing apparatus, Surf by GIATEC SCIENTIFIC, is shown in Figure 2.5. Before each test, a little amount of conductive gel was applied on each probe so the probes could connect better to the surface of the cylinder. The apparatus calculates the resistivity in four perpendicular directions, averages all the measurements, and provides one resistivity value. This test was performed on each cylindrical specimen at all ages before performing the three previously described tests. Table 2.3 shows the relation of chloride penetrability classification and surface electrical resistivity at 23°C.

Figure 2.5 Surface Electrical Resistivity Test Setup

Table 2.3 Relation between Surface Resistivity and Chloride Penetrability at 23°C [55]

Chloride Penetration	Resistivity (kΩ.cm)
High	<10
Moderate	10-15
Low	15-25
Very low	25-200
Negligible	>200

2.4.6 Setting Time Test

Setting time of mortar (neat) specimens was determined by Acme penetration resistance in accordance with the specifications of ASTM C403 [56]. The Acme penetration resistance test estimates the setting times of mortar sieved from fresh concrete mixtures. Initial setting time

Figure 2.6 Setting Time Test Apparatus

Figure 2.7 Drying Shrinkage Test Specimens and the Length Comparator

corresponds to penetration resistance of 500 psi; final setting time corresponds to penetration resistance of 4000 psi. The penetration resistance was measured using various needles at different times until each mixture reached its final set.

After mixing, the fresh mortar was poured into 6× 6-in. cylindrical molds and then, based on the working time of each material, either externally vibrated for about 15 seconds or rodded for consolidation. Typical set up for this test is shown in Figure 2.6.

2.4.7 Drying Shrinkage Test

Drying shrinkage of six 3×3×16-in. specimens of each material was measured in accordance with the specifications of ASTM C157 [32]. The casting of the prisms was done in two lifts, with consolidating using a vibration table after each lift. Three specimens were demolded at an age of 4 hours (per specifications of the ASTM C928 [37]), and three were demolded at 24 hours. Their length change was measured using a standard-length comparator along with a reference bar (Figure 2.7). To capture the full-length change behavior of the materials, several length measurements in time intervals as short as 10 to 30 minutes were

carried out in the first 6 hours or so after demolding, followed by daily and then weekly measurements for up to 28 days.

Specimens were air-cured by immediately being transferred to a temperature-controlled room with 23±2 ˚C temperature and 50±5 % RH. Before demolding, the specimens were covered with plastic sheeting to avoid moisture loss. In addition to being covered by plastic, the top surface of the specimens made with materials P4 and P5 were constantly sprayed with water for an hour after being moved to the curing room, thus keeping the top surface from drying out. This was done per manufacturer's request. The change of length due to drying shrinkage was calculated according to ASTM C157 Eq. 1.

2.4.8 Autogenous Shrinkage Test

For each material, autogenous shrinkage was measured in accordance with the specifications of ASTM C1698 beginning at the time of final set (as determined by performing the setting time test on a specimen made out of the same batch) and using three replicate specimens. Specimens were stored in the same conditions as the drying shrinkage test specimens.

It should be noted that, considering the very short working time of the materials, sieving the materials pre-extended with aggregates into mortar was not feasible. Therefore, the autogenous shrinkage test was not performed on the materials containing aggregates and fibers

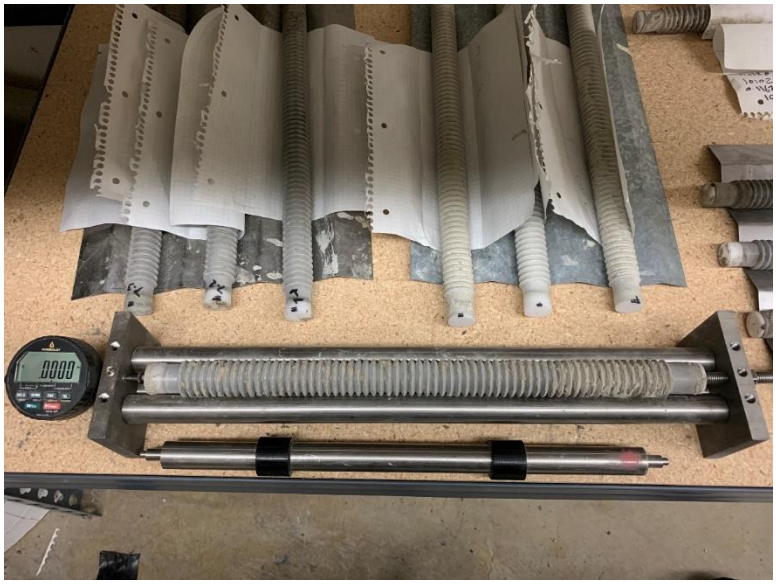

Figure 2.8 Autogenous Shrinkage Test Specimens and Measuring Device

(this is discussed later). The testing apparatus along with the reference bar can be seen in Figure 2.8.

2.4.9 Restrained Ring Shrinkage

The resistance to cracking due to restrained shrinkage was evaluated by the restrained ring shrinkage test, performed in accordance with the specifications of AASHTO T 334 [57]. This test determines the average time to cracking under restrained shrinkage conditions. The restrained shrinkage ring test setup is shown in Figure 2.9. The standard requires 24 hours of curing and then demolding the specimens, but since repair media were expected to perform well at early age, the test method was also modified to begin at the age of 4 hours. Therefore, two ring specimens were prepared for each material. One was demolded at 4 hours, and the other was demolded at 24 hours.

Figure 2.9 Restrained Ring Shrinkage Test Specimens Connected to the Data Acquisition System

Four equally-spaced strain gauges of 350 Ω resistance, compatible with the data acquisition system, were installed on the inner surface of each ring and were protected by applying liquid coating followed by butyl rubber sealant. Strain measurements were recorded every 10 minutes on a Campbell Scientific CR1000 datalogger. For each ring, the measurements and monitoring the crack development were continued for two weeks after cracking.

Circular wooden plates were also prepared to further protect the strain gauges and wires at the time of pouring and casting specimens. To prevent the constraint by the contact between the bottom surface of the concrete ring and the base form, the two surfaces were separated by a layer of plastic sheeting. For each ring, the pouring was done in three lifts, with 75 times rodding per lift to consolidate the specimen. The base form was tapped a couple of times after all three lifts were finished.

Specimens were transferred to the temperature-controlled room immediately after casting. Then, the tie-downs of the steel ring were released, and the strain gauges were connected to the data acquisition system to begin monitoring. To prevent moisture loss from the top surface of the concrete ring, a sheet of rubber mat was pressed over the surface using silicon caulk. To prevent any corrosion caused by applying the caulk, the steel rings were protected by spraying urethane coating. Similar to the drying shrinkage, the top surface of the specimens made from materials P4 and P5 were constantly water sprayed for an hour after being moved to the curing room while being covered by plastic. For these specimens, the rubber mat was installed after water spraying was finished.

2.4.10 Bond Strength Test (Slant Shear)

Bond strength of the repair materials to the substrate concrete was measured by performing the slant shear test in accordance with the specifications of ASTM C882 [29] and modified by ASTM C928 [37] for rapid setting repair media. UDOT requirements for the slant shear test [58] were considered and applied. For each material, nine 4×8 in cylindrical specimens were prepared and tested at ages of 4 hours, 24 hours, and 28 days (three specimens at each age). The substrate concrete mix design is presented in Table 2.4 and was supplied by Geneva Rock Products, a ready-mix concrete supplier in Logan, Utah. The design strength was 5,000 psi.

Substrate concrete cylindrical specimens were water cured for at least 28 days and then saw cut at a 45° angle through the long axis into two equally-sized sections, per UDOT recommendation. The saw cutting setup is displayed in Figure 2.10. Before casting, the slant surface of the substrate was pre-wet, and the fresh repair material was then poured on top of it. The composite specimen was then rodded for consolidation followed by capping and being moved to the curing room to be moist cured.

Figure 2.10 Saw Cutting Setup for Slant Shear Test

Figure 2.11 Slant Shear Bond Strength Test Setup

The testing machine and procedure for running the slant shear was the same as the compressive strength test. The peak load at failure and the failure mode were recorded. The bond strength was calculated by dividing the peak compressive load by the eclipse area (0.7854 times long diameter times short diameter of the cylinder). The slant shear test setup is shown in Figure 2.11.

Table 2.4 Substrate Concrete Mix Design for the Slant Shear Test

Material Type	Description	Design Quantity	Specific Gravity	Volume (ft^3)
Cement	CEMENT TYPE II-V	564 lbs.	3.15	2.87
Fly Ash	TYPE F FLY ASH, ASTM C 618	141 lbs.	2.30	0.98
Coarse Aggregate	ROCK - 3/4" X #4 WASHED	1689 lbs.	2.58	10.49
Fine Aggregate	SAND - WASHED CONCRETE	1044 lbs.	2.60	6.43
Water	POTABLE WATER	33.8 gal	1.00	4.52
Admixture	AIR ENTERING ADMIXTURE - ASTM C260	19 lq. oz.	--	--
Admixture	WATER REDUCER - ASTM C494 TYPE A, D	21 lq. oz.	--	--
	Air Content	6.30 %	--	1.70
	Yield	3720 lbs.	--	27.00

3.0 LABORATORY RESULTS

3.1 Introduction

In this section, the results and the data gathered through conducting mechanical and durability tests in the laboratory are presented. The tests include setting time, compressive strength, splitting tension strength, static modulus of elasticity, slant shear bond strength, surface electrical resistivity, autogenous shrinkage, drying shrinkage, and restrained ring shrinkage. For each test, the performance of the selected rapid repair materials is discussed and compared using plots and tables. At the end of the section, a summary of the properties evaluated in the laboratory study phase is provided.

3.2 Setting Time

As discussed in the previous section, the initial and final setting times of the selected repair media are measured through the penetration resistance test using a penetrometer manufactured by Humboldt. The initial setting time is almost the end of the workability time, and the final setting time is the point at which the mixture, now fully hardened, starts rapid strength development. Therefore, the setting time is a critical measurement that needs to be considered. The repair materials evaluated in this study showed varied setting times which can be generally categorized in three categories, namely flash set, quick set, and normal set [7]. A flash set material hardens in less than 10 minutes, while a quick set material starts to get rigid within 10 to 45 minutes and is fully rigid before 1 hour after water addition. On the other hand, a normal set material is workable for at least 45 minutes and becomes rigid in 1 to 3 hours after the addition of water. It should be noted that the accuracy of the setting time measurement is affected by several factors, including material and ambient temperature. All setting time measurements in this study were taken at room temperature, which was about 72°F, and are tabulated in Table 3.1 along with the type of setting category. Also, the measured setting times are graphically compared in Figure 3.1.

Based on Table 3.1 and Figure 3.1, which show the measured initial and final setting times for each repair material, there are no materials that can be categorized as flash set.

Table 3.1 Initial and Final Setting Time of Rapid Repair Materials

Product	Initial Set (min)	Final Set (min)	Time between Initial and Final Set (min)	Setting Category
P1	35	50	15	Quick
P2	72	113	41	Normal
P3	24	28	4	Quick
P4	23	32	9	Quick
P5	30	45	15	Quick
P6	24	30	6	Quick
P7	65	87	22	Normal
P8	25	28	3	Quick

The initial setting times for all materials are between 20 and 35 minutes, except for materials 2 and 7. Both materials 2 and 7 have an initial setting time of more than one hour, and therefore can be categorized as normal set. All other materials become fully solidified in less than an hour, and therefore can be labeled as quick set. Material 4 has the lowest initial setting time (23 minutes), while for material 2 reaching the initial set time took 72 minutes. In other words, materials 4 and 2 have the lowest and the highest working time, respectively. Similarly, materials 2 and 7 are the only materials with a final setting time of more than an hour. For all other materials, the final setting time is measured between 30 to 50 minutes. Here, materials 3 and 8 have the lowest final set time (28 minutes). For material 2, becoming fully rigid took about 2 hours, similar to a conventional high-early-strength concrete.

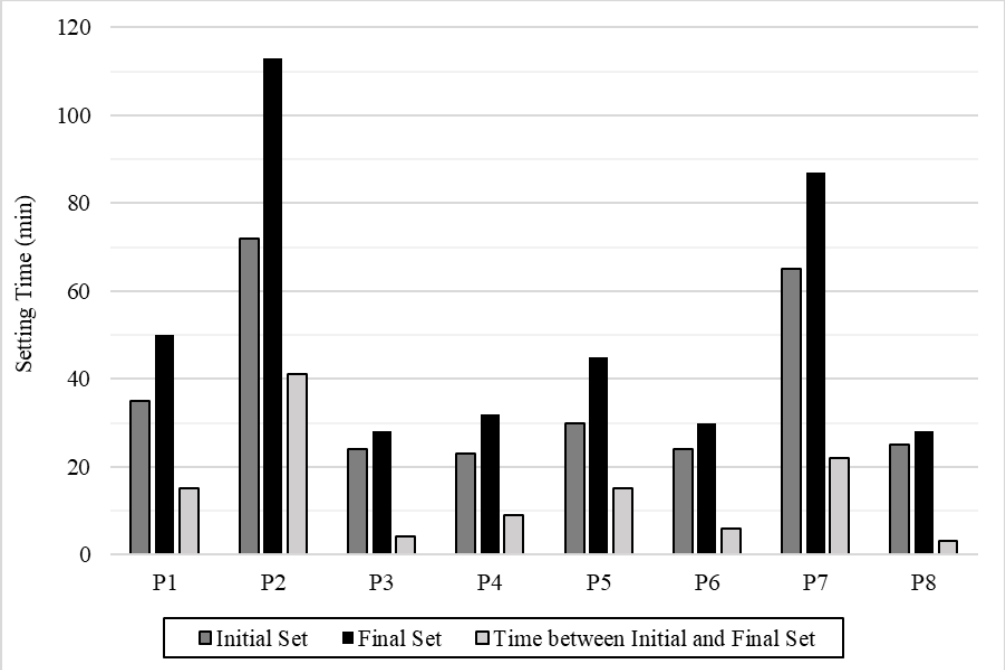

Figure 3.1 Initial and Final Setting Time of Rapid Repair Materials

The time between the initial and final set for most of the tested materials (75% of materials) is around 5 and 15 minutes. For materials 2 and 7, which have the highest initial and final setting time, reaching the final set is relatively gradual and took 20 to 40 minutes. Most materials started to gain strength rapidly, commonly in less than 45 minutes.

The ability to set very fast is desired in terms of reducing the lane closure, but this also limits the placing and finishing time. Materials with a very rapid setting time (materials 3, 4, 6, and 8) are not suitable for large repair areas. When using these kinds of materials, the size and quantity of batches should be small. Also, the placing, compacting, and finishing should be done very quickly. In contrast, materials that set slower (materials 2 and 7) are desired for large repair areas and high ambient temperatures. It should be noted that all materials generated considerable heat upon setting and strength gain.

3.3 Compressive Strength

Repair often takes place at night to avoid interference with traffic and is typically done in 8 hours. About half of this time is needed for surface preparation, therefore mixing, placing, finishing, and curing of the repair material should be done in 4 hours. That is why the mechanical performance at the age of 4 hours is considered critical by UDOT. Gaining a compressive strength of >3,000 psi in 4 hours is desired to ensure the repaired area can be opened to the traffic and carry the loads. The long-age strength is also important in terms of compatibility and durability performance, and a 28-day compressive strength of >5000 psi is expected considering the typical compressive strength of substrate concrete. Therefore, the required or target compressive strength for rapid repair materials evaluated in this project is considered as 3,000 psi in 4 hours, 4,000 psi in 24 hours, 5,000 psi in 7 days, and >5,000 psi in 28 days and beyond. It should be noted that these performance criteria also match the compressive strength requirements set by ASTM C928 [37].

Moreover, a system of classification proposed by the Strategic Highway Research Program (SHRP) was adopted to categorize the selected rapid repair media based on the rate of compressive strength development. In this classification, a material able to develop a compressive strength of at least 3,000 psi in 4 hours is named very early strength (VES). A high

early strength (HES) is a material gaining at least 5,000 psi compressive strength in 24 hours, and finally materials developing a strength of over 10,000 psi in 28 days are labeled as very high strength (VHS) [7]. Table 3.2 presents the average compressive strength of all eight repair materials corresponding to different ages, along with their SHRP classification.

Table 3.2 Average Compressive Strength of the Repair Materials at Different Ages

Product	Average Compressive Strength (psi)				SHRP Category
	4 Hours	24 Hours	7 Days	28 Days	
P1	5,067	6,334	9,442	10,942	VES, HES, VHS
P2	5,106	6,044	9,876	10,966	VES, HES, VHS
P3	3,065	4,088	4,967	8,573	VES
P4	4,709	7,050	7,971	8,266	VES, HES
P5	5,238	6,880	7,356	8,490	VES, HES
P6	5,545	6,600	7,781	8,747	VES, HES
P7	5,611	5,854	6,382	7,893	VES, HES
P8	5,293	5,660	5,956	6,879	VES, HES

VES: Very early strength
HES: High early strength
VHS: Very high strength

Based on Table 3.2, all materials satisfy the required compressive strength at very early ages, with the minimum and maximum at 4 hours being about 3000 psi and 5600 psi, respectively. Thus, all materials fall into the VES category. Also, all materials, except for material 3, can be classified into HES category as their 24-hour strength is more than 5,000 psi. However, all materials meet the target strength at 24 hours, which is 4,000 psi. This is also true for target strength at 7 days, since all materials have at least 5,000 psi. The late-age compressive strength of all materials is also desirable (between 6,800 and 11,000 psi). The only materials that can be labeled VHS are materials 1 and 2. It should be noted that SHRP classification is helpful in terms of deciding on the repair volume and speed. VES materials quickly develop enough strength and they're a good choice for a small repair area, while HES allows for the pavement to be reopened to traffic in 24 hours. When there is a substrate with a high compressive strength, a VHS material will be a preferred choice, but it should be considered that with high strength comes higher risk of shrinkage-induced cracking and related problems. Another important thing to be discussed is the rate of strength development, which is shown in Figure 3.2.

As illustrated in Figure 3.2, all of the tested materials satisfy the project-required compressive strength. Different strength development behaviors can be observed in Figure 3.2. Materials 1, 2, and 3 develop not only a noticeable compressive strength at early ages (more than 1,000 psi from 4 to 24 hours), but also significantly and continuously gain strength after 24 hours. In these three materials, the late-age compressive strength (at 28 days) is nearly twice their 24 hours' strength. Materials 1 and 2 also have the highest 7 and 28-days strength among all materials. This could be due to the noteworthy hydration potential remaining in these materials after setting rapidly and quickly and also indicates a desirable performance in terms of compressive strength at both early and late ages.

Conversely, materials 7 and 8 have a low strength gain at early ages and also insignificant strength development at late-ages, but still meet the project strength requirement very well. Materials 4, 5, and 6 show a considerable strength gain at early ages (about 1,500 to 2,000 psi increase), but the rate of strength gain beyond 24 hours in these materials is not as high as materials 1, 2, and 3. Nevertheless, materials 4, 5, and 6 show desirable compressive strength gain and performance at both early and late ages. Another observation is that the difference between the compressive strength of all materials increase with their age. It can be seen in Figure 3.2 that the data points at 4 hours are somewhat concentrated and close together, but with the increase in age, they keep being separated and widened. Overall, all repair materials can be

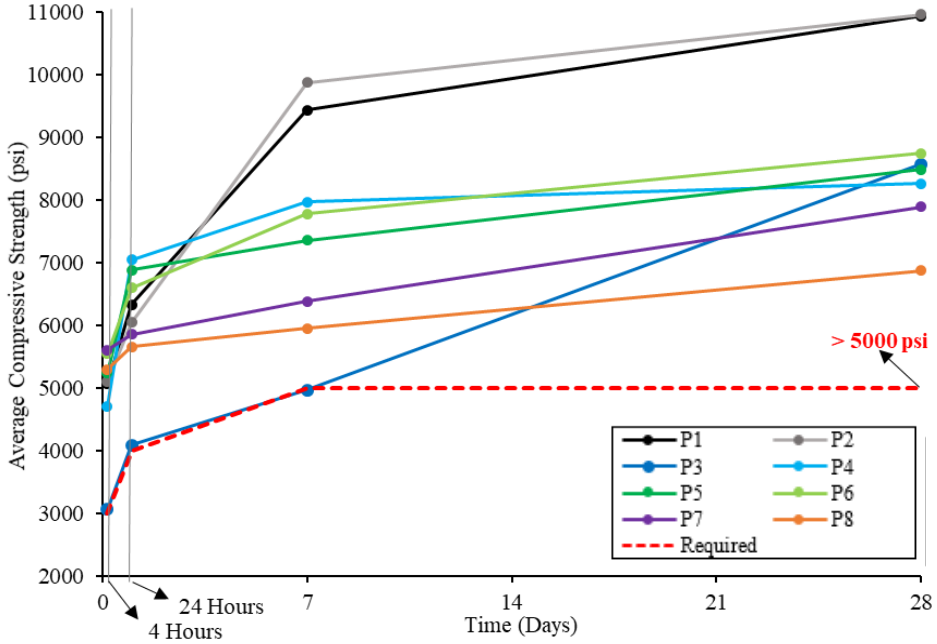

Figure 3.2 Rate of Compressive Strength Development for the Selected Repair Materials

exposed to traffic after 4 hours and meet the requirement of long age strength being equal to or greater than that of the substrate.

Finally, a linear regression model for predicting and calculating the compressive strength as a function of time can be developed for each material and is presented in Table 3.3. Obviously, these equations can only be used if the mixing, casting, and curing conditions are the same as this study. It can also be seen that the R^2 value for most of the equations is more than 0.95, which shows satisfactory correlation. It should be noted that parameter t represents time in days, and can be between 0.167 and 28. Also, f_c' is compressive strength in psi.

Table 3.3 Regression Models for Predicting Compressive Strength (f_c') as a Function of Time (t)

Product	Regression Equation	Correlation (R^2 Value)
P1	$f_c' = 1198.5\ln(t) + 6901.5$	0.979
P2	$f_c' = 1243.3\ln(t) + 6914.5$	0.9496
P3	$f_c' = 182.07t + 3527.2$	0.9758
P4	$f_c' = 678.4\ln(t) + 6407$	0.8886
P5	$f_c' = 587.43\ln(t) + 6479$	0.9506
P6	$f_c' = 621.52\ln(t) + 6626.5$	0.9987
P7	$f_c' = 78.347t + 5726.7$	0.9901
P8	$f_c' = 50.819t + 5487.5$	0.9495

f_c': Compressive strength in psi
t: Time in days, $0.167 \leq t \leq 28$

3.4 Static Modulus of Elasticity

Modulus of elasticity is an indicator of the stiffness of a material, and one of the general requirements for the structural compatibility of repair materials is having a modulus of elasticity close to that of the substrate concrete [8]. If the substrate is assumed to be a typical, normal-weight concrete bridge deck with a nominal compressive strength of 5 ksi, then its modulus of elasticity is around 4000 ksi. Considering that a concrete deck that needs to be repaired has an age of a few years, its modulus of elasticity will be more than 4000 ksi. Therefore, an elastic modulus of 4,000 to 5,000 ksi can be considered as the desired range. The average elastic modulus of the rapid repair materials at different ages are tabulated in Table 3.4.

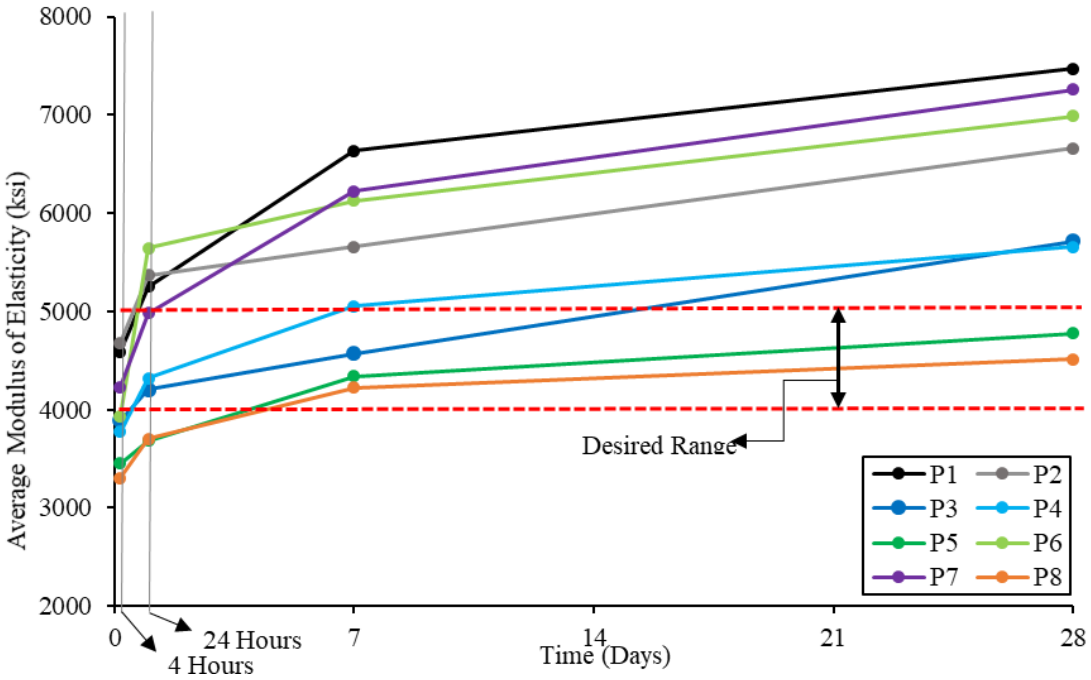

Figure 3.3 Rate of Elastic Modulus Development for the Selected Repair Materials

Based on Table 3.4, the elastic modulus of the selected rapid repair materials at the time of exposure to traffic (4 hours) is between 3,300 and 4,700 ksi. Materials 8 and 2 have the lowest and the highest modulus of elasticity at 4 hours, respectively. At this age, only three materials (1, 2, and 7) have a modulus of elasticity of over 4,000 ksi. At late-ages (28 days), the selected repair materials showed a modulus of elasticity of 4,500 to 7,500 ksi, with materials 8 and 1 having the lowest and the highest value, respectively. Figure 3.3 illustrates the rate of the static modulus of elasticity development for all materials at different ages.

Table 3.4 Average Modulus of Elasticity of the Repair Materials at Different Ages

Product	Average Modulus of Elasticity (ksi)			
	4 Hours	24 Hours	7 Days	28 Days
P1	4,593	5,251	6,633	7,471
P2	4,679	5,365	5,656	6,658
P3	3,893	4,206	4,571	5,718
P4	3,777	4,321	5,052	5,657
P5	3,451	3,685	4,339	4,779
P6	3,932	5,645	6,124	6,991
P7	4,229	4,981	6,223	7,258
P8	3,303	3,700	4,223	4,513

Based on Figure 3.3, and similar to the compressive strength gain (Figure 3.2), different rates of elastic modulus development can be observed. Materials 1 and 7 do not develop much elastic modulus at early ages, but dramatically develop modulus of elasticity beyond 24 hours. These two materials also have the highest elastic modulus at 7 and 28 days. Materials 2, 3, and 6 show a similar trend, but their stiffness development beyond 24 hours is not as high as materials 1 and 7. Material 6 shows the highest increase in stiffness at early ages (4 to 24 hours) among all materials. Materials 5 and 8 do not show a very noticeable stiffness development at either early or late ages. However, these two materials are the only materials that fall in the desired elastic modulus range of 4,000 to 5,000 ksi at late ages.

Similar to compressive strength gain, materials 1, 2, and 6 also show the highest stiffness gain rates. Having a high elastic modulus, however, is not favorable in terms of both structural compatibility with the substrate concrete and durability performance. If the repair material has a higher elastic modulus than the substrate, stresses would not properly be distributed in the repair-substrate system. Higher stiffness means attracting higher loads and higher shrinkage potential.

3.5 Splitting Tensile Strength

Similar to compressive strength, the repair material should have a tensile strength equal to or greater than that of the substrate concrete [8]. For a normal weight concrete with a nominal 28-days compressive strength of 5000 psi, the splitting tensile strength is 400-500 psi. Therefore, the repair materials should have a tensile strength of at least 400 psi to be considered acceptable. Table 3.5 presents the average splitting tensile strength of all eight repair materials corresponding to different ages. It should be noted that, due to some casting limitations, the splitting tensile test at the age of 7 days is skipped for materials 1, 2, 3, and 6.

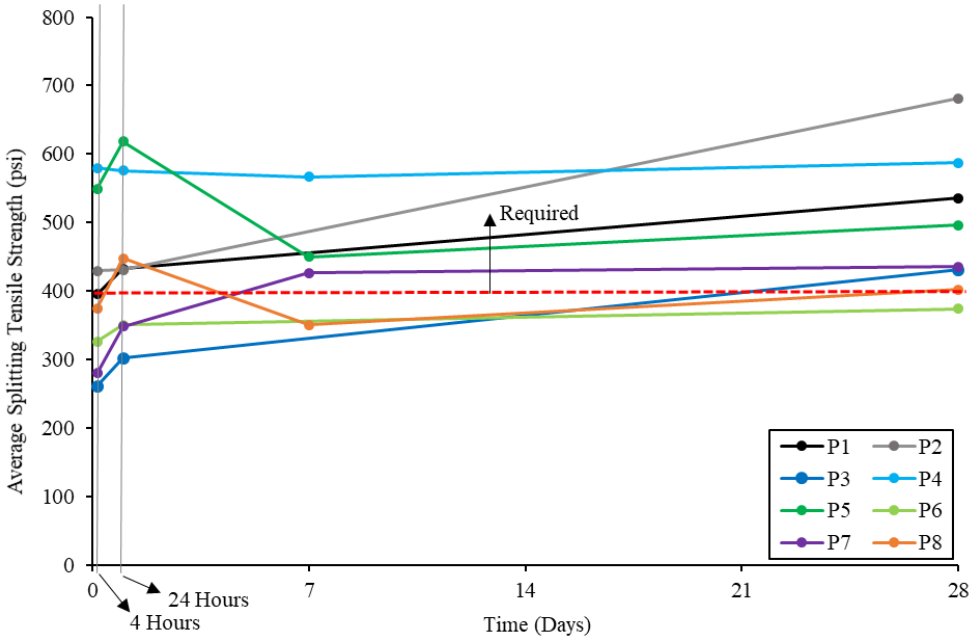

Figure 3.4 Rate of Splitting tensile Strength Development for the Selected Repair Materials

Based on Table 3.5, materials 3 and 4 have the lowest and the highest splitting tensile strength at the critical age of 4 hours, respectively. Four materials (1, 2, 4, and 5) satisfy the splitting tensile requirement at this age, having a strength of about 400 psi or higher. At late ages (28 days), all but one material (6) have a splitting tensile strength of higher than 400 psi. Material 2 has the highest splitting tensile strength at 28 days. Figure 3.4 displays the splitting tensile strength development of the repair media at different ages.

Table 3.5 Average Splitting Tensile Strength of the Repair Materials at Different Ages

Product	Average Splitting Tensile Strength (psi)			
	4 Hours	24 Hours	7 Days	28 Days
P1	395	433	-	536
P2	429	431	-	681
P3	261	302	-	431
P4	580	576	567	588
P5	550	618	450	497
P6	326	351	-	374
P7	280	348	427	435
P8	375	448	351	402

Different trends in splitting tensile strength development can be observed in Figure 3.4. Similar to compressive strength results, materials 1 and 2 have the highest tensile strength

development. Material 3 has the worst tensile strength development at early ages but has managed to satisfy the strength requirement at 28 days. Some materials (4, 5, and 8) do not continuously develop splitting tensile strength. These materials show a decrease in tensile strength from 24 hours to 7 days, but again develop strength beyond 7 days. This behavior is more noticeable in materials 5 and 8 both of which contain fibers. Material 4, despite following the mentioned trend, maintain a high splitting tensile strength all the time. Another behavior observed in materials containing fiber (1, 5, and 8) is displaying a ductile failure upon being split in half, with fibers maintaining the integrity of the cylinder. Other materials have a catastrophic break, starting with developing vertical cracks along the loading plane followed by being split in half in a brittle manner.

3.6 Surface Electrical Resistivity

Surface electrical resistivity is a measure of concrete chloride penetrability, as discussed in the previous section. The average surface resistivity of all materials at different ages along with their chloride penetration potential is tabulated in Table 3.6.

Based on Table 3.6, materials 1, 2, and 3 have a moderate and material 6 have low chloride penetration potential at the critical age of 4 hours. All other materials have very low chloride penetrability at the age of 4 hours. After 4 hours, all materials develop surface resistivity over time and their chloride penetration potential at 28 days is very low. The development in material 1 is exceptional as its surface resistivity significantly increased beyond 24 hours, making its chloride penetrability at 28 days negligible. Materials 6 and 8 show a slight decrease in surface resistivity at late ages, but their chloride penetration potential is still very low. Figure 3.5 shows the rate of surface resistivity development for the selected repair materials at different ages.

The substantial surface resistivity gain of material 1 can be clearly observed in Figure 3.5. No other material has gained a noticeable surface resistivity after the initial development, and based on Figure 3.5, they show a similar steady increase in surface electrical resistivity over time.

Table 3.6 Average Surface Resistivity of the Repair Materials at Different Ages

Product	Average surface electrical resistivity (kΩ-cm)				Long-term Chloride Penetration
	4 Hours	24 Hours	7 Days	28 Days	
P1	12.25	33.82	179.88	264.78	Negligible
P2	11.95	13.96	24.49	41.32	Very Low
P3	12.32	14.76	19.73	31.86	Very Low
P4	34.95	45.34	52.70	77.97	Very Low
P5	34.86	51.66	53.18	56.50	Very Low
P6	23.19	31.60	30.69	28.32	Very Low
P7	27.54	33.44	32.89	33.60	Very Low
P8	49.16	51.74	53.86	43.05	Very Low

3.7 Slant Shear Bond Strength

As discussed in previous sections, the quality of bond between the substrate concrete and repair material and the bond strength is one of the most crucial performance criteria in terms of success of a repair system. Practically, there is a state of shear at the repair-substrate interface, therefore the slant shear test is adopted to measure the bond strength of the selected repair media in this project. According to ASTM C928 [37], the required bond strength for rapid-set

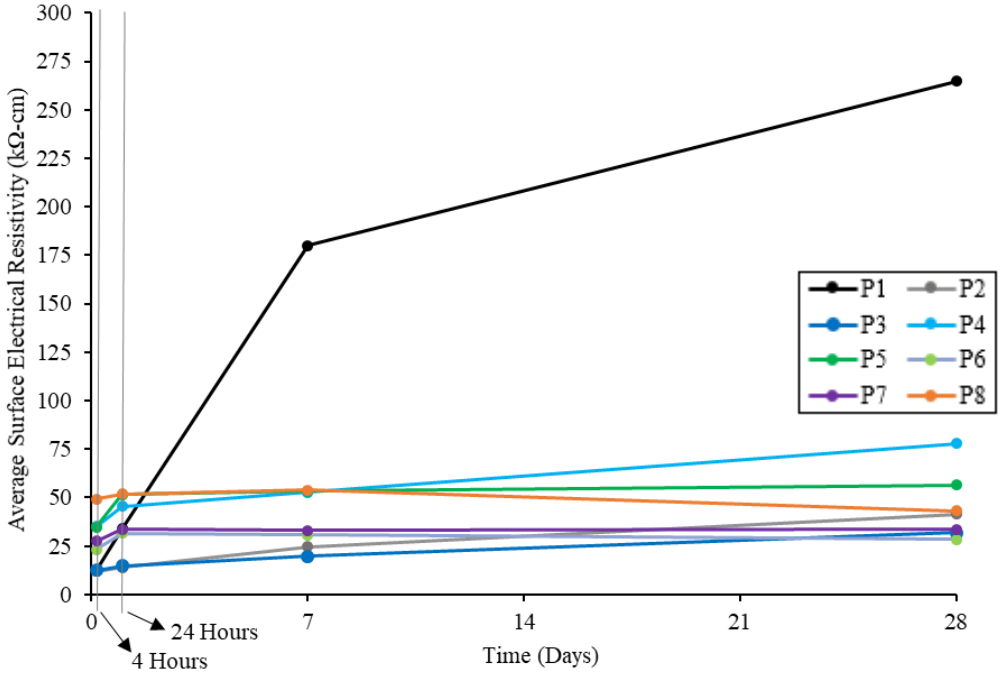

Figure 3.5 Rate of Surface Resistivity Development for the Selected Repair Materials

prepackaged repair materials is 1,000 and 1,500 psi at 1 and 7 days, respectively. Table 3.7 presents the average slant shear bond strength of the repair materials at different ages along with the failure mode observed in three specimens tested at each age.

Table 3.7 Average Slant Shear Bond Strength and Associated Failure Modes of the Repair Materials

Product	Average Slant Shear Bond Strength (psi)					
	4 Hours	Failure Modes	24 Hours	Failure Modes	28 Days	Failure Modes
P1	1943	R, R, R	2,797	R, S, S+R	3285	S, S, S
P2	1625	R, R, R	3,047	S, S, S	3174	S, S, S
P3	878	R, R, R	1,742	R, R, R	3099	R+S, S, R+S
P4	2954	B, B, S	3,198	S, S, S+R	3209	S, S, S
P5	2632	B, B, B	2,720	B, S+B, B	3136	R, S, S+R
P6	2373	R, R, R	2,722	B, R+S, R+S	3260	S+R, S, S
P7	1718	B, R, R	2,913	S+R, R+B, R+B	3434	S, S, S
P8	2071	B, B, B	2,343	B, S+B, R+B	2117	B, R+B, B

R: Repair material failure S: Substrate concrete failure B: Bond failure

Based on Table 3.7, the lowest and the highest bond strength at the critical age of 4 hours is observed in materials 3 and 4, respectively. At the late-ages (28 days), all but one material (8)

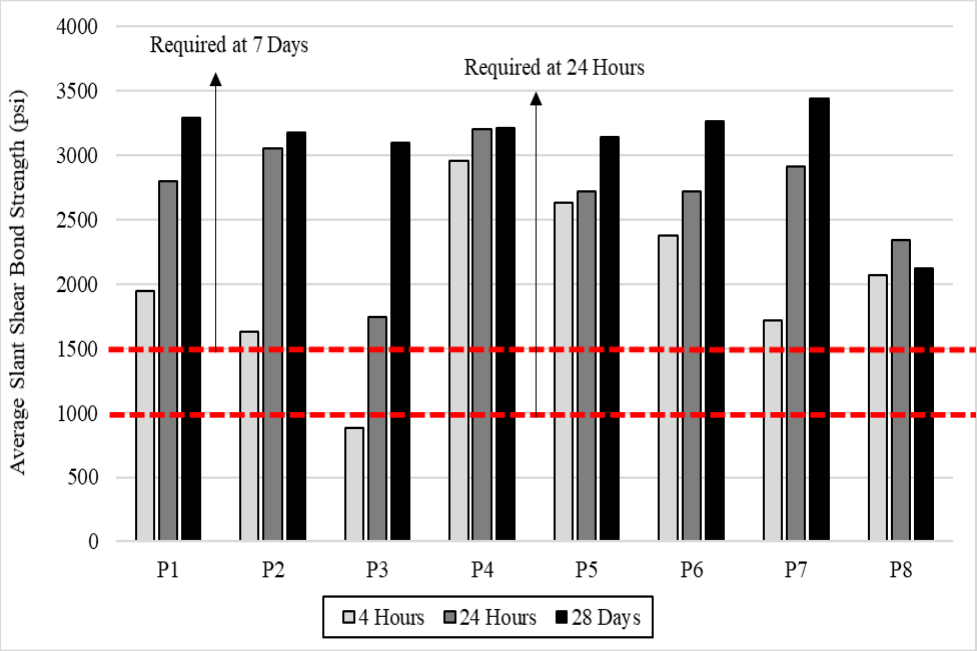

Figure 3.6 Average Slant Shear Bond Strength for the Selected Repair Materials

have a bond strength of over 3000 psi. The early age bond strength of repair materials varies noticeably, but the 28-days bond strength for all materials is very close, except for material 8. Similar to splitting tensile strength, material 8 show an increase-decrease trend and its late-age bond strength is considerably lower than all other materials. Figure 3.6 shows the average slant shear bond strength of repair materials at different ages.

Based on Figure 3.6, all materials meet the ASTM C928 bond strength requirement at the age of 24 hours. In fact, all materials, except for material 3, meet this requirement even at the important age of 4 hours. It can also be observed in Figure 3.6 that the bond strength of repair materials at 4 hours varies noticeably but the difference in bond strength decreases over time, as seven out of eight materials have a bond strength of 3,100-3,400 psi at the age of 28 days. The development rate of slant shear bond of repair materials is plotted in Figure 3.7.

Figure 3.7 shows that all materials also satisfy the 7-days bond strength requirement of ASTM C928. Material 3, which have the lowest bond strength at 4 hours, has the most significant bond strength development among all materials. Materials 2 and 7 have the highest bond strength development from 4 to 24 hours, but material 2 does not develop much bond

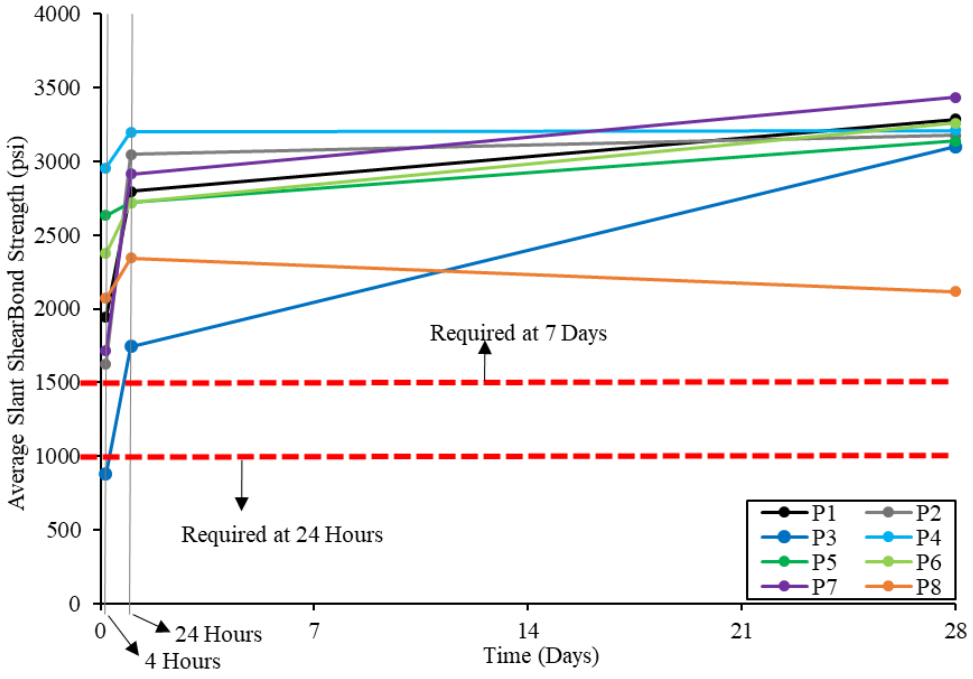

Figure 3.7 Rate of Slant Shear Bond Strength Development for the Selected Repair Materials

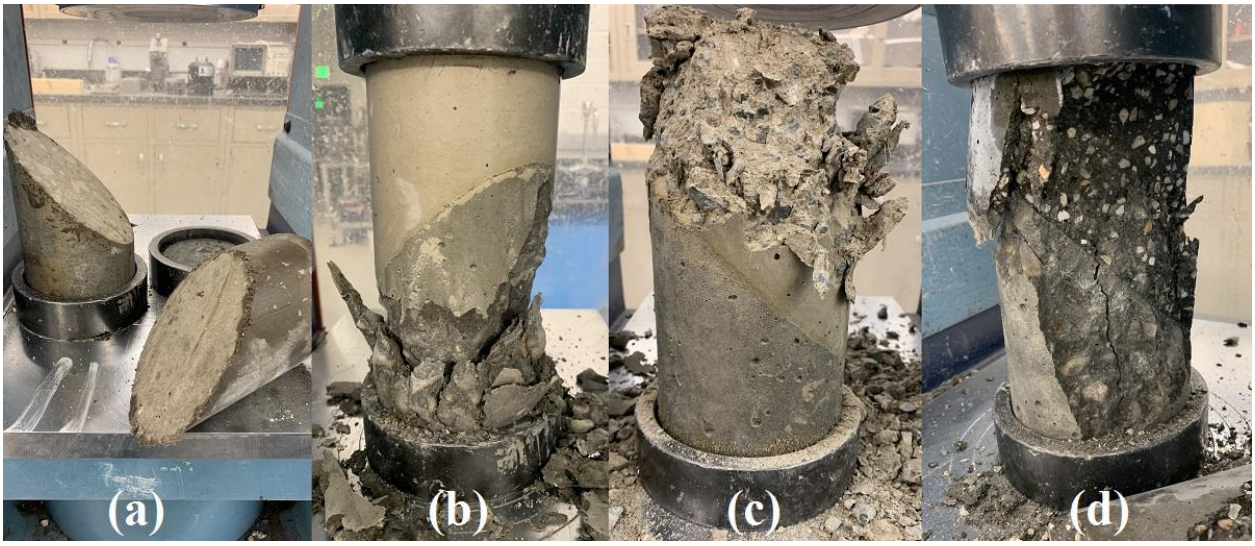

Figure 3.8 Failure Modes Observed in the Slant Shear Bond Strength Tests: (a) Bond Failure, (b) Substrate Concrete Failure, (c) Repair Material Failure, and (d) Combination of Failures

strength beyond 24 hours. This is also true with material 4, which has the highest bond strength at early ages (4 and 24 hours) but developed a negligible amount beyond 24 hours. Materials 1, 5, 6, and 7 show almost a same rate of bond strength development beyond 24 hours. As discussed previously, it can be observed in Figure 3.7 that material 8 follows an increase/decrease trend, similar to its splitting tensile strength development behavior. It has also the lowest 1- and 28-days slant shear bond strength.

Another observation is in failure modes in which materials show all possible failure patterns, including bond failure, repair material failure, substrate concrete failure, and a combination of the three failure modes. Figure 3.8 illustrates the typical failure modes observed in the slant shear test. The failure of the composite repair/substrate system occurring in the substrate concrete (Figure 3.8-b), repair material (Figure 3.8-c), or both (Figure 3.8-d), indicates the repair material has developed a desired bond to the substrate and the composite action of the whole system is expected to be achieved. On the other hand, if the failure plane is at the bond interface, the repair material is considered to have a poor bond to the substrate concrete and premature failure of the repair/substrate system is expected.

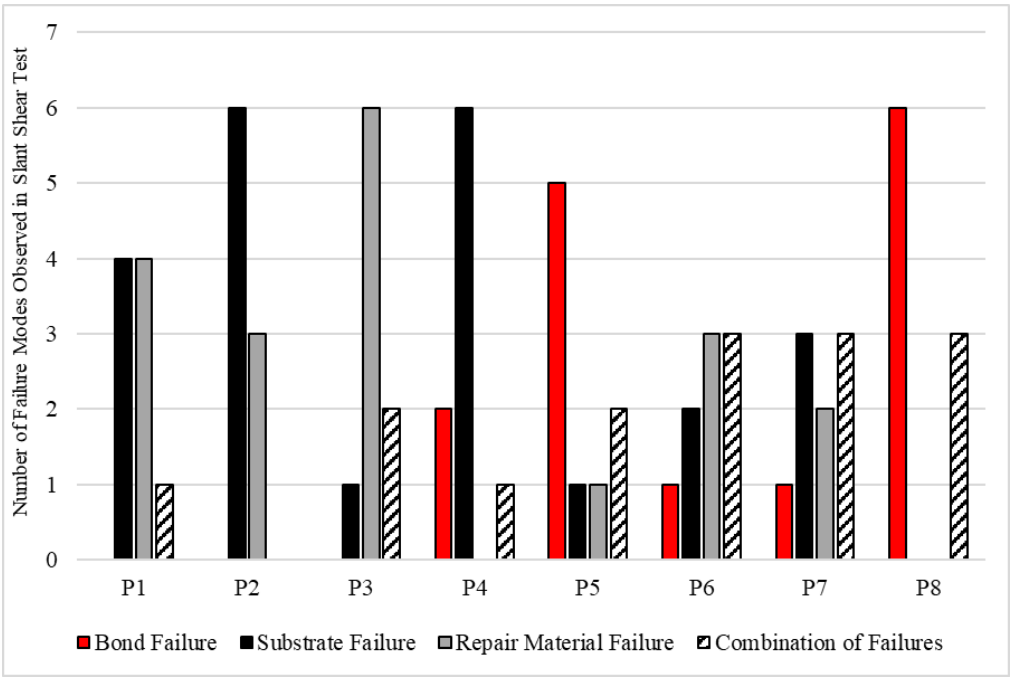

Figure 3.9 Number of Failure Modes Observed for Each Repair Material (Slant Shear Test)

In this project, almost four out of eight repair materials (1, 2, 3, and 6) do not show a bond failure at any age. Other materials (4, 5, and 7) experience bond failure at early ages but not at late ages. Material 8 is the only material having bond failure at both early and late ages. Figure 3.9 graphically shows the number of each failure type observed in the repair materials. It can be seen in Figure 3.9 that materials 5 and 8 have the highest number of bond failures. Material 2 is the only material having only repair or substrate failure modes. Material 2 also has the highest number of substrate failures, along with material 4. Highest number of 'repair material failure' is observed for P3.

3.8 Autogenous Shrinkage

As discussed in Section 1.4.4, autogenous shrinkage of a sealed, thermally-isolated cementitious paste or mortar is caused by the chemical shrinkage (reduction in the absolute volume) of the hydrated cement paste caused by chemical reactions between water and cement. In other words, the absolute volume of the hydrated cement paste is less than the original volume of water and cement (total volume before mixing the two materials together and starting the

hydration process). It should be noted that autogenous shrinkage does not include the effects of moisture loss, temperature variation, or any other outside factor on the volume change.

In this project, the autogenous strain measurements are only taken from materials containing no fiber and/or aggregates (materials 4, 6, and 7), as discussed in Section 2.4.8. The test is performed on a material containing fiber and the data points from three specimens vary significantly, making it impossible to take an average. However, such considerable variation is not observed in specimens filled with materials 4, 6, and 7 when taking the autogenous strain measurements. Figure 3.10 shows the average autogenous shrinkage of the three materials at different ages. The y-axis shows the change in length, therefore negative values indicate shrinkage (reduction in length).

It can be observed in Figure 3.10 that a significant portion of the total autogenous deformation occurs in the first 2-3 days after the addition of water to the repair material. This observation is especially discernable in material 4, in which the rate of autogenous strain development beyond two days is very steady with a slow pace. Material 4 also has the highest

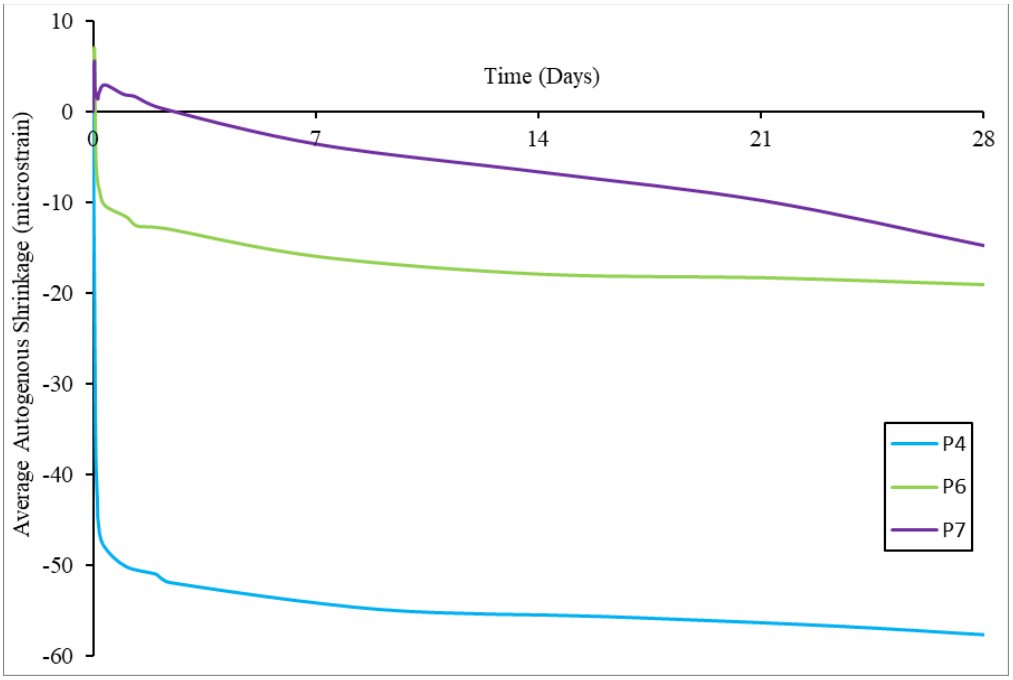

Figure 3.10 Average Autogenous Shrinkage of Materials 4, 6, and 7 at Different Ages

autogenous deformation at all ages, with about 50 and 60 microstrain at 24 hours and 28 days, respectively.

Another observation in Figure 3.10 is that materials 6 and 7 initially and at very early ages show expansion (increase in autogenous strain) but start to shrink and develop negative autogenous strain afterwards. There are two possible reasons for the initial expansion of these materials, namely early heat of hydration which causes thermal expansion, and use of shrinkage compensating admixtures which cause expansion to offset the material shrinkage [36]. It should be noted that both materials are produced by the same manufacturer and the only difference is that material 7 has a higher initial and final setting time (more working time). It can be seen that the material with more working time develops lower autogenous deformation.

3.9 Drying Shrinkage

One of the requirements to satisfy the dimensional (volume) stability between the repair material and the substrate concrete is the long-term shrinkage of the repair material being equal to or greater than that of the substrate [8]. ASTM C928 requires the allowable decrease in length change after 28 days to be 0.15%, for air-cured drying shrinkage test specimens. As discussed in Section 1.4.4, crack development due to shrinkage of the repair material can reduce durability and also cause premature failure of the repair system. Therefore, materials with high shrinkage cracking potential should be avoided. It should be noted that the volume stability can be improved by methods such as internal curing [59], which is not within the scope of this report. To observe the difference due to the demolding time in free shrinkage development of repair materials, for each material three specimens were demolded at 4 hours and three were demolded at 24 hours after the water addition. The results are illustrated in Figure 3.11.

It can be observed in Figure 3.11 that demolding the test specimens at the age of 24 hours resulted in considerably less overall drying shrinkage. The reason is the fact that the majority of chemical reactions, hydration process, and heat development in these materials occur in the first few hours as they set very rapidly and therefore if the specimens are demolded at 24 hours after the addition of water, a significant portion of the shrinkage already developed in the material is missed in the length change measurements. Another reason is that, clearly, the sooner the

specimen is demolded, the more it would be exposed to moisture loss and thus more drying shrinkage is developed. Therefore, evaluating the selected repair materials in terms of free shrinkage and dimensional stability, the specimens demolded after 24 hours are not considered. Based on Figure 3.11-b, the selected repair materials show different rates of drying shrinkage

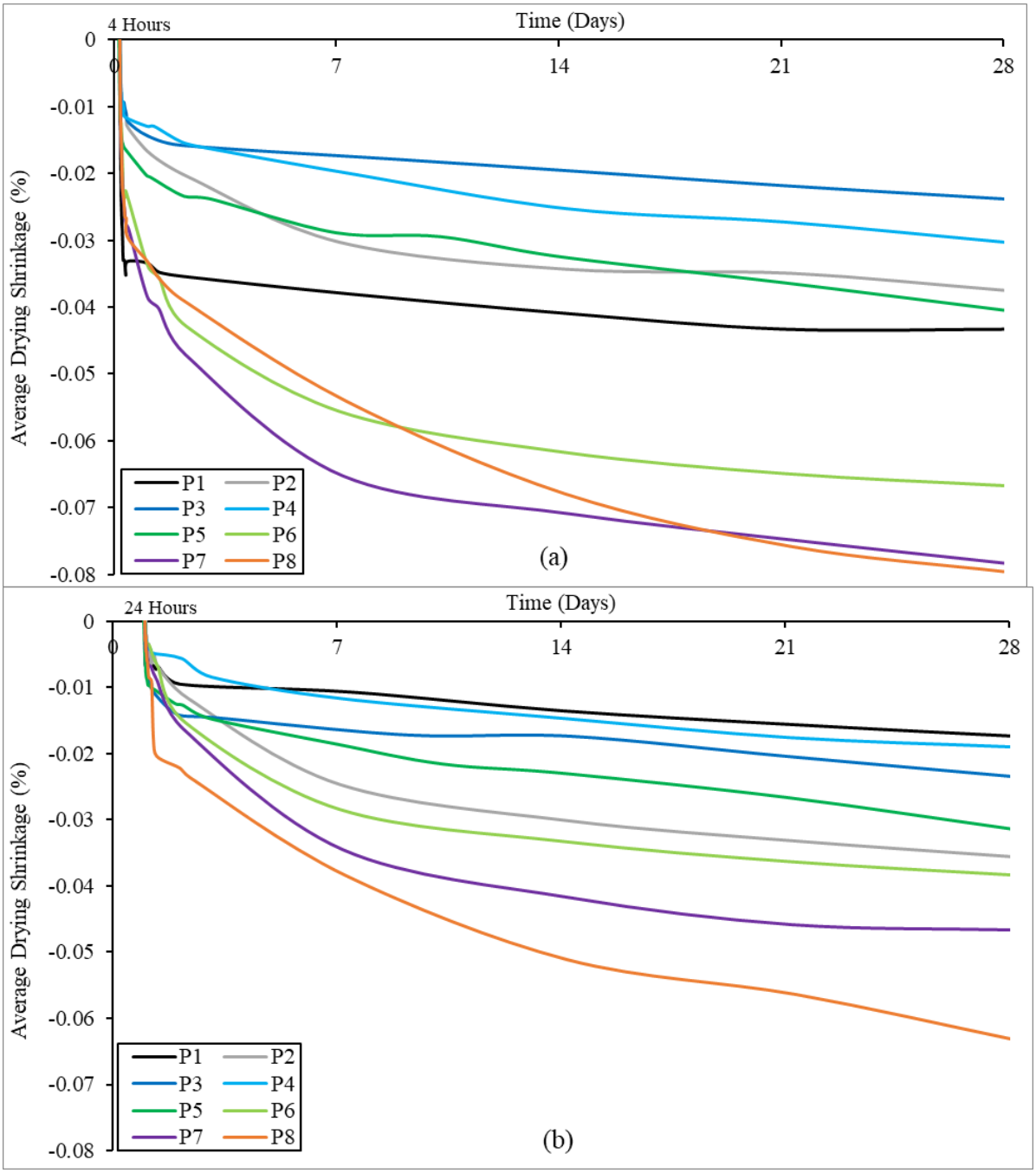

Figure 3.11 Average Drying Shrinkage of Repair Materials at Different Ages, Demolded at: (a) 4 Hours; (b) 24 Hours

development which reflect the fact that they are composed of a variety of cementitious materials and admixtures. Therefore, the entire free shrinkage development behavior should be considered and not just a specific point in time. Material 3 shows the best length change performance, as it develops the lowest drying shrinkage at almost all ages. Conversely, materials 7 and 8 display the highest length change due to free drying shrinkage. Materials 7 and 8 also have a poor mechanical performance in terms of compressive strength, with material 8 having also a very poor splitting tensile strength, modulus of elasticity, and slant shear bond strength. Materials 1 and 2, having the highest compressive strength and very high elastic modulus, tensile strength, and bond strength, also show an acceptable length change development. A substantial portion of the drying shrinkage occur in the first few days, similar to what is observed in the autogenous shrinkage. Specifically, the majority of free shrinkage occur in the first 2-4 days, for materials 1 to 5. These five materials have noticeably less free drying shrinkage than materials 6, 7, and 8. Nonetheless, even materials 6, 7, and 8 which have the highest shrinkage-induced length change significantly satisfy the ASTM C928 requirement, with a 28-days length change of about half the specified limit (<-0.15%).

Another observation in Figure 3.11-a is two different drying shrinkage development behaviors. Materials 2, 3, 4, and 5 show an overall very low drying shrinkage at all ages. They have a small drying shrinkage within the first few hours, possibly due to temperature loss, followed by a slow and steady rate of shrinkage growth over time. Materials 6, 7, and 8 have a

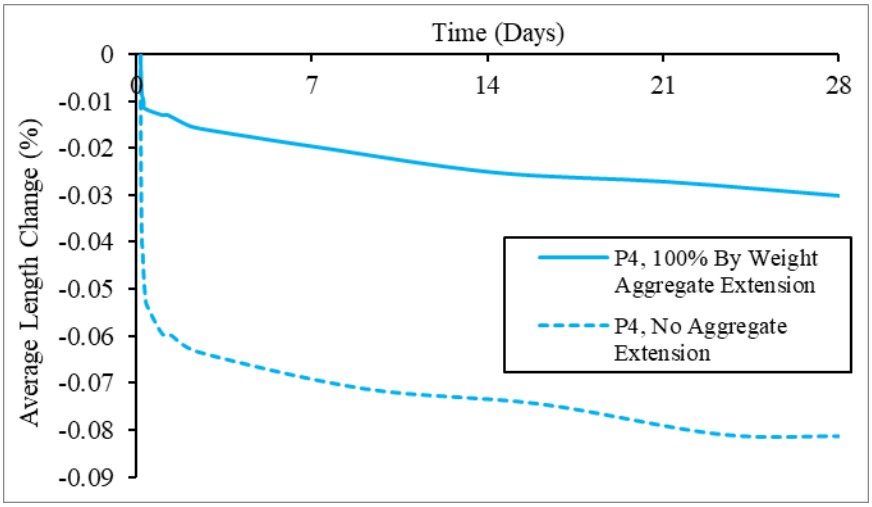

Figure 3.12 Average Drying Shrinkage of Material 4 at Different ages, with and without Aggregate Extension

rapid and large increase in drying shrinkage within the first few days, followed by a continuous and gradual increase in length change over time. Material 1 shows a combination of the aforementioned shrinkage development behaviors; it displays a noticeable and rapid increase in free drying shrinkage in the first two days but have a very slight shrinkage growth beyond that point.

The effect of aggregate extension is also worth discussing. As mentioned in Section 2, material 4 is the only material extended with coarse aggregates by 100% weight. To investigate the effect of aggregate extension, a set of drying shrinkage specimens was also made with neat mortar (no aggregate extension). Figure 3.12 illustrates the free drying shrinkage behavior of material 4, with and without aggregate extension.

It can be clearly observed in Figure 3.12 that aggregate extension tremendously reduces the free drying shrinkage in material 4, as the 28-days length change of the neat mortar, for instance, is about 4 times the length change in the case of aggregate extension. Aggregate extension reduces the cement paste portion of the mixture, and since the drying shrinkage mostly develops in the paste, the overall shrinkage of the material is reduced.

3.10 Restrained Ring Shrinkage

As discussed in Section 2.4.9 of this document, restrained ring shrinkage tests were performed on two specimens for each material. The outer form of the rings was removed at 4-hour and 24-hour ages. The compressive strain of the rings was measured using 4 strain gauges attached to the inner side of the steel ring. A drop of 30 microstrain in one of the gauges usually indicates cracking of the specimen. Each test was run for 28 days. After 28 days, if no drop in compressive strain or no visible crack was observed, the test was terminated, and the specimen was reported as uncracked. If the specimen showed a visible crack, the width of the crack was measured with the help of a crack microscope. A summary of the test results is shown in Table 3.8. Raw test data for ring shrinkage have been provided in Appendix A.

Table 3.8 Summary of Restrained Ring Shrinkage Test

Product	Specimens with Form Removed at 4 Hours				Specimens with Form Removed at 24 Hours			
	Specimen Cracked?	No of Crack	Average Crack Width ($\times 10^{-3}$ in)	Age at Cracking (days)	Specimen Cracked?	No of Crack	Average Crack Width ($\times 10^{-3}$ in)	Age at Cracking (days)
P1	No	N/A	N/A	N/A	No	N/A	N/A	N/A
P2	No	N/A	N/A	N/A	No	N/A	N/A	N/A
P3	No	N/A	N/A	N/A	No	N/A	N/A	N/A
P4	No	N/A	N/A	N/A	No	N/A	N/A	N/A
P5	No	N/A	N/A	N/A	No	N/A	N/A	N/A
P6	No	N/A	N/A	N/A	No	N/A	N/A	N/A
P7	Yes	2	3.72 3.7	2.3	Yes	2	4.249 3.199	4.8
P8	No	N/A	N/A	N/A	No	N/A	N/A	N/A

Only P7 cracked within 28 days, as evident from Figures 3.13 and 3.14. The specimens, demolded at 4-hour and 24-hour ages, cracked at 2.3 and 4.8 days, respectively. Each specimen developed two cracks at 180°. The average crack widths of the 4-hour specimen were 3.72×10^{-3}

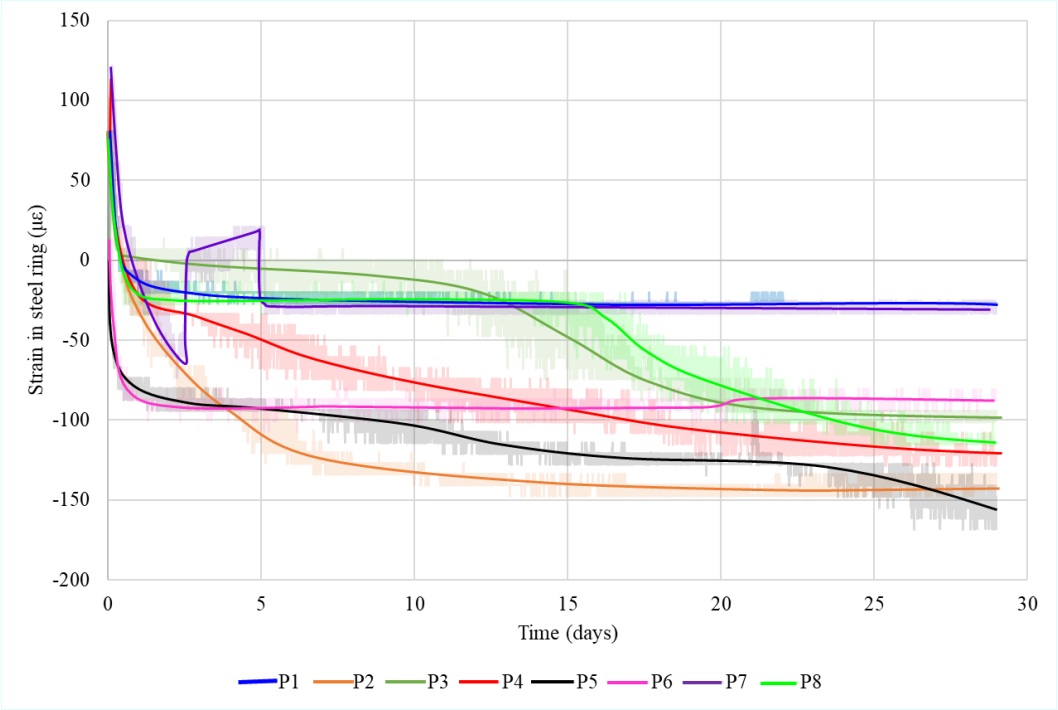

Figure 3.13 Average Strain in Steel Ring (Outer Form Removed at 4-Hour Age)

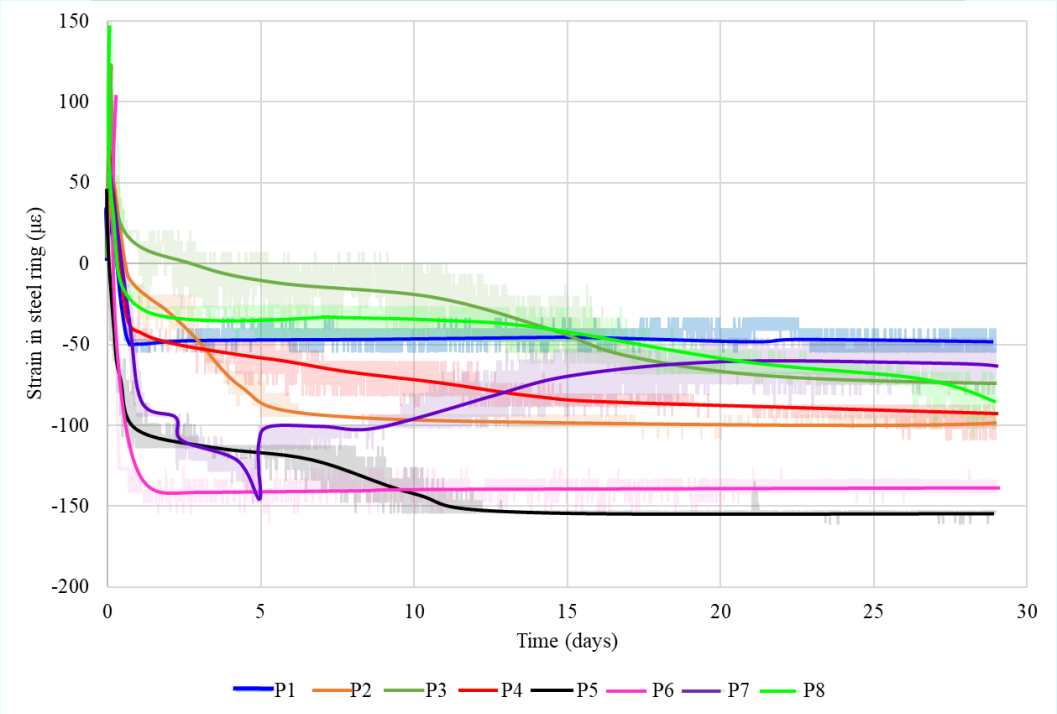

Figure 3.14 Average Strain in Steel Ring (Outer Form Removed at 24-Hour Age)

and 3.7×10^{-3} inch. The average crack widths of the 24-hour specimen were 4.249×10^{-3} and 3.199×10^{-3} inch.

Strain measurements in the steel ring were recorded as soon as the rings were cast, which was around 40 minutes after the product came into contact with water. The plots from Figures 3.13 and 3.14 show only positive strain. After some time, the gauges started to record negative or compressive strain. The time to develop compressive strain in the steel rings varied for each material as shown in Figure 3.15.

The rings with P5 were the fastest to develop compressive strain, which is almost as soon as the strain gauges were connected at around 40 minutes after water was added to the material. For the rest of the products, time to record negative strain ranged from 8.3 hours to 50.9 hours. Except for P3 and P5, the shrinkage, marked by the initiation of negative strain, started within eight to fifteen hours after adding water.

For most of the materials, the time to the removal of outer forms seemed not to affect the development of compressive strain in the steel ring. All but P3 took almost the same time to develop negative strain irrespective of when the outer form was removed. This can be attributed

to the high rate of hydration and heat development of the rapid repair materials at early ages. For 24-hour specimens, by the time the forms were removed, a significant portion of shrinkage already took place. This also confirms the observations made for drying shrinkage specimens. Therefore, it can be said that, for rapid repair materials, removal of outer forms at the 4-hour mark is more sensible.

Another observation from Figures 3.13 and 3.14 can be made regarding the maximum compressive strain in the steel rings. Among the uncracked specimens, P1, P2, P3, and P6 reached a constant compressive strain during the period of testing. The 4-hour specimen of P5 reached a constant strain, although the 24-hour specimen showed an increasing trend. The compressive strains of the steel ring for P4 and P8 seemed to keep increasing during the testing period. Among all the materials, P1 developed the lowest maximum compressive strain, indicating less shrinkage. P1 also showed better mechanical performance than the rest of the materials.

3.11 Summary

This section presents the mechanical and durability performances of the selected rapid repair materials. The laboratory work included setting time, compressive strength, static modulus of elasticity, splitting tensile strength, surface resistivity, slant shear bond strength, autogenous and drying shrinkage, and restrained ring shrinkage tests. In summary, based on the lab performance, P1 and P8 showed the overall best and worst performance in terms of both mechanical and durability performance, respectively.

4.0 FIELD PERFORMANCE OF SELECTED REPAIR MATERIALS

In this section, the field performance of nine total repair materials is presented. In total, nine products were used for repair work, and eight of them were tested in the laboratory. A description of the repair product installation, inspection of crack development over a nine months' period, and a regression model to predict crack development are included in this section.

4.1 Repair Product Installation

The field inspection phase began on June 7, 2019, with the application of the repair materials on the Layton, Utah SR-193 bridge over US-89 (Structure Number 0F 575). The work consisted of identifying and removing patches of distressed concrete from the top layer of the deck, preparation of substrate by sandblasting, and application of repair materials. Prior to the repair product installation, the prepared surfaces were wetted. Due to a scheduling issue, it was possible to observe the construction work only for P1, P4, and P6. Another material, designated as P9, had been used. This material was not included in the preceding laboratory study. Figure 4.1 presents the typical stages of the repair work. A map and a summary of repair areas are provided in Figure 4.2 and Table 4.1. It should be noted that the images of all the repairs cannot be processed due to the large size of patches.

All the products were mixed with a paddle mixer, except for P1, for which the supplier required the use of a barrel mixer. When product P1 was mixed, the ambient temperature and

Figure 4.1 Preparation of Substrate, Pouring, Finishing, and Application of Curing Compound (P6)

humidity were 79 °F and 31%, respectively. Before the pouring, the deck and mixing water temperatures were recorded to be 90 °F and 74 °F, respectively. Each bag of P1 was mixed with 2 quarts of water. Two-thirds of the water was initially mixed with a bag of P1 for 1 minute, and then the rest of water was mixed for an additional 6 minutes. At the pouring, the average temperature of the mix was 80 °F. After one hour, the temperature climbed to 109 °F. At the two hours' mark, the average compressive strength was 4,200 psi, as measured with a Schmidt hammer.

Product P4 was used with 100% extension with pea gravel. The ambient temperature and relative humidity were 77 °F and 34%, respectively. The water, product, aggregate, and deck (substrate) temperatures were 71 °F, 85.6 °F, 102 °F, and 89 °F, respectively. After mixing, the temperature of the mixture was 89.4 °F. Each bag of P4 required 3 to 5.5 quarts of water and 0.09 oz. of a citric-acid-based retarder to increase the setting time. Total mixing time was three minutes. After pouring, a curing compound was applied to the patches. After approximately 1 hour and 15 minutes, the average strength was measured to be 2,630 psi. After 2 hours and 30 minutes, the average strength was recorded to be 4,330 psi. Just after pouring and application of the curing compound, the average temperature of the patches was 86 °F, which rose to an average temperature of 119 °F at the 2 hours and 30 minutes mark. On the fifth day after pouring, shrinkage cracks were observed on the patches with P4.

Product P6 was used for repair patches with 50% extension. The ambient temperature was 74 °F and the relative humidity was 44%. The substrate temperature was 77 °F before the pouring. The temperature of the mix was recorded to be 107 °F, 10 minutes after water was added. As specified, 50% extension (two bags of premix and one bag of aggregate) was used with 11 to 13 quarts of water. Total mixing time was 3 minutes. A broom finish was not achieved before the product set. After one hour, 2,800 psi strength was recorded by using a Schmidt hammer. After five days, the average strength was 4,500 psi. No visible crack was observed after 10 days.

Another product, labelled as P9, was not available for laboratory testing. However, this product was used in repair work in the field. During the repair work, temperatures of the substrate, water, and product were recorded to be 71 °F, 70.5 °F, and 76 °F, respectively. The

ambient temperature and humidity were 61 °F and 35%, respectively. After placement, the repaired patches were covered with plastic sheets. P9 achieved a compressive strength of 4,000 psi in 3 hours and 6,000 psi after 2 days.

A table listing the products with the patch numbers is included in Appendix B. In general, during the installation of repair products, the environmental factors (temperature, humidity, and wind speed) significantly varied and therefore these conditions may affect the field performance. Not all of the repairs were cured in the same way. In some cases, the mix required adjustment, such as additional water or use of retarder, based on the visual appearance. On the other hand, the laboratory experiments, discussed in the previous section, were performed in a controlled condition. Therefore, the environmental factors had minimal effect on the laboratory data.

4.2 Repair Product Field Inspection

All repairs were inspected three times in a span of nine months. Inspection dates were October 27, 2019, February 23, 2020, and June 28, 2020. The inspections were performed between 8:00 AM and 11:00 AM on weekends, when the traffic volume was low as partially closing the lanes would cause minimal obstruction to traffic. Pictures of the repairs were taken, and then cracks were highlighted for identification purposes. An example of the processed pictures with the cracks is presented in Figure 4.3.

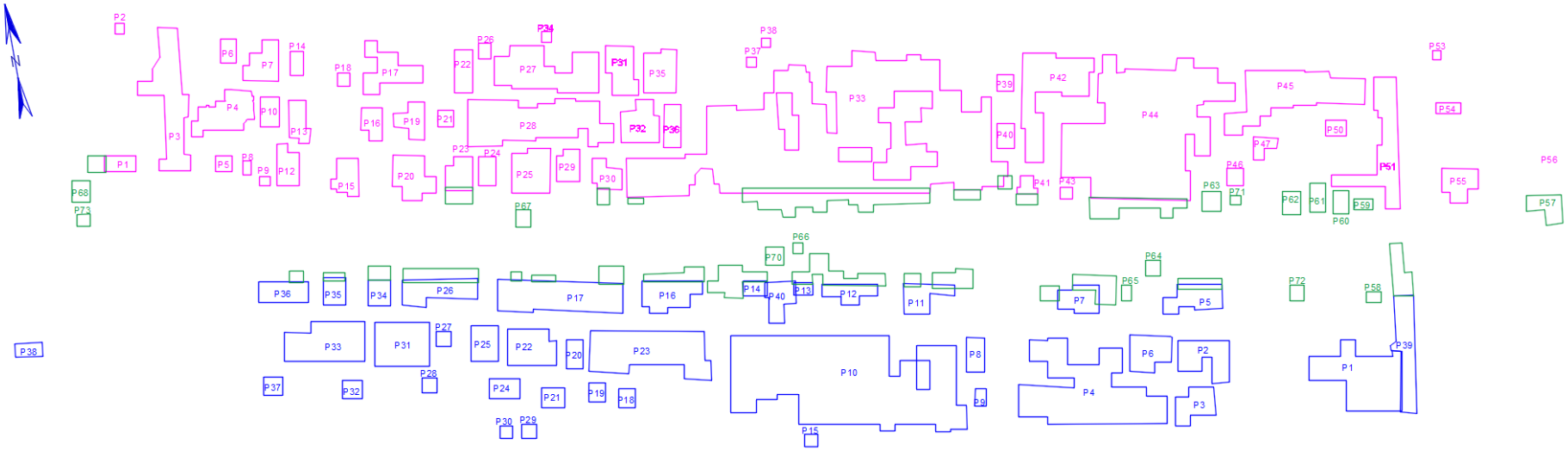

Figure 4.2 Map of the Repair Work (Phase 1: Blue, Phase 2: Green, Phase 3: Magenta)

Table 4.1 Summary of Repair Area

Phase 1			Phase 2			Phase 3		
Repair	Area (ft^2)	Average Depth (in)	Repair	Area (ft^2)	Average Depth (in)	Repair	Area (ft^2)	Average Depth (in)
1	16.33	3.5	57	16.52	3.5	1	91.93	3
2	2.11	2	58	3.43	2.5	2	36.22	3
3	75.98	3.5	59	4.38	3	3	23.85	2.5
4	34.14	3.75	60	9.75	3	4	163.75	3.5
5	5.63	4	61	9.88	3	5	28.72	3.5
6	7.88	3.5	62	9.11	3	6	29.17	3
7	24.14	4	63	7.80	2.5	7	22.57	3.5
8	2.60	4	64	5.06	3	8	13.67	3
9	2.11	3	65	4.38	2.5	9	4.06	3.75
10	12.51	3.5	66	2.24	2.5	10	380.76	3.25
11	-	-	67	5.42	3	11	22.73	3
12	18.81	4	68	8.67	3	12	18.60	3
13	15.14	3.5	70	7.33	2.5	13	5.04	3
14	6.71	3	71	2.24	2	14	7.76	3
15	18.06	3.5	72	5.04	2.5	15	3.67	2.5
16	12.65	3.5	P1-1	6.45	2.5	16	33.06	4
17	35.32	3.5	P1-23	9.87	3.25	17	79.53	4
18	3.50	3	P1-30	4.40	2.5	18	7.20	4
19	18.59	4	P1-33a	2.22	3	19	6.85	4
20	32.05	3.75	P1-33b	63.03	3.5	20	10.42	3.5
21	5.44	3.5	P1-33c	3.99	3.5	21	10.21	3.25
22	17.65	3.5	P1-33d	4.00	3	22	36.73	3.25
23	18.58	4	P1-41	5.02	3	23	100.38	3.25
24	10.63	4	P1-44	29.16	3	24	13.50	3.5
25	36.02	3.5	P3-11a	15.40	3	25	21.27	2.5
26	4.08	3.5	P3-11b	4.81	3	26	34.63	4
27	76.68	2.75	P3-12	27.53	3	27	4.69	3.5
28	118.92	4	P3-14	23.10	3	28	4.78	4
29	14.72	3.5	P3-16	13.98	3	29	4.51	2
30	16.49	4	P3-17a	8.86	2.5	30	3.51	2
31	27.93	3.5	P3-17b	3.50	3	31	54.00	3

Phase 1			Phase 2			Phase 3		
Repair	**Area (ft^2)**	**Average Depth (in)**	**Repair**	**Area (ft^2)**	**Average Depth (in)**	**Repair**	**Area (ft^2)**	**Average Depth (in)**
32	30.47	3.5	P3-17c	2.25	3.25	32	7.44	3
33	613.75	3	P3-26	22.17	3	33	62.49	3.75
34	2.50	2	P3-34	6.50	3	34	12.46	4.25
35	29.54	3	P3-35	3.79	3	35	13.44	4
36	15.57	3.75	P3-36	3.80	2.5	36	22.43	4
37	-	-	P3-39	16.69	4	37	7.79	3.75
38	-	-	P3-5	9.75	2.5	38	9.28	4
39	6.04	3	P3-7a	20.68	3	39	38.97	5.25
40	9.68	3	P3-7b	5.96	2.5	40	20.82	3.5
41	6.37	2.5	73	3.56	2.5			
42	81.10	3						
43	3.20	2.5						
44	335.35	3						
45	92.40	3						
46	6.05	3						
47	8.45	3						
48	-	-						
49	-	-						
50	7.20	3						
51	70.47	5						
52	-	-						
53	1.56	2						
54	6.25	2.5						
55	21.99	3						
56	12.50	3.5						

The delamination was detected using chain drag and hammer sounding. Total crack lengths were then normalized with respect to the area of each repair. Average values of crack length per square foot of area, or Normalized Crack Length (NCL), were calculated according to Equation 4.1 for each inspection and are reported in this document to compare the field

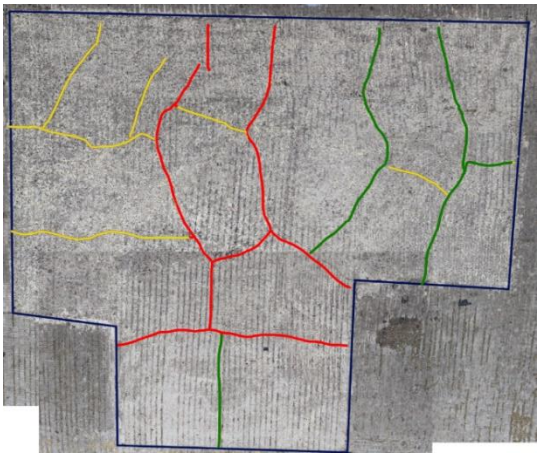

Figure 4.3 Crack Formation on Repairs Identified during First (Red), Second (green), and Third (Yellow) Inspection

performance of the products. NCL is presented in Table 4.2 and Figure 4.4. Comprehensive inspection photos and tables are presented in Appendix B and in Table 4.3, respectively. Note that P2 and P7 materials from the material testing program were not selected for field repairs.

$$\text{NCL} = (\text{Crack Length})/(\text{Area of Repair}) \tag{4.1}$$

Table 4.2 Average Normalized Crack Length (NCL) of Repairs

Product	Average Crack Length (in./ft.^{2})		
	Inspection 1	Inspection 2	Inspection 3
P1	0	0.888	1.32
P3	0	0	0
P4	5.64	7.68	8.88
P5	9.84	11.04	12.6
P6	4.08	5.04	5.52
P8	2.4	3.96	4.32
P9	4.44	8.64	9.24

Table 4.3 Normalized Crack Length (NCL) for Repairs

Product			Inspection 1	Inspection 2	Inspection 3	
	Area (ft^2)	Shape	Crack Length ($in./ft.^2$)	Crack Length ($in./ft.^2$)	Crack Length ($in./ft.^2$)	Cracked?
P1	4.69	Rectangular	0.00	0.00	0.00	NO
P1	4.78	Rectangular	0.00	0.00	0.00	NO
P1	10.21	Rectangular	0.00	1.41	2.46	YES
P1	13.5	Rectangular	0.00	3.47	3.80	YES
P1	21.21	Rectangular	0.00	0.00	0.00	NO
P1	36.73	Irregular	0.00	0.43	1.38	YES
P3	5.04	Rectangular	7.05	15.12	15.12	YES
P3	5.44	Rectangular	8.32	8.32	8.32	YES
P3	12.65	Irregular	7.43	8.69	12.35	YES
P3	17.65	Rectangular	0.00	0.00	0.00	NO
P3	18.32	Irregular	4.04	6.64	7.94	YES
P3	32.05	Irregular	6.78	7.23	9.74	YES
P4	4.06	Rectangular	4.34	0.00	0.00	NO
P4	9.68	Rectangular	12.38	15.66	15.66	YES
P4	12.5	Rectangular	8.94	11.83	13.22	YES
P4	13.67	Rectangular	15.60	17.44	19.66	YES
P4	21.99	Irregular	11.17	11.57	15.20	YES
P4	22.73	Irregular	6.37	9.81	11.67	YES
P5	6.37	Irregular	0.82	2.07	2.07	YES
P5	70.47	Irregular	7.40	8.06	8.94	YES
P6	7.44	Rectangular	0.00	0.00	0.00	NO
P6	7.79	Rectangular	0.00	0.00	0.00	NO
P6	12.46	Rectangular	2.20	6.73	6.73	YES
P6	22.43	Rectangular	1.65	4.37	4.37	YES
P6	38.97	Irregular	8.44	10.58	12.14	YES
P6	54	Rectangular	1.80	2.29	2.54	YES
P8	4.38	Rectangular	0.00	7.48	7.48	YES
P8	5.06	Rectangular	10.17	15.27	15.27	YES
P8	7.33	Rectangular	9.51	15.03	15.03	YES
P8	15.14	Irregular	5.77	8.94	11.84	YES
P8	18.06	Irregular	5.79	5.91	7.21	YES
P8	24.14	Irregular	0.00	0.00	0.00	YES
P9	36.22	Irregular	6.30	11.88	11.88	YES
P9	23.85	Irregular	3.55	7.08	8.46	YES
P9	29.17	Irregular	3.50	6.84	7.49	YES

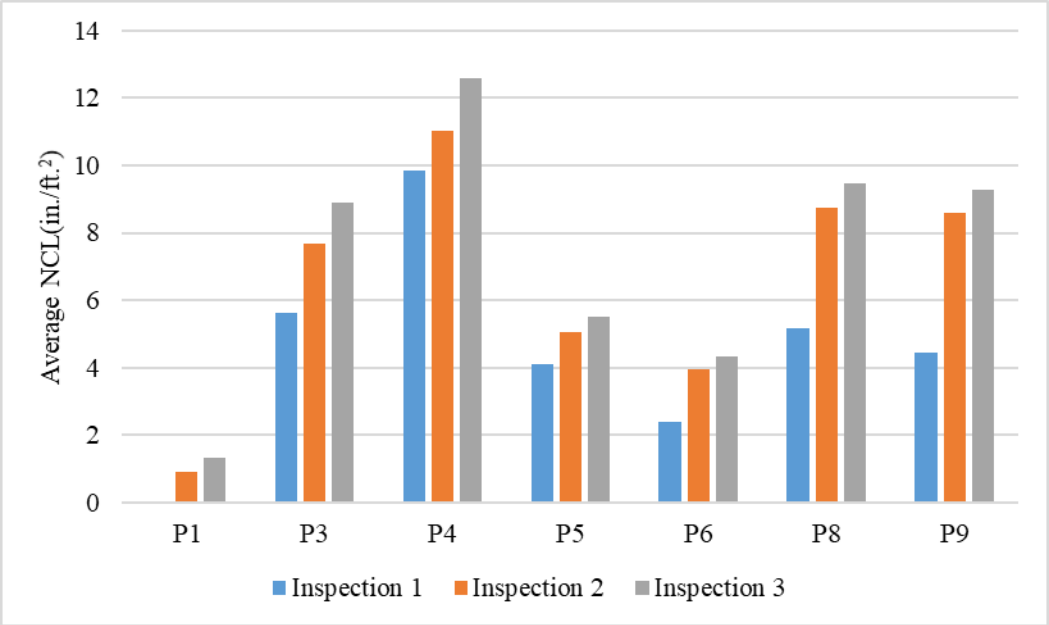

Figure 4.4 Average NCL of Repair Patch

Repairs with product P1 did not show any cracks during the first inspection, while repairs with P4 developed the most cracks (0.82 ft./ft.^{2}), followed by P3, P8, P5, P9, and P6. Generally, cracks increased in length between the first and second inspections as shown in Figure 4.4. Similarly, lengths of cracks generally increased between the second and third inspections. However, relatively few new cracks were identified in the third inspection. Overall, P4 developed the highest length of cracks per square foot at the completion of the field inspection. Out of six repairs fabricated from P1, three did not develop any cracks during the inspection period. For all other products, at least one of the inspected repairs remained uncracked for the duration of the study, except P5 and P9. These repairs were all rectangular in shape and relatively smaller in size (< 20 ft^2).

Figure 4.5 illustrates the increase in NCL as a percentage. As a whole, most cracking increased significantly between inspections one and two, but much less between inspections 2 and 3. Percentages of increase in NCL were highest for the second inspection, ranging from 12% to 70%. By the third inspection, the increment of these percentages reduced to 8% to 16%, except for repairs with P1. Repairs with P1, which did not develop any crack by the first inspection, had 49% more cracks per square feet by the third inspection, compared to the second inspection. This indicates the possibility of further crack formation in these repairs at later ages. An increase in percentage of cracks in P4 by the second and third inspections were 12% and

14%, respectively. Therefore, it can be inferred that, although P4 developed cracks more compared to other products by the first inspection, the crack development in these repairs was almost complete by the third inspection. As all of the repairs eventually showed cracks, all of the repairs may require sealing to protect rebars and stop further deterioration of concrete. If the crack development in repairs was finished early, then it may be possible to seal the crack earlier. As such, given that any crack formed on the repairs is to be sealed, P4 may be more suitable for repair work.

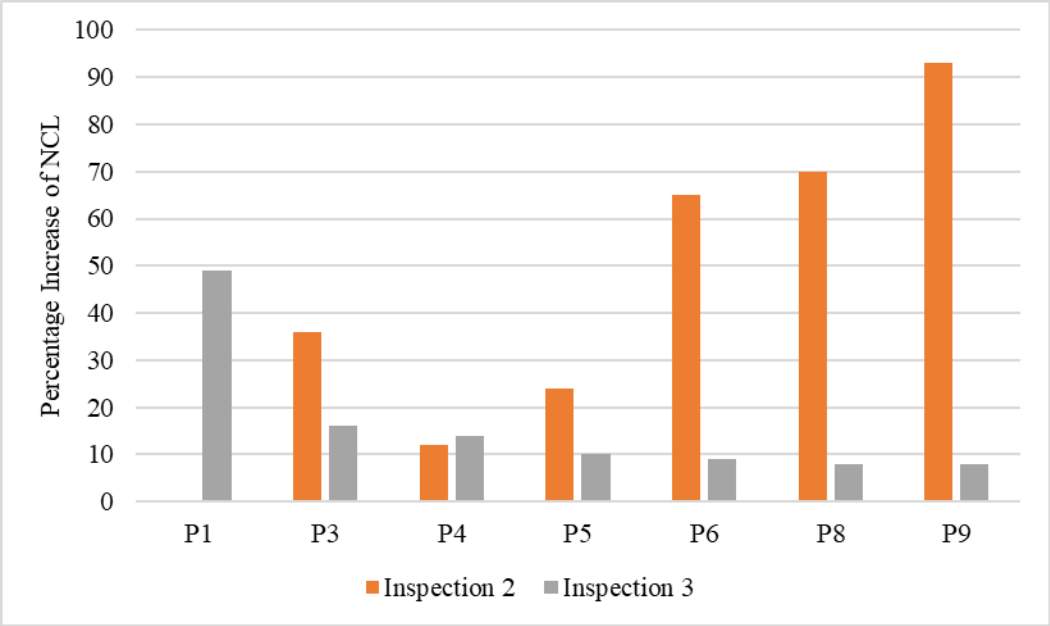

Figure 4.5 Percentage Increase of NCL by Second and Third Inspection

In addition to the cracks, some repairs with materials P1 (1 repair), P4 (5 repairs), P5 (2 repairs), P6 (4 repairs), and P8 (1 repair) developed delamination. No delamination was identified in repairs with P3 and P9. This is summarized in Table 4.4. An example of a repair with delamination is presented in Figure 4.6.

Table 4.4 Delamination in Repair Patch

Product	**P1**	**P2**	**P3**	**P4**	**P5**	**P6**	**P7**	**P8**	**P9**
Delamination?	YES	N/A	NO	YES	YES	YES	N/A	YES	NO

It should be noted that the repairs varied highly in size and shape as shown in Table 4.1 and Figure 4.2. Therefore, it is of interest to understand whether crack size was affecting the

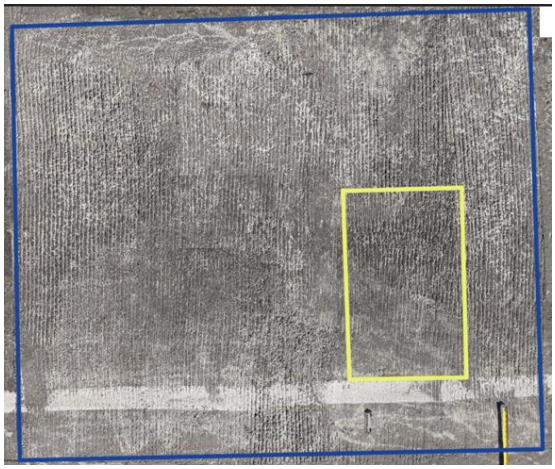

Figure 4.6 Delamination in a Repair Patch Marked with Yellow Box (P6)

crack formation in repairs. In Table 4.5, the repairs are categorized in four bins based on their size, and total summation of the crack length in each bin is presented. The black shaded cells in the table represent that, for that particular bin and material, that size of the repair has not been investigated. Some of the products are entirely absent from the field investigation phase. Due to these limitations, it is difficult to directly compare the field performance among products. In the next section, an attempt is made to identify the best laboratory test result to predict the field performance in terms of crack formation.

Table 4.5 Total Crack Length in Repairs Categorized According to Repair Size

	Inspection 1					Inspection 2					Inspection 3				
	Total Crack Length (inch)														
	< 10 ft²	10 to 20 ft²	20 to 30 ft²	30 to 40 ft²	> 40 ft²	< 10 ft²	10 to 20 ft²	20 to 30 ft²	30 to 40 ft²	> 40 ft²	< 10 ft²	10 to 20 ft²	20 to 30 ft²	30 to 40 ft²	> 40 ft²
P1	0	0	0	0		0	61.2	0	15.96		0	76.32	0	50.64	
P2															
P3	80.76	168		217.2		121.44	231.48		231.84		121.44	301.68		312.24	
P4	137.52	324.96	390.48			151.56	386.28	477.36			151.56	434.04	599.64		
P5	5.196				521.64	13.2				567.84	13.2				630.24
P6	0	27.36	37.08	328.92	97.2	0	83.88	98.04	412.2	123.6	0	83.88	98.04	473.04	137.28
P7															
P8	121.2	191.88	0			220.2	242.16	0			220.2	309.48	0		
P9			255.828	228.084				504.36	429.96				565.32	429.96	

4.3 Correlation Between Laboratory Test Results and Field Performance of Repair Products

To identify the most suitable laboratory test, linear regression analysis has been performed. For this purpose, the laboratory test results at 28th day and field performance (NCL) at the end of each investigation (third inspection) has been selected. In a bid to estimate the crack development, the linear regression equations were developed as a function of the laboratory test results. Not all the products were tested in the field. Products P1, P3, P4, P5, P6, P8 and P9 were used in bridge deck repair and monitored over time for crack development. P9 did not have laboratory data and so is not used in designing the prediction model. The regression models are presented in Figure 4.7. The highly scattered data, as shown in the plots, results in a poor correlation between the variables. This is true for all three inspections. One shortcoming of this analysis is the very limited size of dataset. This increases the difficulty to develop an accurate picture of the relationship between each variable and NCL. Table 4.6 presents the coefficient of determination, R^2, values for the regression models for different parameters. R^2 ranges from 0 to 1. An R^2 value of 1 indicates perfect correlation.

Table 4.6 Coefficient of Determination, R^2

Inspection	f'_c (psi)	$\sqrt{f'_c}$	E (ksi)	T (psi)	SER (kΩ-cm)	SSBS (psi)	Drying Shrinkage demolded at 4 hours (microstrain)	Drying Shrinkage demolded at 24 hours (microstrain)
1	0.4067	0.3877	0.3452	0.0997	0.2857	0.0310	0.1020	0.0002
2	0.6143	0.6021	0.4548	0.0127	0.3791	0.1694	0.0144	0.0483
3	0.5507	0.5381	0.4123	0.0229	0.3415	0.1367	0.0322	0.0253

Table 4.6 and Figure 4.7 illustrate that, based on these datasets, compressive strength is found to be the best predictor of early age cracking. In addition to the linear regression model, an attempt to develop a multivariate Ridge regression was made. However, it also fails to predict the field performance of the repair products based on the laboratory results with any significant level of certainty due to the limited dataset.

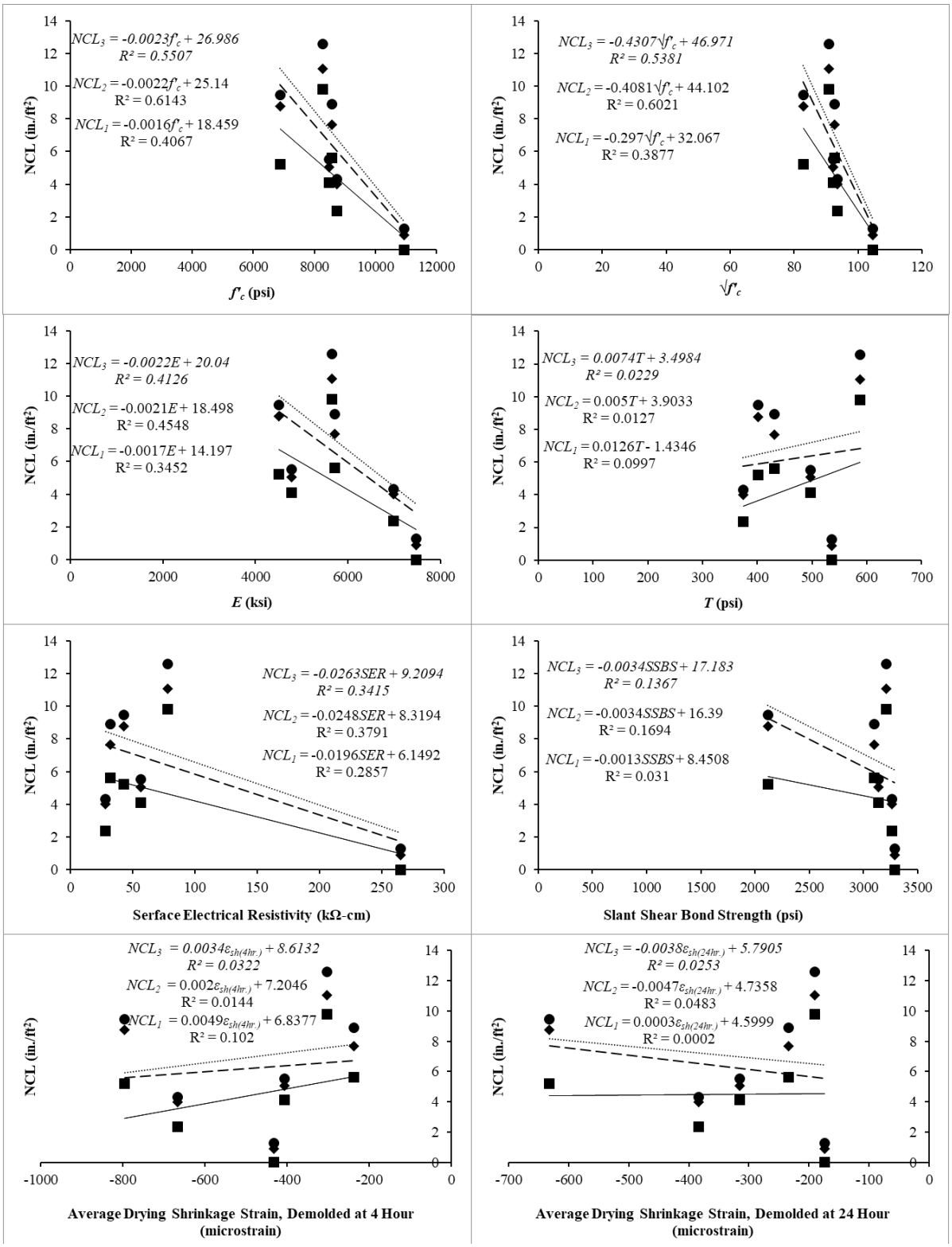

Figure 4.7 Correlation Between Laboratory Results and Normalized Crack Length (■- Inspection 1, ♦- Inspection 2, and ● Inspection 3)

5.0 CONCLUSIONS

As discussed in Sections 3 and 4, extensive laboratory and field investigation have been performed to quantify the comparative mechanical and shrinkage performances of the selected rapid repair materials. Based on these results, the following conclusions have been reached:

Setting Time: Initial and final setting times, two critical measurements for rapid repair products, have been measured through the penetration resistance by using a penetrometer. Products P3, P4, P6, and P8 had initial setting times below 30 minutes. P1 and P5 had initial setting times between 30 and 60 minutes. P2 and P7 had setting times longer than 60 minutes. P2 and P4 had the highest and the lowest working time, respectively. Most materials went from initial to final set in under 15 minutes, and materials commonly started to gain strength in less than 45 minutes.

Based on these results, P1, P3, P4, P5, P6, and P8 have been categorized as quick setting products. These materials are more suitable when the size and quantity of batches are small. P2 and P7 are categorized as normal setting materials. When the repair area is large and the ambient temperature is high, normal setting materials are recommended.

Compressive Strength: The materials were categorized in three different SHRP categories based on their average compressive strengths. These categories are Very Early Strength (VES), High Early Strength (HES), and Very High Strength (VHS). All the products achieved at least 3,000 psi compressive strength within 4 hours. As such, all of the products meet the requirement of VES category. All but product P3 are classified as HES materials as their compressive strengths were at least 5,000 psi after 24 hours. Only two of the products, P1 and P3, can be categorized as VHS material as they developed more than 10,000 psi strength in 28 days.

As SHRP classification is helpful in terms of deciding on the repair volume and speed of reopening the pavement to traffic, these categories can be utilized to choose a specific product for specific projects. All the products, as they fall in VES category, are a good choice for a small repair area. All of HES products can be utilized for repair work when traffic needs to be opened in 24 hours. Among the products investigated for this research, only P3 does not fall into this category. P1 and P2 are recommended when the substrate compressive strength is high.

Static Modulus of Elasticity: For structural compatibility, the repair material is required to have a modulus of elasticity close to that of the substrate. Assuming a typical normal-weight concrete for a bridge deck (substrate) and considering the age of the substrate, a desirable range of elastic modulus should be between 4,000 ksi to 5,000 ksi. Only three materials (P1, P2, and P7) achieved that level of modulus of elasticity within 4 hours (the time of exposure to traffic). All of the products had a modulus of elasticity over 4,000 ksi at late stages (7 days and 28 days). It should be noted that P5 and P8 were the only materials that fell in the desired range of elastic modulus at late stage. Modulus of elasticity values for all other products were over 5,000 ksi at 28^{th} day.

However, high elastic modulus is not necessarily favorable in terms of structural-compatibility, as higher stiffness means attracting higher loads, higher shrinkage potential, and improper distribution of stresses in the repair-substrate system.

Splitting Tensile Strength: For a repair material installed on a substrate made of normal-weight concrete, the tensile strength of at least 400 psi is deemed acceptable. All but P6 achieved that level of splitting tensile strength at late stage. Products P2, P4, and P5 were the only materials which achieved sufficient tensile strength at 4 hours. All the products, except P3, P6, and P7, failed to gain the desired tensile strength within 24 hours. Only the materials containing fibers (P1, P5, and P8) displayed ductile failures.

Surface Resistivity: At the critical age of 4 hours, P1, P2, and P3 registered a moderate chloride penetration potential based on the result from surface electrical resistivity test. P6 had a low chloride penetration potential. All other product had very low chloride penetration potential. Interestingly, P1 displayed exceptional development of chloride penetration potential and was the only product to have a negligible long-term chloride penetration. Other products failed to gain noticeable surface electrical resistivity beyond initial stage.

Slant Shear Bond Strength: ASTM C 928 specifies that a rapid-set prepacked repair product should have a required bond strength of 1000 and 1500 psi at 1 and 7 days, respectively. All materials, except for P3, had a slant shear bond strength of over 1,500 psi at 4 hours, whereas the required bond strength at 24 hours was 1,000 psi. At 24 hours, all materials but P3 had a slant shear bond strength of over 2,000 psi, twice the required slant shear bond strength at 24 hours

and exceeding the required strength of 1,500 psi at 7 days. Nevertheless, P3 still satisfied the required slant shear bond strength at 24 hours. P5 and P8 exhibited higher proportions of bond failures.

Shrinkage: All materials generally had a satisfactory performance but with different trends of autogenous (sealed) or drying shrinkage development. It should be noted that autogenous strain measurement was only taken for three materials (P4, P6, and P7) as only these materials did not contain fiber and/or aggregates. When autogenous shrinkage measurements were taken on material containing fiber, the results varied so significantly that taking an average was impossible. Materials with higher working time developed lower autogenous deformation.

All materials performed satisfactorily in terms of free drying shrinkage. The maximum shrinkage was less than 800 microstrain in P7 and P8, 600 microstrain in P6, and less than 400 microstrain in the remaining materials, well below the ASTM C928 limit of 1,500 microstrain. Aggregate extension significantly reduced the free drying shrinkage of material as the extension reduced the paste portion of the mixture.

All material, except for P7, remained uncracked during 28-day restrained ring shrinkage tests. P7 cracked after about 2 days when demolded at 4 hours, and after about 5 days when demolded at 24 hours. P1 exhibited the best restrained shrinkage performance overall.

Field Investigation: Based on the field investigation on repair materials placed on a concrete bridge deck, P1 developed the least amount of shrinkage cracking. In terms of total crack development, P4 performed the worst among the rapid repair materials used on this deck. Crack development of P4 was mostly complete by the first inspection. For all of the products, sealing of cracks may be required in the future. Therefore, the product which finished the crack formation the earliest can be more suitable, as those repairs can be sealed earlier. But due to significant variation in size and shape of repair area, and high variability in ambient condition during pouring on the deck, the laboratory performances of the materials, under controlled temperature and humidity, are more reliable indicators to compare the performance of the materials.

Based on the linear regression models, although no strong correlation between the laboratory tests and field performance could be established, compressive strength was found to

be the best predictor of early age cracking. A multivariate Ridge regression also failed to provide any meaningful correlation, which was attributed to the limited dataset.

It should be noted that only early age cracking of repairs has been studied for this project. In the long term, these repairs are exposed to repeated thermal and mechanical loading cycles. In such scenarios, the long-term performance of the repairs may very well be different.

Overall, and based on the lab performance and the field investigations provided in this report, P1 and P8 show the best and the worst performance in terms of both mechanical and durability properties, respectively.

REFERENCES

[1] ACI 546.3R-14 (2014) "Guide to materials selection for concrete repair" *American Concrete Institute*, 1-72.

[2] Ram, P. V., J. Olek, and J. Jain (2013) "Field trials of rapid-setting repair materials" Publication FHWA/IN/JTRP-2013/02. *Joint Transportation Research Program,* Indiana Department of Transportation and Purdue University, West Lafayette, Indiana.

[3] Cervo, N. M., & Schokker, A. J. (2010) "Bridge Deck Patching Material Evaluation" *ASCE Journal of Bridge Engineering, 15(6),* 723-730.

[4] Quezada, I., Thomas, R.J., Maguire, M. (2019), "Rapid Concrete Repair", Report No. UT-19.08, Utah Department of Transportation, Salt Lake City, Utah.

[5] Barde, A., Parameswaran, S., Chariton, T., Weiss, J., and Cohen, M. D. (2006) "Evaluation of rapid setting cement-based materials for patching and repair" Publication FHWA/IN/JTRP/2006-11. *Joint Transportation Research Program*, Indiana Department of Transportation and Purdue University, West Lafayette, Indiana.

[6] Wilson, T.P., Smith, K.L., and Romine, A.R. (1999) "Materials and procedures for rapid repair of partial-depth spalls in concrete pavements - Manual of Practice" FHWA Report No. FHWA-RD-99-152, *Federal Highway Administration*, U.S. Department of Transportation.

[7] Yang, Z., Brown, H., Huddleston, J., and Seger, W., (2016) "Performance evaluation of rapid-set prepackaged cementitious materials for rehabilitation of surface distress of concrete transportation structures" *PCI Journal*, March-April 2016, pp. 81-96.

[8] Quezada, I. (2018) "Investigating rapid concrete repair materials and admixtures" *Ph.D. Dissertation Thesis*, Utah State University, Logan, Utah, USA.

[9] Richards, J.P., Xi Y. (2006) “An experimental study on rapid setting concrete repair materials” In: Gdoutos E.E. (eds) *Fracture of Nano and Engineering Materials and Structures*, Springer, Dordrecht

[10] Lee, B. J., and Kim, Y. Y., (2018) “Durability of latex modified concrete mixed with a shrinkage reducing agent for bridge deck pavement” *International Journal of Concrete Structures and Materials*, *12(2)*, 2018.2, 259-267.

[11] Li, M., and Li, V. C. (2009) “Influence of material ductility on the performance of concrete repair” *ACI Materials Journal*, *106(5)*, pp. 419-428.

[12] Li, J., Xu, G., Chen, Y., and Liu, G. (2014) “Multiple scaling investigation of magnesium phosphate cement modified by emulsified asphalt for rapid repair of asphalt mixture pavement” *Constr. Build. Mater.*, *69*, 346−350.

[13] Kastiukas, G., Zhou, X.M., Castro-Gomes, J., Huang, S., and Saafi, M. (2015) “Effects of lactic and citric acid on early-age engineering properties of Portland/calcium aluminate blended cements” *Constr. Build. Mater, 101*, 389–395.

[14] Won, J. P., Kim, J. M., Lee, S. J., Lee, S. W., and Park, S. K. (2011) “Mix proportion of high-strength, roller-compacted, latex-modified rapid-set concrete for rapid road repair” *Constr. Build. Mater., 25*, 1796–1800.

[15] Wang, Y., Kong, L., Chen, Q., Laud, B., and Wang, Y. (2017) “Research and application of a black rapid repair concrete for municipal pavement rehabilitation around manholes” *Constr. Build. Mater., 150*, 204-213.

[16] Song, L., Li, Z., Duan, P., Huang, M., Hao, X., and Yu, Y. (2017) “Novel low cost and durable rapid-repair material derived from industrial and agricultural by-products” *Ceram. Int., 43(16)*, 14511-14516.

[17] Roy, M., Ray, I., and Davalos, J. F. (2013) “High-performance fiber-reinforced concrete: development and evaluation as a repairing material” *ASCE J. Mater. Civ. Eng*., *26*, 04014074.

[18] Yue, L. and Bing, C. (2015) "New type of super-lightweight magnesium phosphate cement foamed concrete" *ASCE J. Mater. Civ. Eng*., *27(1)*, 0001044.

[19] Ghasemzadeh, F., Sajedi, S., Shekarchi, M., Layssi, H., and Hallaji, M. (2013) "Performance evaluation of different repair concretes proposed for an existing deteriorated jetty structure" *ASCE J. Perform. Constructed Facil., 28 (4),* pp. 1-10.

[20] Laskar, S.M., and Talukdar, S. (2017) "Development of ultrafine slag-based geopolymer mortar for use as repairing mortar" *ASCE J. Mater. Civil Eng., 29 (5),* 0001824.

[21] ASTM Standard C125 − 15a, (2015) "Standard terminology relating to concrete and concrete aggregates" *ASTM International*, West Conshohocken, Pennsylvania.

[22] Jeon, S., Nam, J.H., An, J.H., and Kwon, S.A. (2009) "Physical properties of rapid-setting concrete using ultra fine fly ash" *ASCE GeoHunan International Conference*, August 3-6, 2009, Changsha, Hunan, China.

[23] Emmons, E., Vaysburd, A., & McDonald, J. (1993) "A rational approach to durable concrete repairs" *Concrete International, 15*(9), 40-45.

[24] Mangat, P. S., and Limbachiya, M. K. (1995) "Repair material properties which influence long-term performance of concrete structures" *Constr. Build. Mater., 9*(2), 81-90.

[25] Talbolt, C., Pigeon, M., Beaupré, D., & Morgan, D. (1994) "Influence of surface preparation on long term bonding of shotcrete" *ACI Materials Journal, 91*(6), 560-566.

[26] Courard, L., Piotrowski, T., & Garbacz, A. (2014) "Neat-to-surface properties affecting bond strength in concrete repair" *Cement & Concrete Composites, 46*, 73-80.

[27] Momayez, A., Ramezanianpour, A., Rajaie, H., & Ehsani, M. (2004) "Bi-Surface Shear Test for Evaluating Bond between Existing and New Concrete" *ACI Materials Journal, 101*(2), 99-106.

[28] ASTM Standard C1583/C1583M, (2013) “Standard test method for tensile strength of concrete surfaces and the bond strength or tensile strength of concrete repair and overlay materials by direct tension (Pull-off method)” *ASTM International*, West Conshohocken, PA.

[29] ASTM Standard C882/C882M – 13a, (2013) “Standard test method for bond strength of epoxy-resin systems used with concrete by slant shear” *ASTM International*, West Conshohocken, PA.

[30] Soliman, H., and Shalaby, A. (2014) “Characterizing the Performance of Cementitious Partial-Depth Repair Materials in Cold Climates,” *Constr. Build. Mater.*, *70*, 148-157.

[31] Morgan, D. (1996) “Compatibility of concrete repair materials and systems” *Construction and Building Materials*, 57-67.

[32] ASTM Standard C157/C157M, (2014) “Standard test method for length change of hardened hydraulic-cement mortar and concrete” *ASTM International*, West Conshohocken, PA.

[33] ASTM Standard C1581/C1581M − 09a, (2009) “Standard test method for determining age at cracking and induced tensile stress characteristics of mortar and concrete under restrained shrinkage” *ASTM International*, West Conshohocken, PA.

[34] http://germann.org/products-by-application/autogenous-shrinkage/autogenous-shrinkage

[35] ASTM Standard C1698, (2014) “Standard test method for autogenous strain of cement paste and mortar” *ASTM International*, West Conshohocken, PA.

[36] Yang, Z., Brown, H., Huddleston, J., and Seger, W., (2016) “Restrained Shrinkage Cracking and Dry Shrinkage of Rapid-Set Prepackaged Cementitious Materials” *ASCE J. Mater. Civ. Eng., 28(6):* 04016014.

[37] ASTM Standard C928/C928M, (2013) “Standard specification for packaged, dry, rapid-hardening cementitious materials for concrete repairs” *ASTM International*, West Conshohocken, PA.

[38] Hwang, S.D., and Khayat, K.H., (2008) "Effect of mixture composition on restrained shrinkage cracking of self-consolidating concrete used in repair" *ACI Mater J, 105 (5)*, pp. 499-509.

[39] Myintlay, K. (2007) "Early age shrinkage and bond at interface between repair material and concrete substrate" *Ph.D. Dissertation Thesis*, National University of Singapore, Singapore.

[40] ASTM Standard C531 - 00, (2012) "Standard specification for linear shrinkage and coefficient of thermal expansion of chemical-resistant mortars, grouts, monolithic surfacings, and polymer concretes" *ASTM International*, West Conshohocken, PA.

[41] Ghazy, A., and Bassuoni, M. T., (2017) "Shrinkage of nanomodified fly ash concrete as repair material" *ACI Materials Journal, 114(6)*, 877-888.

[42] Choi, P., and Yun, K.K., (2014) "Experimental analysis of latex-solid content effect on early age and autogenous shrinkage of very-early strength latex-modified concrete" *Constr. Build. Mater., 65*, 396–404.

[43] Mansi, A. S., Abdulhameed, H. A., and Yong, Y. K. (2018) "development of low-shrinkage rapid set composite and simulation of shrinkage cracking in concrete patch repair" *ASCE International Conference on Transportation and Development*, July 15-18, 2018, Pittsburgh, Pennsylvania, USA.

[44] ASTM Standard C666/C666M – 15 (2015) "Standard test method for resistance of concrete to rapid freezing and thawing" *ASTM International*, West Conshohocken, PA.

[45] ASTM Standard C418 – 12 (2012) "Standard test method for abrasion resistance of concrete by sandblasting" *ASTM International*, West Conshohocken, PA.

[46] Moffatt, E. G., and Thomas, M. D. A. (2018) "Durability of Rapid-Strength Concrete Produced with Ettringite-Based Binders" *ACI Materials Journal, 116(1)*, 105-115.

[47] Moffatt, E. G., and Thomas, M. D. A. (2017) "Performance of rapid-repair concrete in an aggressive marine environment" *Constr. Build. Mater., 132,* 478-486.

[48] Maler, M., Najimi, M., and Ghafoori, N. (2017) "Frost resistance of high early-age strength concretes for rapid repair" *ASCE 17th International Conference on Cold Regions Engineering*, September 10-13, 2017, Duluth, Minnesota, USA.

[49] Yeon, J., Kang, J., and Yan, W. (2018) "Spall damage repair using 3D printing technology" *Autom. Constr., 89,* 266–274.

[50] ASTM C39 "Standard Test Method for Compressive Strength of Cylindrical Concrete Specimens", *ASTM International, West Conshohocken, PA*

[51] ASTM C496 "Standard Test Method for Splitting Tensile Strength of Cylindrical Concrete Specimens", *ASTM International, West Conshohocken, PA*

[52] Olufunke, A. (2014) "A Comparative Analysis of Modulus of Rupture and Splitting Tensile Strength of Recycled Aggregate Concrete" *American Journal of Engineering Research (AJER), 3(2),* 141-147.

[53] ASTM C 469 "Standard Test Method for Static Modulus of Elasticity and Poisson's Ratio of Concrete in Compression", *ASTM International, West Conshohocken, PA*

[54] AASHTO TP 95 "Standard Method of Test for Surface Resistivity Indication of Concrete's Ability to Resist Chloride Ion Penetration", *Association of State and Highway Transportation Officials.*

[55] Kessler, R.J., Powers, R.G., Vivas, E., Paredes, M.A., and Virmani Y.P. (2008) "Surface Resistivity as an Indicator of Concrete Chloride Penetration Resistance" *Concrete Bridge Conference,* St. Louis, Missouri, May 4-7.

[56] ASTM C403 "Standard Test Method for Time of Setting of Concrete Mixtures by Penetration Resistance", *ASTM International, West Conshohocken, PA*

[57] AASHTO T 334, “Standard Method of Test for Estimating the Cracking Tendency of Concrete”, *American Association of State and Highway Transportation Officials.*

[58] UDOT (2004), “Concrete Fast Set Repair Materials Bond (Slant/Shear) Test”, *Materials Manual and Instruction,* Section 976

[59] Quezada, I., Thomas, R. J., and Maguire, M., "Internal Curing to Mitigate Cracking in Rapid Set Repair Media*." Advances in Civil Engineering Materials* 7.4 (2018): 660-671.

APPENDIX A: RESTRAINED RING SHRINKAGE TEST DATA

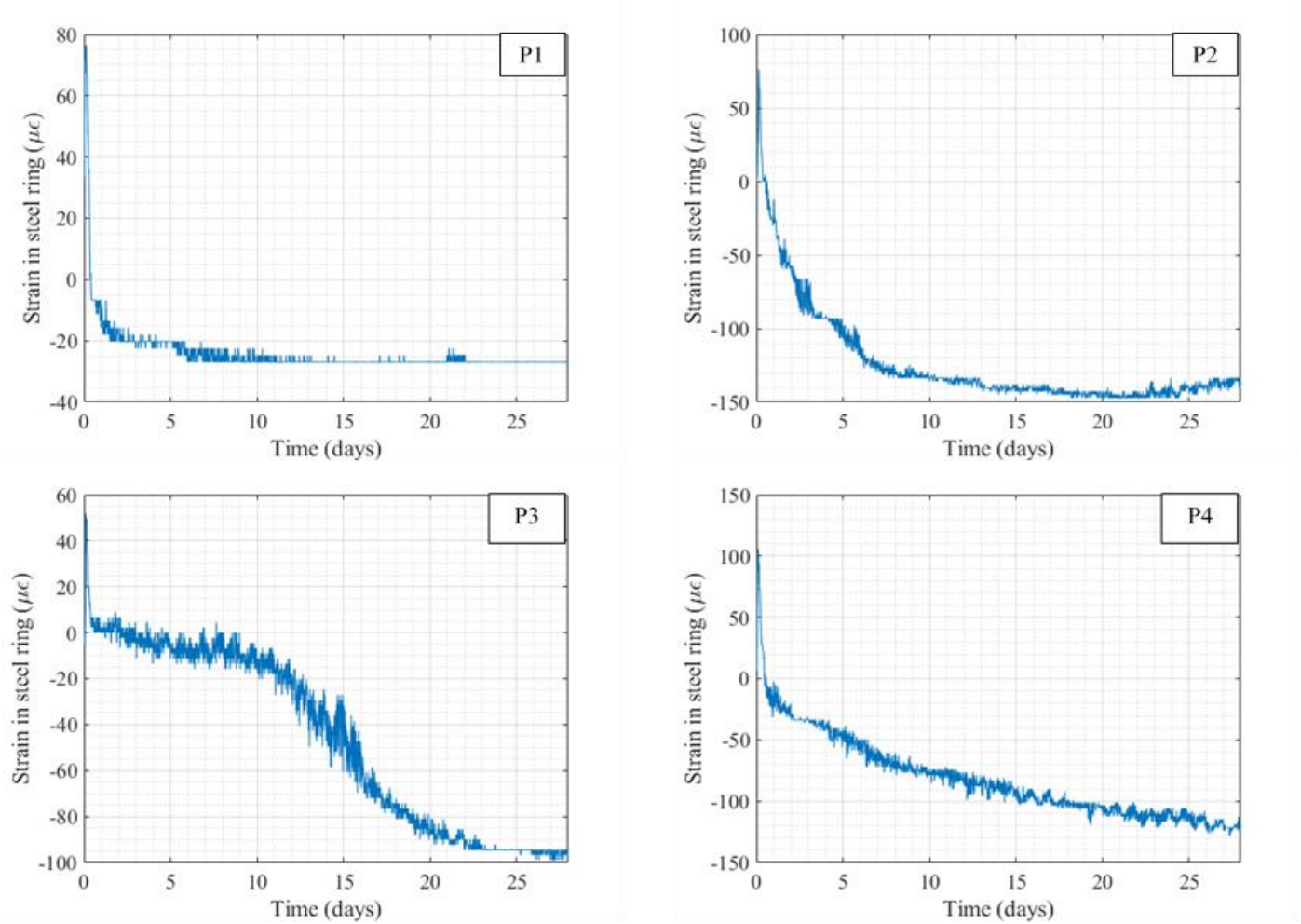

Figure A.1 Average Strain in Steel Ring for P1, P2, P3, and P4 (Outer Form Removed at 4-Hour Age)

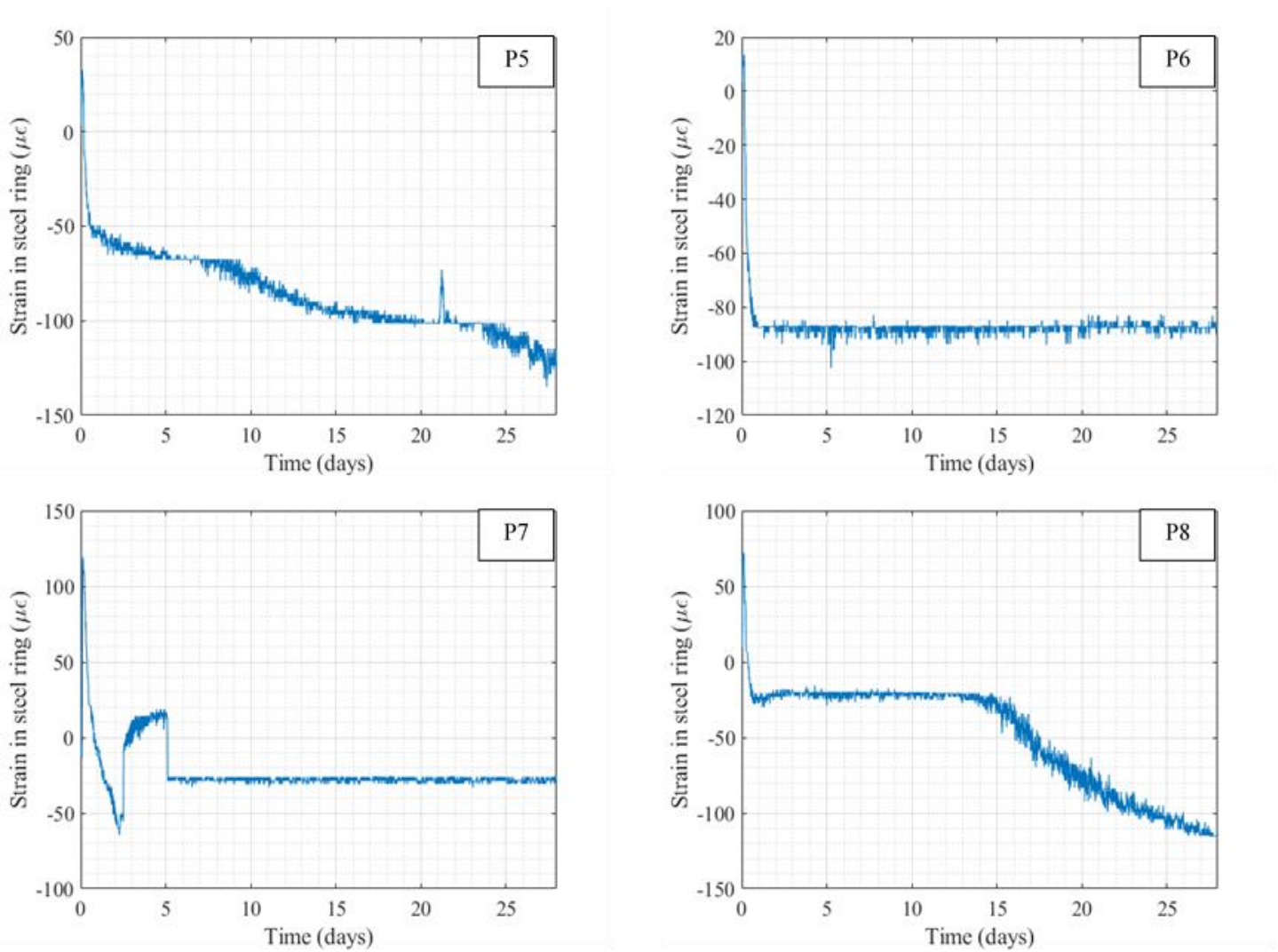

Figure A.2 Average Strain in Steel Ring for P5, P6, P7, and P8 (Outer Form Removed at 4-Hour Age)

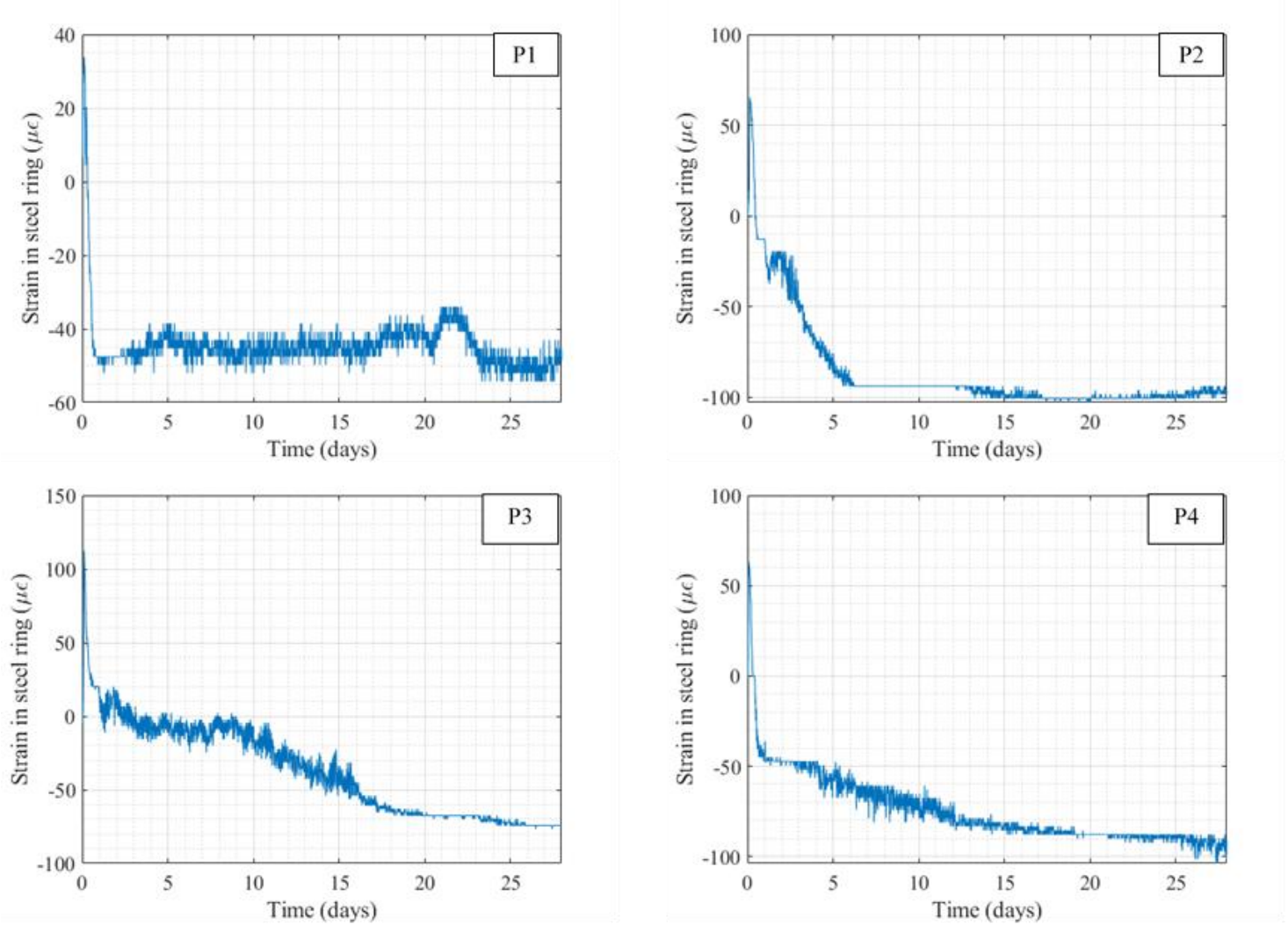

Figure A.3 Average Strain in Steel Ring for P1, P2, P3, and P4 (Outer Form Removed at 24-Hour Age)

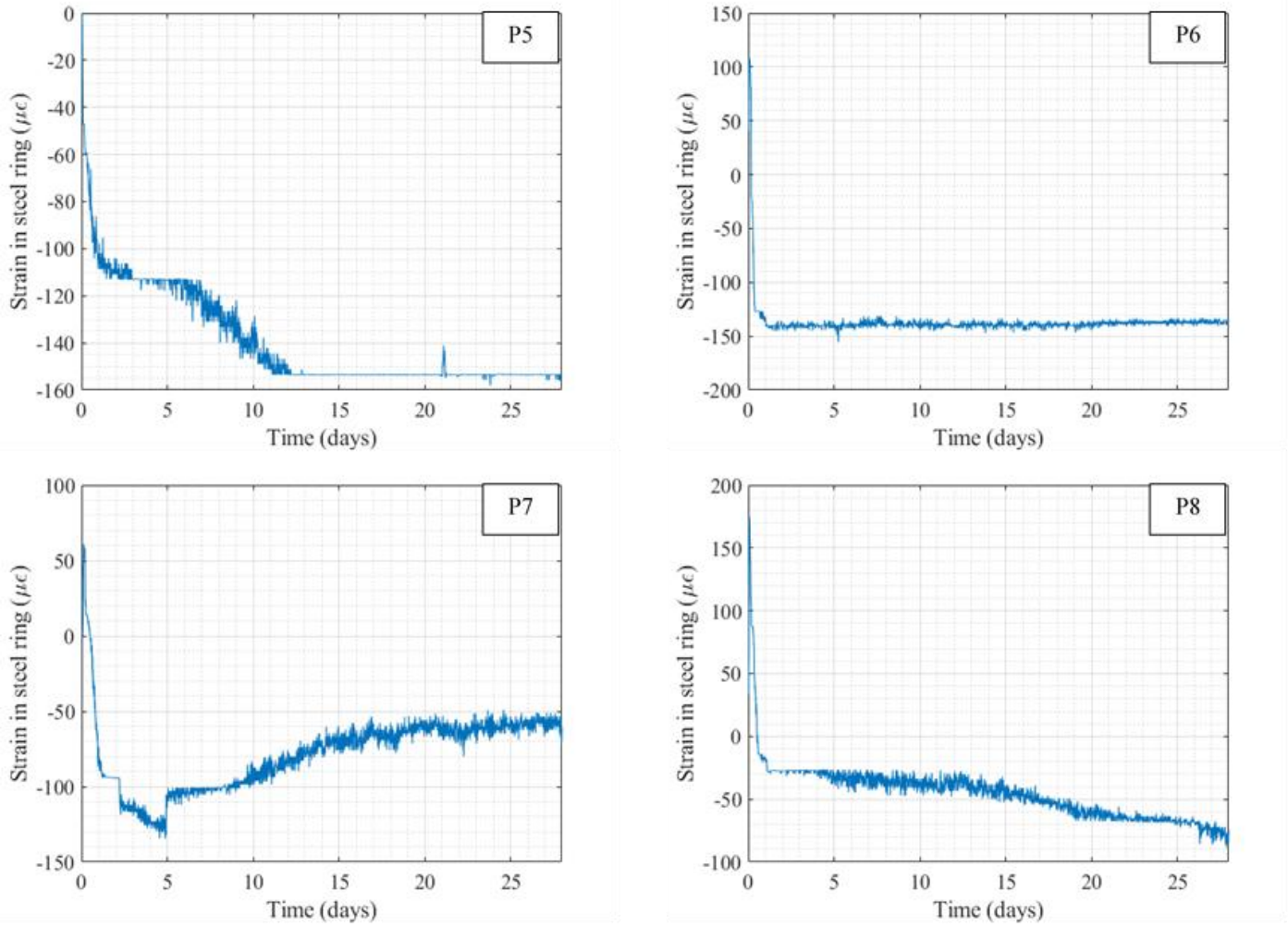

Figure A.4 Average Strain in Steel Ring for P5, P6, P7, and P8 (Outer Form Removed at 24-Hour Age)

APPENDIX B: FIELD INVESTIGATION PICTURES AND REPAIR INFORMATION

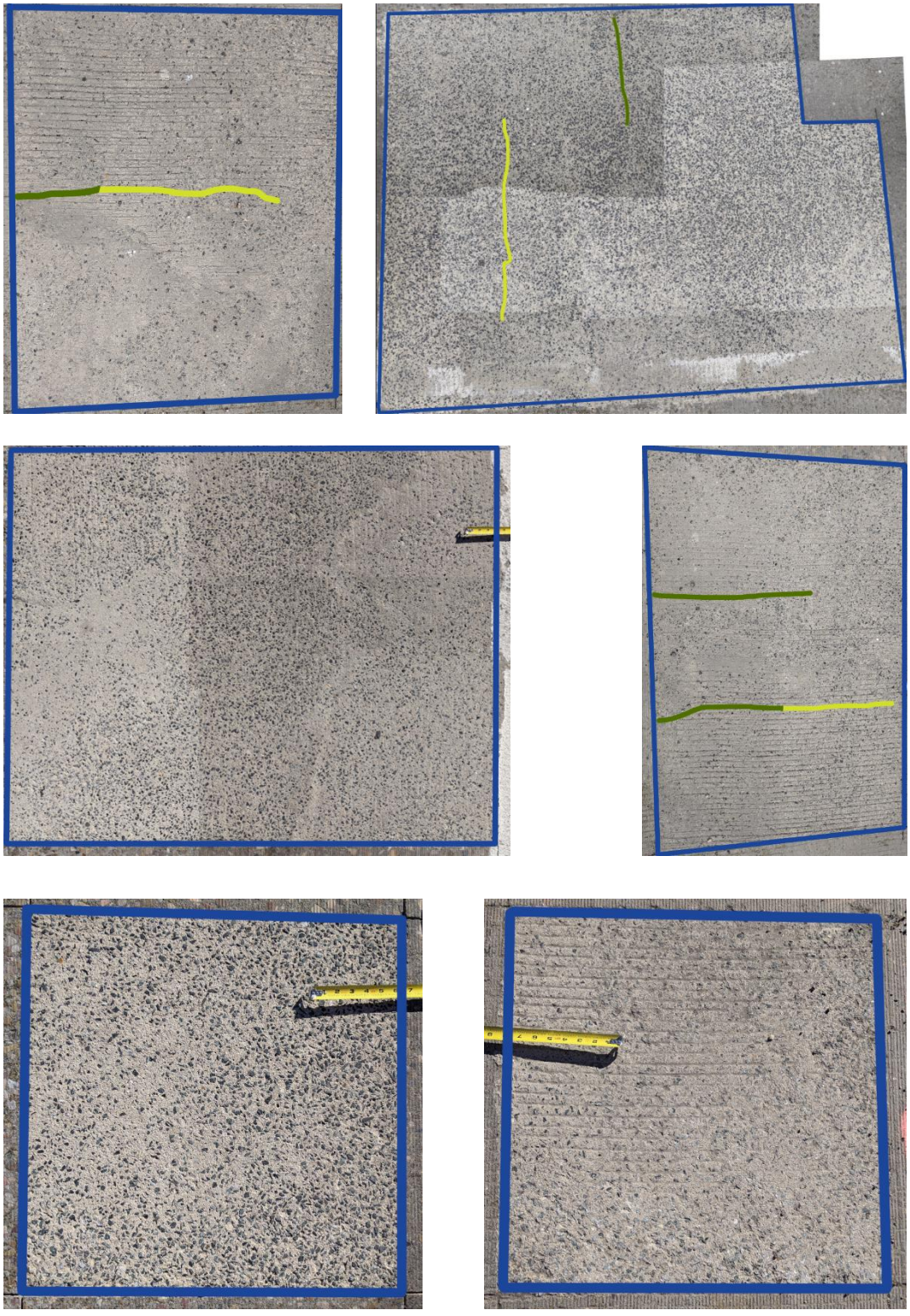

Figure B.1 Crack Formation in Patches with P1 during First (Red), Second (Green), and Third (Yellow) Inspection

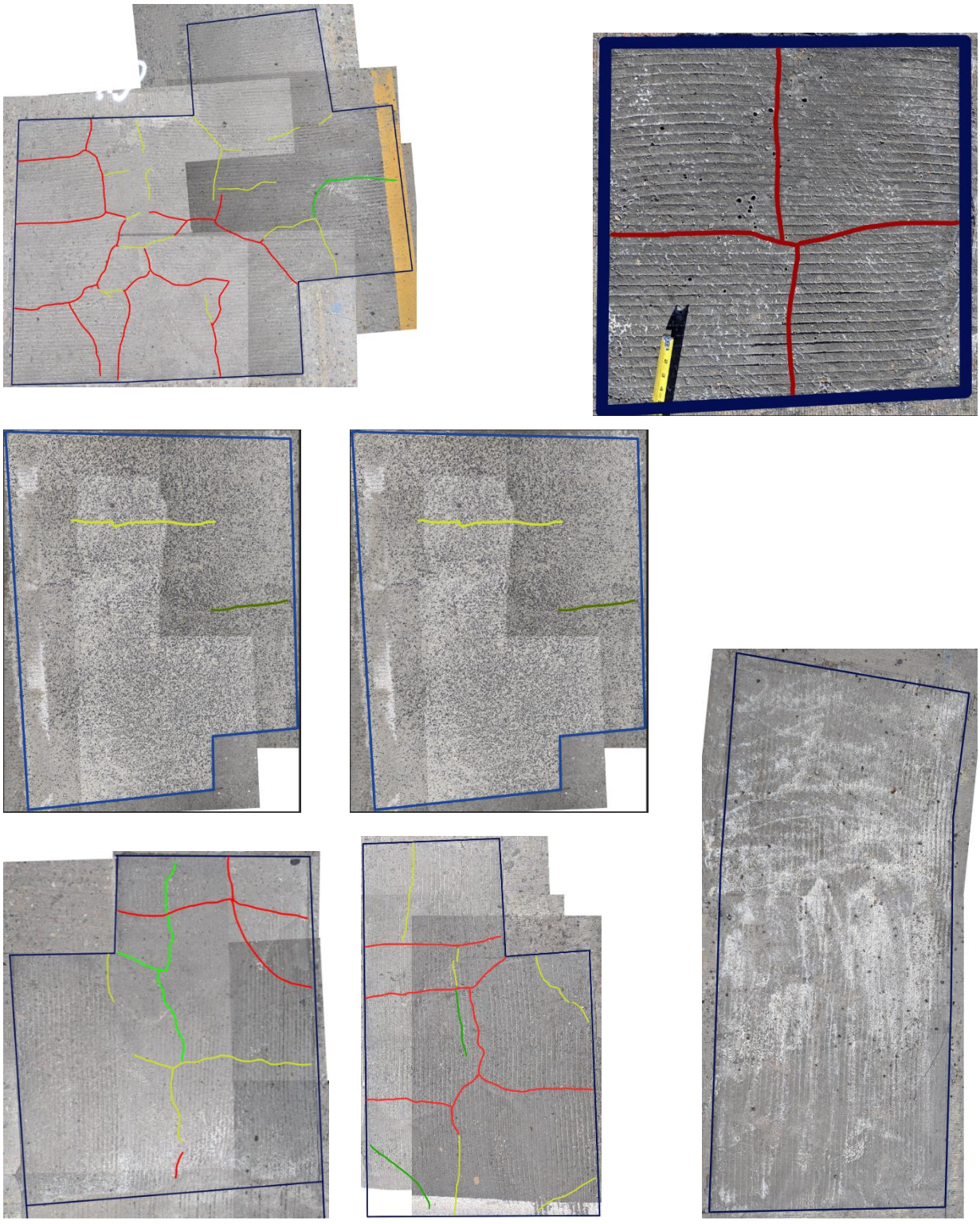

Figure B.2 Crack Formation in Patches with P3 during First (Red), Second (Green), and Third (Yellow) Inspection

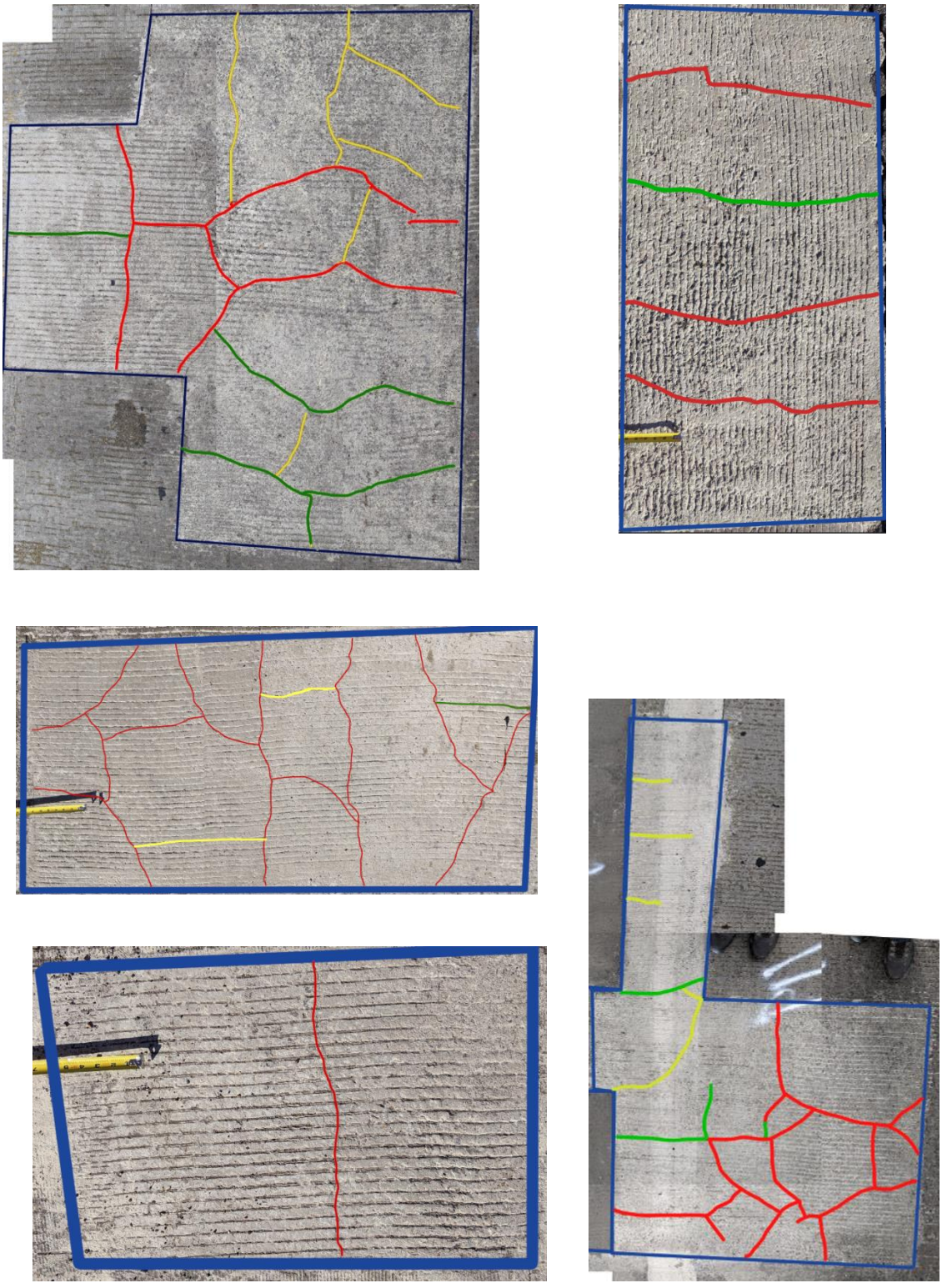

Figure B.3 Crack Formation in Patches with P4 during First (Red), Second (Green), and Third (Yellow) Inspection

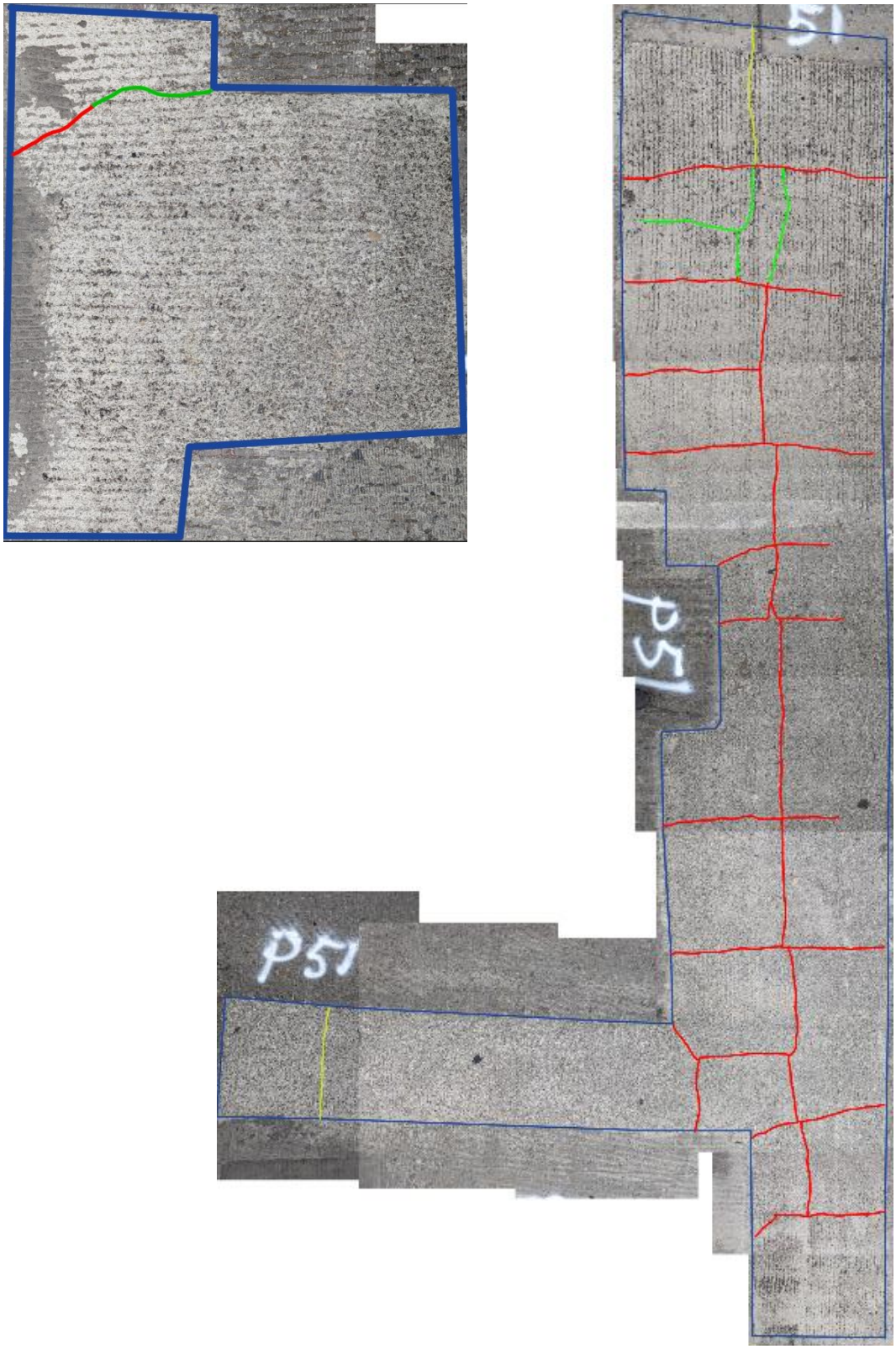

Figure B.4 Crack Formation in Patches with P5 during First (Red), Second (Green), and Third (Yellow) Inspection

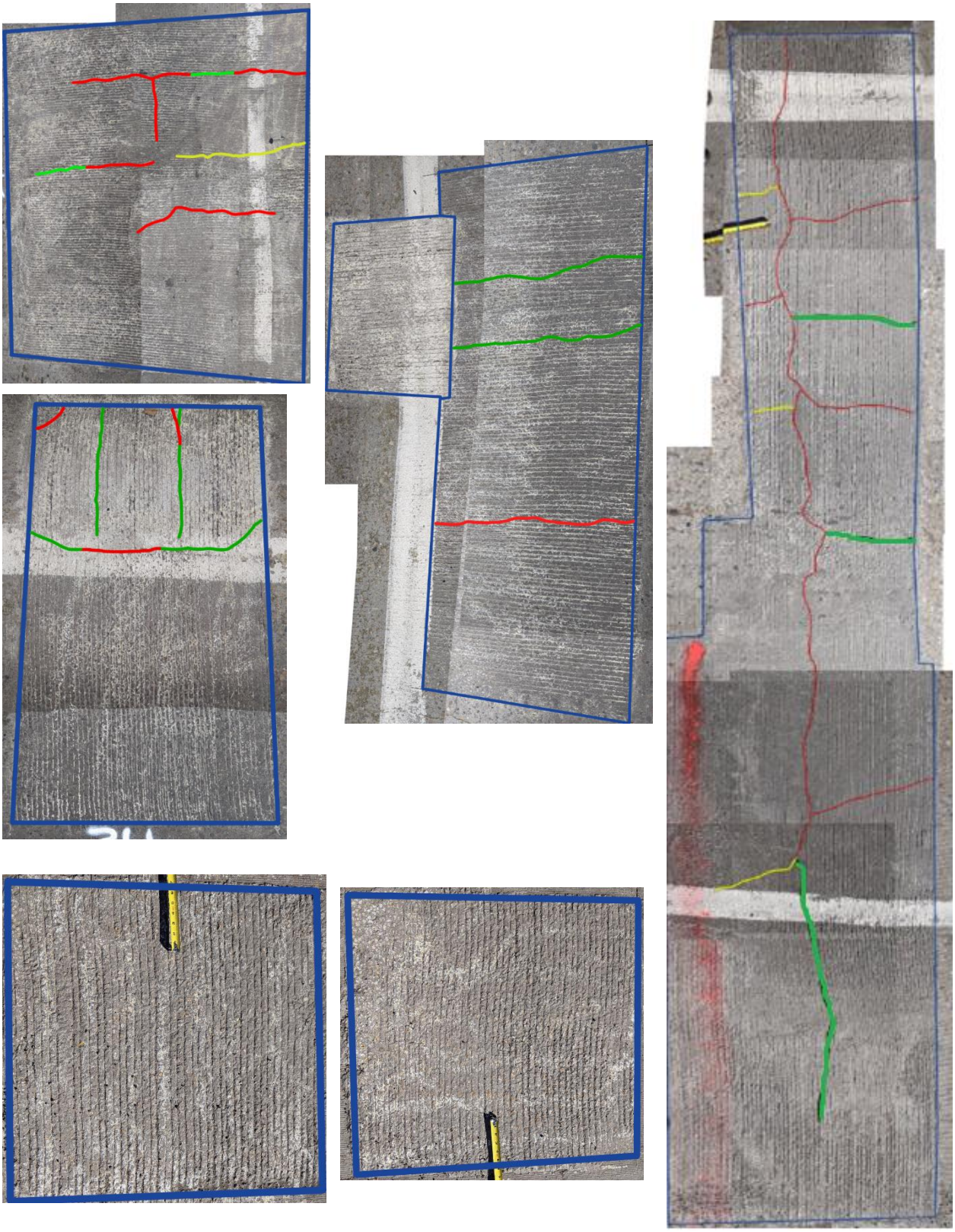

Figure B.5 Crack Formation in Patches with P6 during First (Red), Second (Green), and Third (Yellow) Inspection

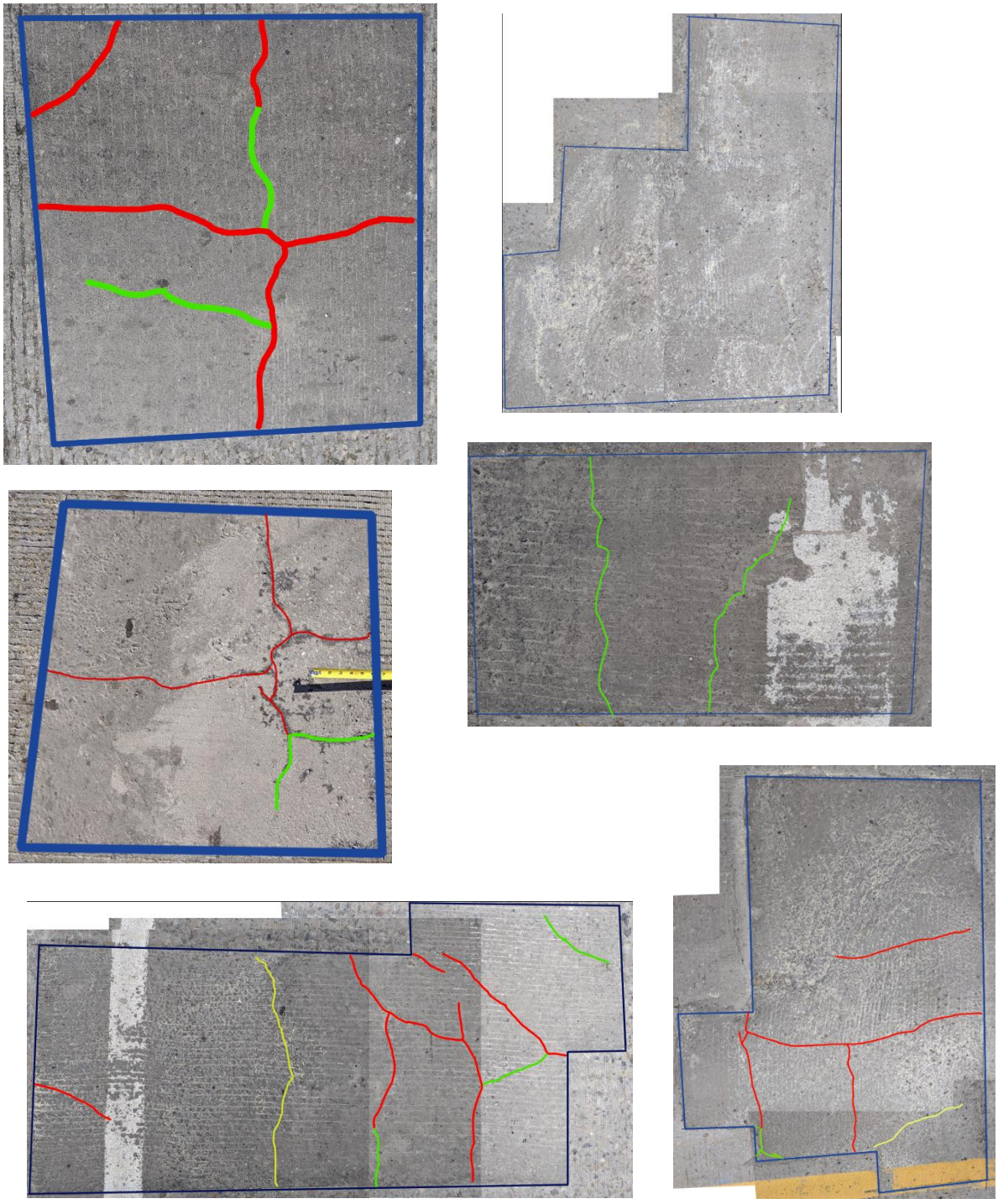

Figure B.6 Crack Formation in Patches with P8 during First (Red), Second (Green), and Third (Yellow) Inspection

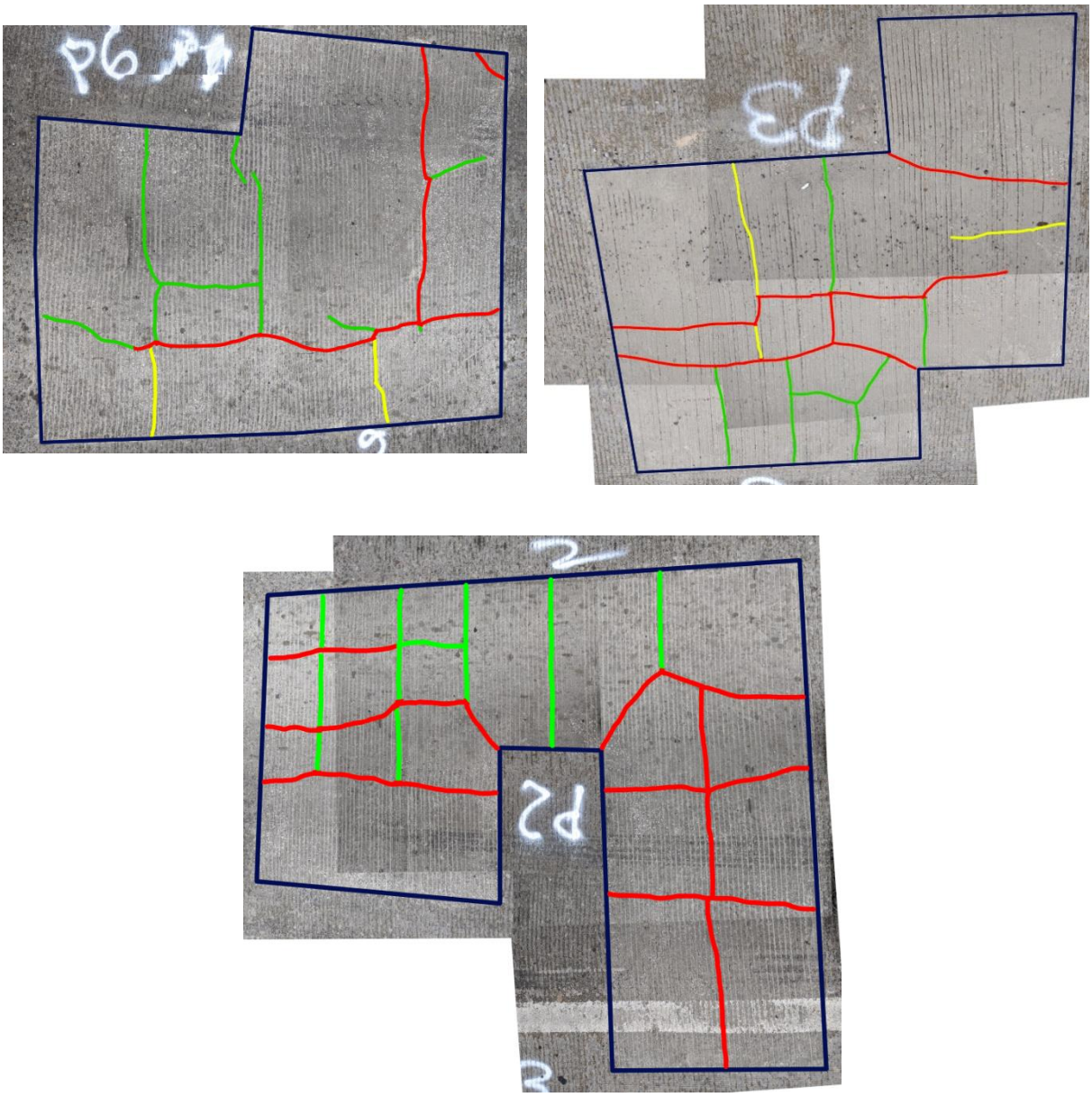

Figure B.7 Crack Formation in Patches with P9 during First (Red), Second (Green), and Third (Yellow) Inspection

Table B.1 Details of Repair Work (Phase 1)

Pothole	Area (SF)	Average Depth (IN)	Material Type	Notes
1	16.33	3.5	Dayton HD50	
2	2.11	2	Dayton HD50	
3	75.98	3.5	Dayton HD50	
4	34.14	3.75	Dayton HD50	
5	5.63	4	Dayton HD50	
6	7.88	3.5	Dayton HD50	
7	24.14	4	Dayton HD50	
8	2.60	4	Dayton HD50	
9	2.11	3	Dayton HD50	
10	12.51	3.5	Dayton HD50	
11				Combined with 7
12	18.81	4	Dayton HD50	
13	15.14	3.5	Dayton HD50	
14	6.71	3	Dayton HD50	
15	18.06	3.5	Dayton HD50	
16	12.65	3.5	Sika 421	
17	35.32	3.5	Sika 421	
18	3.50	3	Dayton HD50	
19	18.59	4	Sika 421	
20	32.05	3.75	Sika 421	
21	5.44	3.5	Sika 421	
22	17.65	3.5	Sika 421	
23	18.58	4	Sika 421	
24	10.63	4	Sika 421	
25	36.02	3.5	Sika 421	
26	4.08	3.5	Sika 421	
27	76.68	2.75	Sika 421	1-Jul
28	118.92	4	Sika 421	
29	14.72	3.5	Sika 421	1-Jul
30	16.49	4	Sika 421	1-Jul
31	27.93	3.5	Sika 421	1-Jul
32	30.47	3.5	Sika 421	1-Jul
33	613.75	3	Rapid Set Volumetric	
34	2.50	2	Sika 421	1-Jul
35	29.54	3	Rapid Set	
36	15.57	3.75	Sika 421	1-Jul
37			Rapid Set Volumetric	Combined with P33/Error

Pothole	Area (SF)	Average Depth (IN)	Material Type	Notes
38			Rapid Set Volumetric	Combined with P33/Error
39	6.04	3	Rapid Set	
40	9.68	3	Rapid Set	
41	6.37	2.5	Rapid Set Volumetric	
42	81.10	3	Rapid Set Volumetric	
43	3.20	2.5	Rapid Set	
44	335.35	3	Rapid Set Volumetric	
45	92.40	3	Rapid Set Volumetric	
46	6.05	3	Rapid Set	
47	8.45	3	Rapid Set	
48				Combined with P45
49				Combined with P45
50	7.20	3	Rapid Set	
51	70.47	5	Rapid Set Volumetric	
52				Combined with P45
53	1.56	2	Rapid Set	
54	6.25	2.5	Rapid Set	
55	21.99	3	Rapid Set	
56	12.50	3.5	Rapid Set	

Table B.2 Details of Repair Work (Phase 2)

Pothole	Area (SF)	Average Depth (IN)	Material Type	Notes
57	16.52	3.5	Sika 421	
58	3.43	2.5	Sika 421	
59	4.38	3	Sika 421	
60	9.75	3	Sika 421	
61	9.88	3	Dayton HD50	
62	9.11	3	Dayton HD50	
63	7.80	2.5	Dayton HD50	
64	5.06	3	Dayton HD50	
65	4.38	2.5	Dayton HD50	
66	2.24	2.5	Dayton HD50	
67	5.42	3	BASF 1060	
68	8.67	3	BASF 1060	
70	7.33	2.5	Dayton HD50	
71	2.24	2	Sika 421	
72	5.04	2.5	Sika 421	
P1-1	6.45	2.5	BASF 1060	
P1-23	9.87	3.25	BASF 1060	
P1-30	4.40	2.5	BASF 1060	
P1-33a	2.22	3	BASF 1060	
P1-33b	63.03	3.5	BASF 1060	
P1-33c	3.99	3.5	BASF 1060	
P1-33d	4.00	3	Dayton HD50	
P1-41	5.02	3	Dayton HD50	
P1-44	29.16	3	Dayton HD50	
P3-11a	15.40	3	Dayton HD50	
P3-11b	4.81	3	Dayton HD50	
P3-12	27.53	3	Dayton HD50	
P3-14	23.10	3	Rapid Set	
P3-16	13.98	3	BASF 1060	
P3-17a	8.86	2.5	BASF 1060	

Pothole	Area (SF)	Average Depth (IN)	Material Type	Notes
P3-17b	3.50	3	BASF 1060	
P3-17c	2.25	3.25	BASF 1060	
P3-26	22.17	3	BASF 1060	
P3-34	6.50	3	BASF 1060	
P3-35	3.79	3	BASF 1060	
P3-36	3.80	2.5	BASF 1060	
P3-39	16.69	4	Dayton HD50	
P3-5	9.75	2.5	Dayton HD50	
P3-7a	20.68	3	Dayton HD50	
P3-7b	5.96	2.5	Dayton HD50	
73		2.5	BASF 1060	Found with drone

Table B.3 Details of Repair Work (Phase 3)

Pothole	Area (SF)	Average Depth (IN)	Material Type	Notes
1	91.93	3	BASF 1060	
2	36.22	3	Fastrac	
3	23.85	2.5	Fastrac	
4	163.75	3.5	Fastrac	
5	28.72	3.5	Fastrac	
6	29.17	3	Fastrac	
7	22.57	3.5	Fastrac	
8	13.67	3	Rapid Set	
9	4.06	3.75	Rapid set	
10	380.76	3.25	Rapid Set 3/4	
11	22.73	3	Rapid set	
12	18.60	3	Rapid Set	
13	5.04	3	Rapid Set	
14	7.76	3	Rapid Set	
15	3.67	2.5	Rapid set	
16	33.06	4	BASF 1060	
17	79.53	4	Pavemend	
18	7.20	4	Pavemend	
19	6.85	4	Pavemend	
20	10.42	3.5	Pavemend	
21	10.21	3.25	Pavemend	
22	36.73	3.25	Pavemend	
23	100.38	3.25	BASF 1060	
24	13.50	3.5	Pavemend	
25	21.27	2.5	Pavemend	
26	34.63	4	Pavemend	
27	4.69	3.5	Pavemend	
28	4.78	4	Pavemend	
29	4.51	2	BASF 1060	
30	3.51	2	Pavemend	
31	54.00	3	BASF 1060	
32	7.44	3	BASF 1060	
33	62.49	3.75	BASF 1060	
34	12.46	4.25	BASF 1060	
35	13.44	4	BASF 1060	
36	22.43	4	BASF 1060	
37	7.79	3.75	BASF 1060	

Pothole	Area (SF)	Average Depth (IN)	Material Type	Notes
38	9.28	4	BASF 1060	
39	38.97	5.25	BASF 1060	
40	20.82	3.5	Rapid set	No cure applied

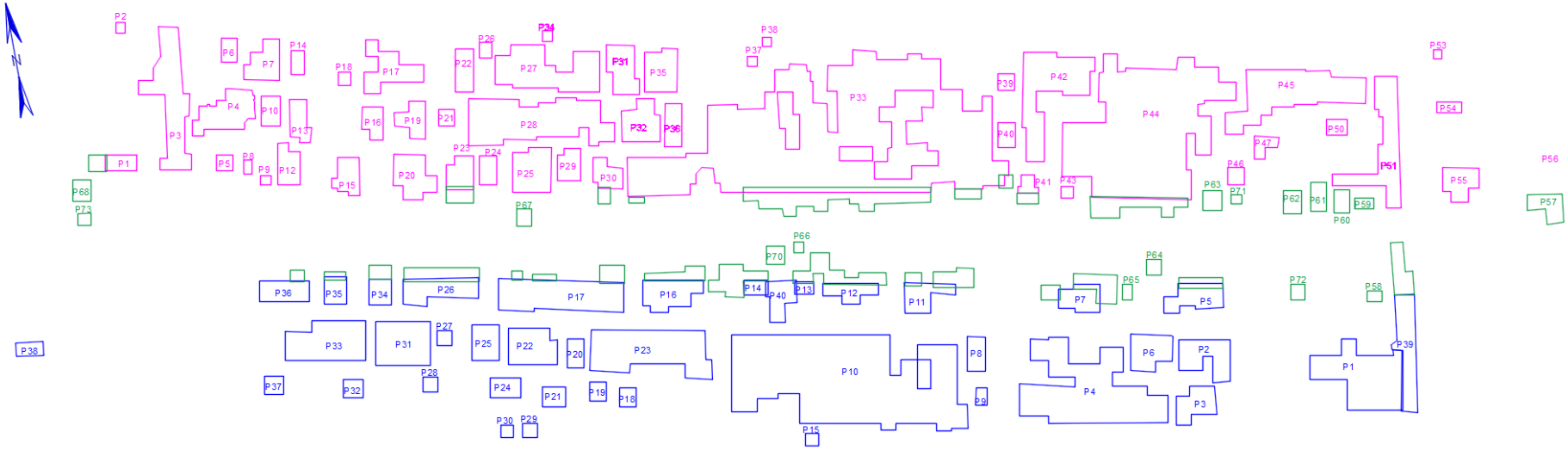

Figure B.8 Map of the Repair Work (Phase 1: Blue, Phase 2: Green, Phase 3: Magenta)

APPENDIX C: PRODUCT INFORMATION

Table C.1: Product Keys

Product	Pavemend DOT Line	Sika 321	Sika 421	CTS DOT Line	CTS DOT Concrete	BASF 1060	BASF 1061	Dayton HD50	FasTrac
Key	P1	P2	P3	P4	P5	P6	P7	P8	P9

Table C.2: Material Specification

Question	Western Material Design FasTrac 246	Sika Sika 421	Aquafin Pavemend DOT Line	BASF BASF 1060	CTS CTS DOT Repair Mix	Dayton Superior Dayton HD50
Does the material come in 50lbs bags?	It comes in 60 lb. bags	It is sold only in 65-lbs bags because it is pre-extended with aggregate	No. The product is specifically formulated to 53.5 lbs. due to a 2 qt water ratio.	Yes. It comes in 50# bags and in 3000# totes	It comes in 55# bags. We can also package it in 3000# totes.	Yes, it comes in 50# bags
Can the product be extended? If so, what percent?	It is pre-extended	It is pre-extended, aggregate is already in the bag. No need to extend further. This eliminates potential contractor errors of extending material at the job site	No. The product is already pre-extended with 3/8" granite aggregate. Formulation is based on performance at this yield. Extension will result in dilution of formula and change of specific water ratio.	Yes, up to 100% by weight	Yes. Up to 100%. A 55# sack extended 100% yields 0.84-0.90 Cubic Feet	Yes, 60%
What is the product yield per bag? Not extended (top). Extended, if applicable (bottom)	0.45 cubic feet	0.5 cubic feet	0.4 cubic feet	0.57 Cubic Feet	0.5 cubic feet	0.42 Cubic Feet
	N/A	N/A	N/A	0.77 Cubic Feet	0.84-0.90 Cubic Feet	0.60 Cubic Feet
Minimum patch depth (it is assumed that if the product is extended, that the minimum depth would be based on the agg. used to extend - 3xDiameter)	1 in	Minimum application depth is 1"	The minimum profile thickness is 1.25"	1/2 inch (If extended with a 3/8" pea gravel (most typical), saw cut the perimeter of the area being repaired into a square with a minimum depth of 1 inch, but the rest of the area of the repair should be 1.5 inches minimum for best performance of the patch)	Depends on size of aggregate. We can go down to ½" when not extended	1/2 inch (Minimum depth is 0.5" and 1" if extended)

Question	Western Material Design FasTrac 246	Sika Sika 421	Aquafin Pavemend DOT Line	BASF BASF 1060	CTS CTS DOT Repair Mix	Dayton Superior Dayton HD50
Approximate cost per bag	It would be approximately **$15** per bag in Utah	approximately **$15**/bag	**$39**	Approximate cost per bag is **$25-$22** depending on quantity purchased.	**$25-$30**	**$20**
Product availability: Where can the product be locally sourced?	The product could be purchased through a local distributor	It is readily available and can be sourced at the following Sika distributors: Smalley & Co./Lowry's-Pro Coat/For Shor/White Cap/Intermountain Concrete	Product Availability by receipt of PO. Can be sourced from Salt Lake City.	It is locally stocked in Salt Lake City and the surrounding areas through several major distributors like Intermountain Concrete Specialties, HD Supply, Smalley and Company, and ProCoat Systems. It is made in Newark, California and shipped to our distributor partners.	White Cap for bags, totes would come out of DuPont, WA or Southern CA	This product is available at most local Concrete Supply Warehouses (Intermountain Concrete Supply, ForShore, WhiteCap, etc.).
Is a primer required?	No primer is required	No special primer is required. Typically, a scrub coat of Sikacrete 421 CI Rapid is applied to the SSD surface of the patching area as per data sheet and industry accepted standards	No. No bonding agent. Just SSD. (Saturated Surface Dry).	No separate "primer" is required, although, a scrub coat / key coat of mixed 1060/1061 mortar is required to be worked into the SSD substrate prior to placing material as per direction on the Product Data Guide	No	No
Does the material contain Magnesium Phosphate?	NO	NO	No, product is Pozzolan	NO	NO	NO
How soon after placement ca the product be overlaid		can be coated with a vapor barrier type coating (epoxy, polyester etc.) after minimum cure time of 24-hours @ 66-95 degrees F, 48-hours @ 56-65 degrees F, and 5-days @ 45-55 degrees F.	2 hours	As far as time before overlaying, it depends on what is the overlay material is, how deep the patch is as well as temperature and humidity. For applications 2 inches or less, typically epoxy materials can be placed (after required surface prep) in 4 hours on the 1060 @ 70° F 50% RH, while our polyurethane	After proper curing. 1.5-2 hours. Remember 98% of the water is used during hydration so there is no bleed water, thus overlays can be applied immediately-the advantage of this CSA cement. Wet burlap is the preferred method of curing or else the cure compound will act as a debonder with the overlay	Can be overlaid in less than 4 hours or when Patch has less than 4% moisture content.

Question	Western Material Design FasTrac 246	Sika Sika 421	Aquafin Pavemend DOT Line	BASF BASF 1060	CTS CTS DOT Repair Mix	Dayton Superior Dayton HD50
				coatings will require 24 hours under these same conditions. The 1061 requires a little more time for the epoxies (6 hours @ 70° F 50% RH) but still only 24 hours for polyurethane materials. For applications greater than 2 inches then you would either wait 48 hours to be safe or conduct a moisture test to determine that all residual moisture have dissipated before proceeding with overlay.		